MAS-RELATED G PROTEIN-COUPLED RECEPTOR B2 ACTIVATION MEDIATES BLADDER WALL BIOMECHANICS

By

Pragya Saxena

A DISSERTATION

Submitted to
Michigan State University
in partial fulfillment of the requirements
for the degree of

Pharmacology and Toxicology – Doctor of Philosophy

2024

ABSTRACT

Approximately 43 million men and 71 million women suffer from troublesome lower urinary tract symptoms (LUTS) in the US alone, representing a significant public health burden. Among the many different origins of LUTS, inflammation in the bladder wall alters urothelial signaling, detrusor contractility, and bladder wall biomechanics – all of which could disrupt normal storage and voiding function. The Mas-related G protein-coupled receptor B2 (Mrgprb2) is an orphan receptor traditionally believed to be expressed on mast cells that drives "pseudo-inflammation" through IgE-independent degranulation of mast cells. The exact role of Mrgprb2 in altering bladder function is unknown. Thus, this dissertation pursues the following hypothesis: Mrgprb2 receptor activation promotes Matrix metalloprotease-mediated collagen degradation leading to altered mechanical compliance. We observed that the Mrgprb2 agonist, compound 48/80, rapidly increases mechanical compliance of whole bladders during *ex vivo* filling while paradoxically increasing detrusor excitability. Compound 48/80 also caused overactivity when administered intravesically during conscious cystometry. Unexpectedly, these changes persisted in mast cell-deficient mice, suggesting that the effects of compound 48/80 are independent of mast cells. Visualization of collagen fibers within the wall showed that Mrgprb2 agonism leads to a significant reduction in bladder wall thickness combined with a disruption in MMP-2/TIMP-2 balance hence it is likely that the former is a product of the latter. Also, collagen remodeling still occurs in the absence of urothelial permeabilization. Together, these findings suggest that the material properties of the bladder wall are more labile than we imagined. Mrgprb2 activation in the bladder wall can lead to rapid and profound changes in compliance mediated by imbalances in the MMP-TIMP family of enzymes. Understanding the pathophysiology of this mechanism is of significance since it uncovers various druggable targets for inflammatory LUTS outside of

mast cell degranulation. This dissertation provides novel insights into the critical role of Mrgprb2 in driving rapid changes in bladder function, thereby contributing to a better understanding of the consequences of pro-inflammatory pathway activation in the urinary bladder.

This thesis is dedicated to my husband, Suvir, for being my pillar of strength and my biggest cheerleader.

ACKNOWLEDGEMENTS

I would like to express my deepest gratitude to my mentor, Dr. Nathan Tykocki. He encouraged me to find the confidence within me and be the best version of myself throughout my time in his lab. He taught me the importance of hard work, kindness, and perseverance during a PhD career, and I will always be indebted to him for the young scientist I have become. In addition to my mentor, I would like to thank my committee members, Dr. Anne Dorrance, Dr. William Jackson, and Dr. Sara Roccabianca for guiding me in times of need and always redirecting my focus to what is important. Their knowledge and insight in their respective fields were invaluable to me. I would like to thank my parents, Dr. Ratnesh Saxena and Dr. Punita Saxena, for helping me build the wings I could fly with. Everything that I am and everything that I do is because of them and for them. I would also like to thank my brother Dhruv, for being the only family I had away from home and for always listening to me rant about failed experiments. Lastly, I would like to thank the wonderful friendships I have built in this department, Osvaldo and Jess, I could never have completed my degree if it wasn't for the constant support and love I derived from them. To the rest of my family and friends; just like raising a child, it takes a village to propose, perform, and present a dissertation, and I am so grateful for all the support I have received through it all. Finally, I have spent the last five years trying to learn everything I can about bladder biomechanics but the most important lesson I'll always carry with me has been to embrace failure and be persistent in one's pursuits.

"When you get into a tight place and everything goes against you … never give up then, for that is just the place and time that the tide will turn."

Harriet Beecher Stowe, Oldtown Folks, 1869

TABLE OF CONTENTS

LIST OF ABBREVIATIONS

ATP	Adenosine triphosphate
BK	Large conductance potassium channels
ECM	Extracellular Matrix
GAG	Glycosaminoglycans
IC/BPS	Interstitial cystitis/bladder pain syndrome
LOX	Lysyl Oxidase
LP	Lamina Propria
LUTS	Lower Urinary tract symptoms
MC	Mast cells
MMP	Matrix metalloproteases
OAB	Overactive bladder
P2X	Purinergic receptor type X
SEM	Standard error of mean
SK	Small conductance potassium channels
TPE	Transient pressure events

AN OVERVIEW OF BLADDER WALL STRUCTURE AND FUNCTION

1. PHYSIOLOGY OF THE URINARY BLADDER

The urinary bladder performs three main functions: filling, storage and voiding of urine. Despite its apparent structural simplicity, the bladder wall is equipped with a complex arrangement of layers that interact with each other to adequately perform its functions. The innermost layer of the bladder is a stratified epithelium, the urothelium [4]. The sub urothelial layer, called the lamina propria, is a network of ECM proteins, blood vessels, immune cells, interstitial cells, and afferent and efferent nerve endings [4, 5]. In some species, such as humans, the lamina propria also has muscle fibers organized in a muscularis mucosae layer similar to the gut implying that the bladder develops from the hindgut in an embryo [6]. Some studies also propose that species such as guinea pigs have a muscularis mucosae layer due to their specific ethology [7]. The outermost layer of the bladder is the detrusor muscle layer. All bladder wall layers singularly contribute to bladder function; however, the focal point of this section will be to discuss how the different cellular components of the bladder can interact with each other to change biomechanical properties of the acellular matrix proteins.

1.1 T*he urothelium: a multi-faceted transitional epithelium of the bladder*

Epithelial tissues that line hollow organs, such as the gastrointestinal tract, the respiratory tract, and the genitourinary tract, face a challenge in maintaining a balance between their core functions: protection, transport, secretion, and tissue repair. The urothelium represents a great example of a stratified epithelia in our body since it serves as one of the least permeable barriers while enabling expansion of bladder surface area to accommodate large volumes [8]. As noted in Figure 1, The urothelium is composed of three different histological layers: basal, intermediate, and superficial [9]. The basal cuboidal cells are the progenitor cells that differentiate into intermediate cells [4]. The intermediate layer plays an important role in the regeneration and repair of the urothelium during inflammation and injury [10]. The superficial layer of the urothelium is formed by highly differentiated and polarized binuclear umbrella cells. The umbrella cells are responsible for creating a protective barrier between urine and underlying layers by forming tight junctions [11]. The urothelium has 5-7 structural layers when the bladder is relaxed, but the bladder can stretch tremendously to store large volumes of urine. At this stage, the urothelium is able to condense to 3-4 structural layers without jeopardizing structural integrity; hence it is called a transitional epithelium [12]. During filling, the urothelium must withstand high osmotic pressures and mechanical stretch while maintaining a strong barrier. Umbrella cells transition from a parasol shape to a squamous flat form upon filling in order to maintain their barrier function [11]. Even so, a significant drop in transepithelial electric resistance (TER) occurs during mechanical stretch, suggesting that active stretch on the bladder wall can lead to a leakier barrier [13]. Simultaneously, the drop in TER is accompanied by increased transepithelial membrane capacitance that occurs due to apical membrane exocytosis [14]. The classical model of bladder filling suggests that umbrella cells undergo both exocytosis

and endocytosis induced by stretch and pressure respectively [12]. The rates of both processes are as such that the net effect is to add membrane as the bladder fills to store more urine [15].

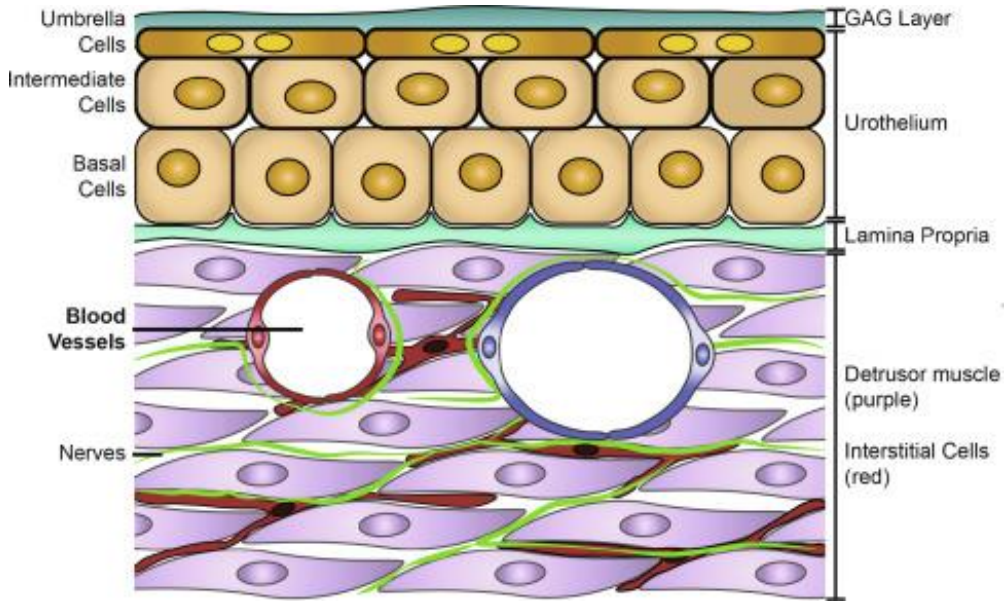

Figure 1 The different layers of the murine urinary bladder wall. The structure of bladder wall is depicted. Layers from top to bottom represent the following: (1) Urothelium layer comprising of a GAG layer, umbrella cells, intermediate cells and basal cells, (2) Lamina propria comprising of the extracellular matrix proteins such as collagens and elastin, and (3) Detrusor muscle layer that consists of smooth muscle cells, interstitial cells and blood vessels. GAG: Glycosaminoglycans. Image courtesy: Nathan R. Tykocki, image adapted from [2]

The urothelium also acts as the first responder to most chemical and mechanical stimuli, releasing several mediators to communicate with underlying layers of the bladder wall [8, 16, 17]. The urothelial cells respond to chemical, mechanical, and thermal stimuli by virtue of all the receptors and ion channels expressed on their surface, including (but not limited to): α- and ß-adrenergic receptors [18] muscarinic receptors [19]; purinergic $P2X_{1\text{-}7}$ and $P2Y_{1,2,4}$ receptors [20, 21]; and transient receptor potential (TRP) channels (TRPV1, TRPV2, TRPV4 and TRPM8) [8]. Muscle excitability can be altered [22] via release of soluble mediators [23] from the urothelium, including ATP [24, 25] and prostaglandins [26]. Both surfaces of the urothelium can release ATP after it experiences changes in hydrostatic pressure [21]. The urothelium can also undergo changes to its barrier and transport function upon stimulation of these input pathways [15].

It is imperative to characterize signaling molecules that are released by the urothelium since it acts as a transmural signaling hub that can significantly alter detrusor activity and bladder capacity. Defects in the transmural signaling likely contributes to the pathogenesis of various bladder dysfunctions, such as interstitial cystitis and overactivity [27].

1.2 *Urinary bladder contraction and relaxation*

The detrusor muscle is the outermost layer of the bladder wall and is arranged in layers of longitudinal and circular orientation much like the gastrointestinal tract however they are more loosely arranged in the bladder [28]. Since the detrusor is the only muscle component in the bladder wall, it is significantly responsible for maintaining proper bladder function by contracting and relaxing [29]. Detrusor contraction and relaxation is regulated by the parasympathetic and sympathetic innervation in the bladder, respectively. Detrusor contraction is regulated by both muscarinic and purinergic efferent nerve signaling; however, muscarinic control dominates in humans [30]. Once G_q–coupled muscarinic M_3 receptors are activated, the

subsequent formation of inositol 1,3 bisphosphate (IP_3) potentiates release of sarcoplasmic intracellular calcium stores [31]. While less clearly studied, M_2 receptors also contribute to detrusor contraction by either inhibiting the relaxing effects of adrenergic ß$_3$ receptors [32] or inhibiting K_{ATP} channels [33]. Detrusor relaxation is regulated in part by ß$_3$ adrenoreceptors and by the opening of small conductance Ca^{2+}-dependent K^+ channels (SK channels) and large conductance Ca^{2+}-dependent K^+ channels (BK channels). These channels only open with increased intracellular calcium and cause membrane hyperpolarization, closure of L-type voltage-gated calcium channels ($Ca_V1.2$ channels), and relaxation of detrusor smooth muscle [34].

As for the afferent outflow to the CNS, spontaneous phasic contractions, which occur in randomized areas of the detrusor, are responsible for driving sensation of fullness [35, 36]. The ability of the bladder to have spontaneous contractions without significantly increasing overall intravesical pressure is very specific to detrusor smooth muscle. Detrusor myocytes are not as well coupled as other smooth muscle cells. If muscle bundles were well coupled, intravesical pressure would change spontaneously making it very difficult to store urine [37-39]. The interplay between contraction and relaxation pathways maintains a low muscular tone within the detrusor until bladder fullness is sensed.

1.3 *Lamina propria: the functional hub of the bladder*

Just below the urothelium is the lamina propria, which sits in between the basement membrane of the urothelium and the detrusor muscle layer [40]. The lamina propria is home to multiple cells (e.g., fibroblasts, myofibroblasts and mast cells), the highly specialized bladder vasculature, a rich lymphatic network, and matrix proteins (e.g., elastin and collagen fibers) [5, 41]. Mechanical stretch and purinergic signaling can initiate calcium events through the lamina

propria before it reaches the detrusor muscle layer, insinuating that the lamina propria is a functional layer capable of communicating signals between the urothelium and detrusor layers [42, 43].

The LP contains a novel cell population that have the structural characteristics of myofibroblasts but are also similar to the interstitial cells of Cajal found in the gut [40]. Interstitial cells have not been studied extensively but their role within the bladder is currently of significant research interest. Interstitial cells respond to cholinergic and purinergic signaling [42, 44] and also express both PGE_2 receptors (EP_1 and EP_2) indicating that prostaglandins released from the urothelial cells can illicit downstream effects via interstitial cells [45-47]. The LP also contains a complex network of both efferent and afferent nerves. Nerves are also present in LP that contain the characteristic sensory neuron peptides, CGRP, Substance P, and Neurokinin A [48] It is possible that nerves in the LP are involved in mechanosensory pathways within the bladder that include the urothelium and detrusor layers.

Lastly, the cells within the bladder wall greatly depend on adequate oxygen supply from the blood to perform their functions. The bladder vasculature is an important part of the lamina propria that delivers oxygen and nutrients to the cells of the bladder even in the face of mechanical stretch and spatial changes. Vessels within the bladder are extremely tortuous and have frequently spaced interlacements [49]. The structure and arrangement of bladder vessels have not been studied in great detail and their functional role in normal and pathological states of the bladder remain to be fully established.

1.4 *Preliminary Findings*

A large part of this dissertation focuses on exploring previously unknown receptors that may be expressed in the urothelial layer and understand how the mediators that are released upon their activation can signal downstream to alter bladder function. One such receptor is the Mas-related G protein-coupled receptor b2 (Mrgprb2) that is known to be expressed in the bladder however its role in driving bladder dysfunction is not explored. I characterized the effects of Mrgprb2 agonism on bladder wall compliance and detrusor contractility (see Chapter 3). My findings show that exposure to compound 48/80 increases mechanical compliance and properties of the transient pressure events that occur in the bladder as it fills mediated via Mrgprb2 receptors. These effects were studied further to elucidate the mechanism downstream of Mrgprb2 receptor activation (see Chapter 4) that leads to increased compliance however, the increases in amplitude and leading slope of transient pressure events is not explored further. Section 1.2 and 1.3 outline the mediators that can be released from the urothelium and alter detrusor contractility and integrity of the extracellular matrix. Specifically, purinergic signaling and prostaglandin release were explored. Figure 2 shows that the effects of compound 48/80 on compliance and contractility are likely both mediated by ATP. Other than ATP, prostaglandins were also explored as a cause for increased contractility. The COX inhibitor indomethacin was also able to inhibit the dual effects of compound 48/80 (Figure 3). The proposed pathway for dual effects of compound 48/80 discussed in chapter 5 explains the possibility of ATP and prostaglandin release when mechanical stretch is induced.

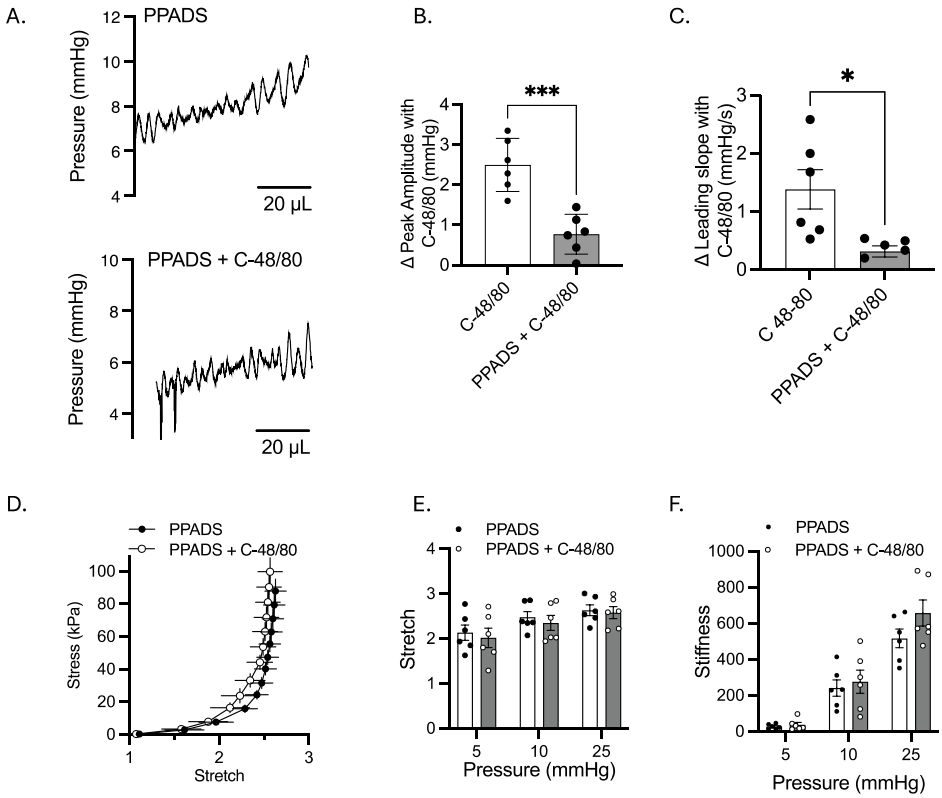

Figure 2 P2X receptor antagonist PPADS blocks both effects of compound 48/80. **A,** Representative traces of transient pressure events in presence of the P2X antagonist, PPADS (10 µM) alone and after addition of the Mrgprb2 receptor agonist compound 48/80 (10 µg/mL). The increase in peak amplitude **(B)** and leading slope **(C)** were reduced by PPADS (P=0.0005 for peak amplitude and P=0.012 for leading slope). PPADS blocks the increase in mechanical compliance caused by compound 48/80, signified by the absence of rightward shift in the stress vs. stretch curve **(D)** and a significant increase in stretch at 5, 10, and 25 mmHg **(E).** Stiffness remains unchanged in both groups. N=6. *P* values were determined using Unpaired *t*-test for equal variance. *:<0.05, ***:<0.001

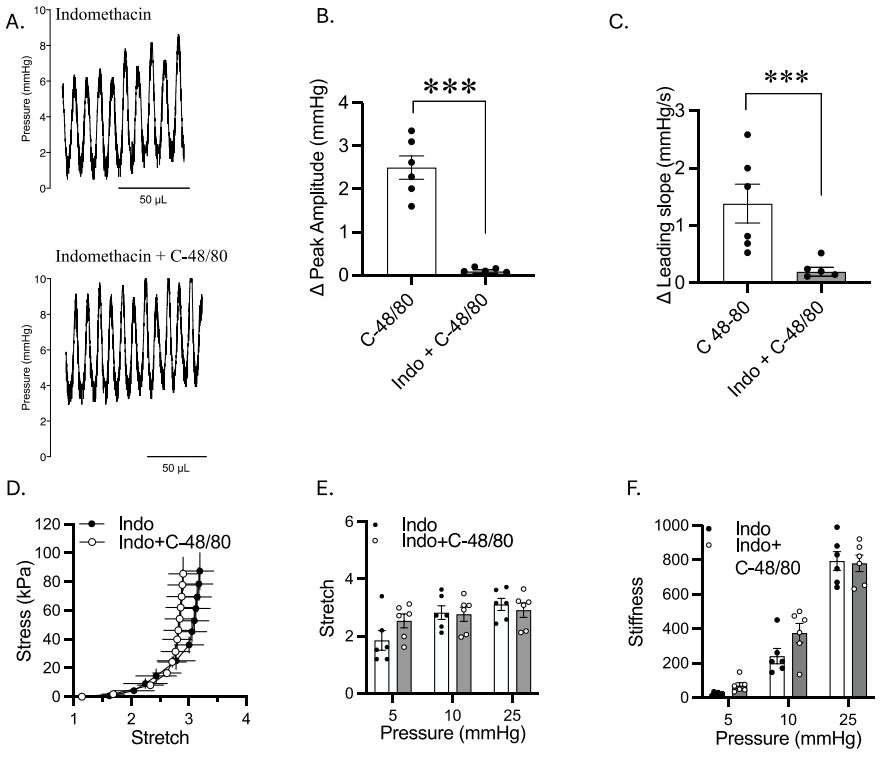

Figure 3 Nonselective COX inhibitor, Indomethacin blocks both effects of compound 48/80. A, Representative traces of transient pressure events in presence of the COX inhibitor, Indomethacin (10 µM) alone and after addition of the Mrgprb2 receptor agonist compound 48/80 (10 µg/mL). The increase in peak amplitude **(B)** and leading slope **(C)** were reduced by Indomethacin (P=0.0002 for peak amplitude and P=0.006 for leading slope). Indomethacin blocks the increase in mechanical compliance caused by compound 48/80, signified by the absence of rightward shift in the stress vs. stretch curve **(D)** and a significant increase in stretch at 5, 10, and 25 mmHg **(E).** Stiffness remains unchanged in both groups. N=6. *P* values were determined using Unpaired *t*-test for equal variance. *:<0.05, ***:<0.001

2. STRUCTURE OF THE BLADDER WALL

Extracellular matrix within the bladder plays a major role in stretching of the bladder wall to accommodate urine and bringing it back to its original state after voiding has occurred [5]. The ECM continuously undergoes changes in arrangement and composition to provide structural support and integrity to the bladder wall. The majority of ECM is made up of fibrillar collagen types I and III. Other ECM components include elastin fibers (made up of tropoelastin and microfibrils), proteoglycans, and adhesive proteins, such as laminins and fibronectins (Figure 2). The ECM remains the most complex structural organization of proteins in organisms [50]. Historically, we believed that tissues and organs were a collection of connective tissue fibers that are arranged nonspecifically and originated spontaneously [50]. Characterization of collagen and elastin fibers only became possible in the early 1900s through modern microscopy techniques [51]. While recent research helped identify important constituents of the ECM and their contributions to organ structure and function, it is important to note that organization of ECM may not be conserved between organs.

This section will examine the current state of knowledge of matrix biology of the bladder while also drawing comparisons from other organs to shed light on what could be the role of ECM components within the bladder wall. Due to the constant filling and emptying cycles the bladder must go through, the bladder needs to be highly distensible. However, its distensibility is not just by virtue of the muscle. The content and organization of the ECM play a large role in maintaining the mechanical integrity of the bladder wall during filling and storage. We discuss the bladder ECM in terms of ECM molecules, crosslinking, adhesive receptors in development and pathophysiology.

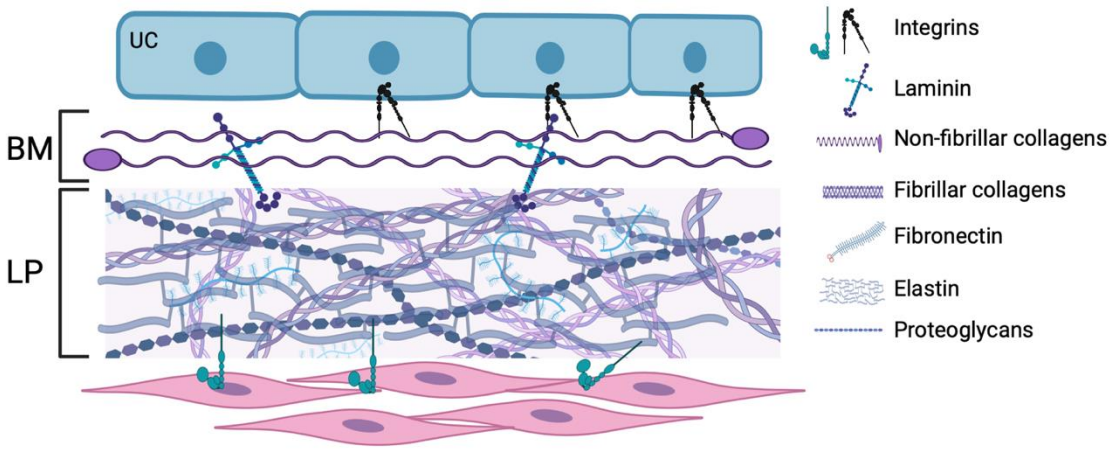

Figure 4 Extracellular matrix (ECM) compartments. Schematic representation of two compartments of the ECM in the bladder: basement membrane (BM) and lamina propria (LP). The distinction between the two compartments is more nebulous in the bladder. The legend indicates the identity of each ECM component.

2.1 *Contents of the Extracellular Matrix*

Broadly, ECM in our body can be categorized into two parts: the basement membrane closest to the epithelial cells and the interstitial matrix that is located in the lamina propria and the muscle layer [52, 53] (Fig 2). While the bladder ECM has similar components, it is dissimilar in the distinct compartmentalization. It is easier to understand the anatomy of bladder ECM by categorizing it into different types of proteins. Bladder ECM is made up of fibrillar proteins, polysaccharide molecules known as glycosaminoglycans, adhesive proteins and ECM receptors [5].

The fibrillar proteins in the bladder ECM are collagen and elastin fibers. Collagen type I and type III represent the bulk of the bladder wall, with collagen type III specifically associated with compliance (an overview of collagen arrangement and their contribution to mechanical function is explained in Section 2.2). Elastin is secreted as tropoelastin by fibroblasts or smooth muscle cells [54] and is primarily responsible for the bladder's ability to recoil to its original shape after continued distention. Tropoelastins are embedded in a scaffold of microfibrillar components and covalently link with other monomeric tropoelastin molecules to form elastin fibers. These fibers contain a core fiber surrounded by the microfibrillar proteins fibrillin 1, fibrillin 2, fibulin 3, and microfibril associated glycoprotein (MAGP) [55]. However, elastin fibers are extremely long lasting and have a very low turnover. Studies done in vascular tissue show that a loss of elastin can alter the orientation and function of smooth muscle cells due to the elastin fragments aberrantly binding to the elastin binding protein (EBP) [56].

A large part of ECM function is responding to cellular signals thus, adhesion to cells is an integral part of their characteristics. Adhesive proteins in the ECM help with the cellular adhesion and are important for remodeling, morphogenesis, and cellular growth. Laminins and

fibronectins are the two main adhesive proteins in the bladder ECM. Laminins are large trimers of 15 alpha, beta, and gamma chains that are mostly present around the smooth muscle cells [57]. Adhesion of laminins to detrusor smooth muscle cells may improve their survival during filling [58]. Fibronectin is a glycoprotein in bladder ECM that is also generally involved in wound healing in organs that are exposed to toxins, such as the gut and lungs. In the bladder, it is a very important molecule that promotes adhesion, cellular migration, and tissue patterning. Fibronectin is directly involved in the fibrillogenesis of collagen, making it a vital part in the pathophysiology of remodeling in the bladder [59].

There are several ECM receptors that are now being heavily investigated, but integrin receptors are mainly studied for cell-cell and cell-ECM interactions in the bladder wall. Integrin $\alpha 6\beta 4$ is the primary receptor in the urothelium that binds to laminin. Integrins $\alpha v\beta 3$, $\alpha 5\beta 1$, $\alpha 3$, $\alpha 2$, and $\alpha 1$ are expressed in the smooth muscle and bind to collagen and fibronectin. Stretch stimulus leads to increased binding of integrin receptors to the ECM due to their transformation to a high affinity state. These transformed integrins can induce downstream signaling pathways leading to ECM remodeling [60].

The continuous remodeling of the bladder requires synthesis and breakdown of ECM components. Collagen and elastin fibers form cross-links that are vital to provide tensile strength and elasticity to the bladder. LOX (Lysyl oxidase) and other LOX-like proteins, which mediate elastin formation from tropoelastin also mediate collagen-elastin crosslinking. Apart from LOX, advanced glycation end (AGE) products can also induce cross-linking to make the ECM stiffer and are commonly seen in aged or diabetic bladders [61].

2.2 *Collagen fiber arrangement during filling and storage*

Collagen type I and collagen type III represents the bulk of structural ECM proteins in the bladder wall [62]. Studies performed to understand collagen structure in tendons show us that type I collagen fibers are more crimped in conformation and straightens up when tension is applied on them [63]. Hence, the structural properties of type I and III collagen play a critical role in the mechanics of the bladder.

Barring less abundant collagens that are difficult to classify (e.g., fibril associated with interrupted triple helices (FACITs), collagens found in the detrusor layer can be either classified as fibrillar or non-fibrillar [57, 64]. All collagens are made up of three alpha-chains that consists of the repeating Gly-Pro-X sequence to give them a triple helical structure (Figure 3). The triple helix strengthens the collagen, makes it less susceptible to proteases and provides tensile strength to the bladder [65]. While fibrillar collagens are highly repetitive, the same is not seen with non-fibrillar collagens, such as type II and type IV. These collagens have a variable sequence and are more sheet-like in conformation. These exist mainly in the basement membrane to act as a barrier for migrating cells [5]. Fibrillar collagens type I and III exist in the lamina propria and in the endomysium surrounding the detrusor. Type I fibers are found as super-helices of 1.5 nm in diameter that gives it the strength for maintaining proper bladder function. Type III fibers are thinner but more distensible, forming heterotypical fibrils with type I to regulate their diameter [66]. Loss of collagen type III is associated with increased bladder compliance [67].

As the bladder expands the heavily coiled collagen fibers in the lamina propria as well as the endomysium gradually uncoil, leading to a reduction in thickness of the bladder wall [68]. There are a few schools of thought about which layer of the bladder wall can be attributed to its high compliance. Many studies offer hypotheses for different layers of the bladder bearing the load

during different phases of filling but there is not enough scientific evidence to conclude that this is the case. Some studies attribute the bladder compliance completely to the lamina propria and propose that the smooth muscle layer is only present as a protective measure to avoid over distention [69]. This dissertation aims to show that collagens in the lamina propria, endomysium, and the smooth muscle cells themselves stretch to allow distention of the bladder during filling. It is the contribution of all these components – and not sequential load bearing – that allows for the intravesical pressure to rise and the bladder to fill.

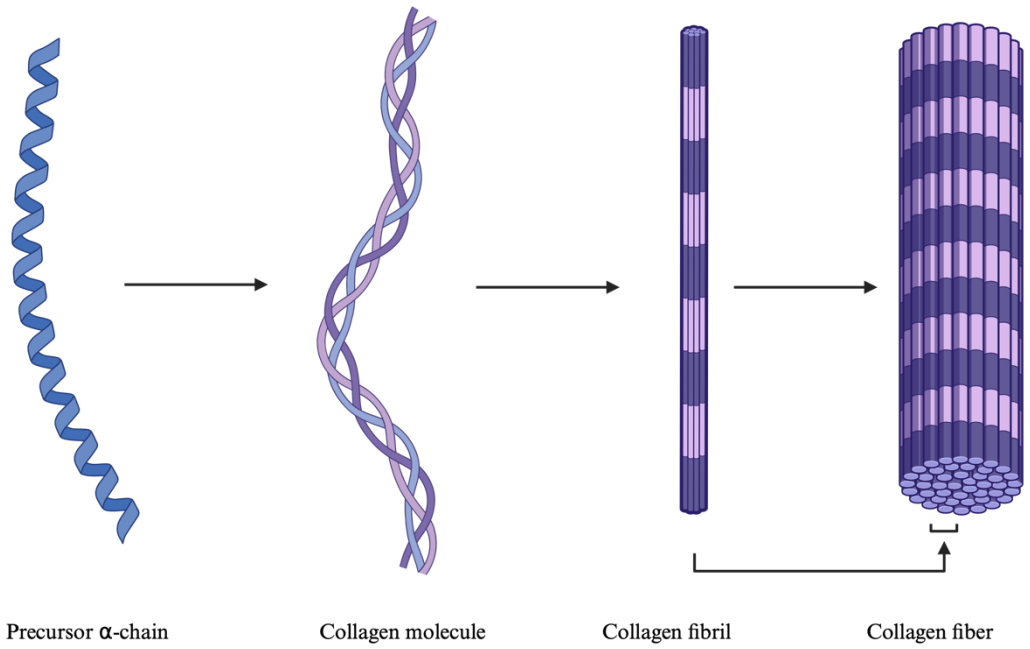

Figure 5 Formation and crosslinking of collagen fibers. Three independent precursor alpha-helix chains form hydrogen bonds to assemble into a triple-helix intertwined structure called procollagen (not shown) that possesses the basic mechanical strength of collagen. Procollagen is then assembled into a collagen molecule with the help of metalloproteinases. Next, collagen molecules are laterally stacked in peptide chains by LOX-mediated catalysis. These stacks are known as collagen fibrils, and they are further stacked laterally and connected by covalent bonds to form collagen fibrils. Collagen fibrils are the most basic constituent of the ECM and possesses enhanced mechanical strength due to the LOX-catalyzed crosslinking between the collagen molecules.

2.3 *Collagen deposition and degradation*

Collagens are usually synthesized in the extracellular matrix by cells, such as fibroblasts and myofibroblasts [70]. The exception is collagen type IV, which can also be synthesized by epithelial cells [71]. Optimal deposition of both collagens type I and III is integral to bladder function since reduced type I content is linked to urinary incontinence [72, 73] and type III content is inversely related to bladder compliance [67]. Collagen type IV has mostly been studied in the pathophysiology of urothelial cancer, however its sensitivity to inflammation makes it important in other lower urinary tract diseases – especially ones that may arise due to inflammation.

Since ECM turnover is continuous and necessary to the integrity of the bladder wall, there are proteins present within the ECM that carry out degradation of ECM components. Matrix metalloproteases (MMPs) play a dominant role in breaking down existing ECM molecules and potentiating the formation of new ones. MMPs are a family of more than 27 Zinc-dependent endopeptidases that were historically named according to their substrate of choice (e.g., collagenases, gelatinases, stromelysins, and matrylisins); however recent studies have shown that MMP specificity may be too broad to categorize [70]. MMPs can be produced by various cell types, including fibroblasts, epithelial cells, and leukocytes. During homeostasis their expression and activity are low and controlled by their endogenous inhibitors, Tissue inhibitors of metalloproteases (TIMPs) [74]. Under homeostatic conditions, MMPs contribute to collagen turnover but in the event of bladder instability, MMP activity and expression can be altered to significantly alter bladder function. Excess deposition or degradation of ECM proteins, especially collagen fibers, can lead to direct effects on bladder compliance and stiffness suggesting that MMPs represent a great target to understand inflammation driven alteration of

bladder wall biomechanics. There are several inflammatory mediators that can induce MMP activity, including cytokines, growth factors, and neutral proteases released by activated mast cells [75]. Matrix metalloproteases in the ECM can also be activated by mediators including neutral proteases [75] and ATP released by neighboring cells in the bladder wall [76]. The different types of MMPs have different substrates in the ECM however some overlap exists [77]. An outline of MMPs and their specific substrates is given in Table 1. The catalytic activity of MMP is controlled at the transcriptional level, during pro-peptide cleavage from tissue inhibitors of matrix metalloproteases (TIMPs) and by specific inhibitors such as tetracycline derivatives [78, 79]. MMPs are activated in several ways through removal of the pro-domain to expose the active site that is protected by a cysteine residue (Figure 4) [80]. Removal of the cysteine residue takes place in the pericellular space and is triggered by multiple mediators including but not limited to TIMPs, other activated endoproteinases, and reactive oxygen species [78, 81]. Once the MMPs are activated by cleaving the pro-domain and revealing the substrate binding cleft for the substrate peptide to bind. The carbonyl group of the peptide coordinates with the active Zn^{2+} site and displaces the water molecule to promote hydrolysis of the peptide itself [74]. The pocket beside the active Zn^{2+} site holds the side chain of the peptide and varies in size with different types of MMPs hence, certain MMPs are specific for their substrate. The most common types (MMP-2, MMP-1, MMP-8 and MMP-13) can degrade fibrillar collagens (type I and type III) and cause an increase in bladder compliance [82]. In this dissertation, I studied the overall effects of MMP activation on collagen content upon activation of a pseudo-inflammatory pathway within the bladder.

Table 1. MMPs and their substrates with a focus on MMPs that are known to be present in the urinary bladder [74].

Enzyme	MMP Classification	Substrate
Collagenases	MMP-1	Collagens I, II, III, VII, X, gelatin, aggrecan
	MMP-8	Collagens I, II, III, aggrecan
	MMP-13	Collagens I, II, III, gelatin, fibronectin, laminin
Gelatinases	MMP-2	Gelatin, collagens I, IV, V, VII, X, fibronectin, laminins, aggrecans
	MMP-9	Gelatin, collagen IV, V, XIV, elastin, aggrecan
Stromelysins	MMP-10	Collagen IV, fibronectin, aggrecan
	MMP-11	Fibronectin, gelatin, laminins, collagen IV, aggrecan
Membrane-type MMPs	MMP-14	Activates proMMP-2 and proMMP-13
Matrilysin	MMP-7	Gelatin, fibronectin, laminins, collagen IV, tenascin-C, elastin, aggrecan

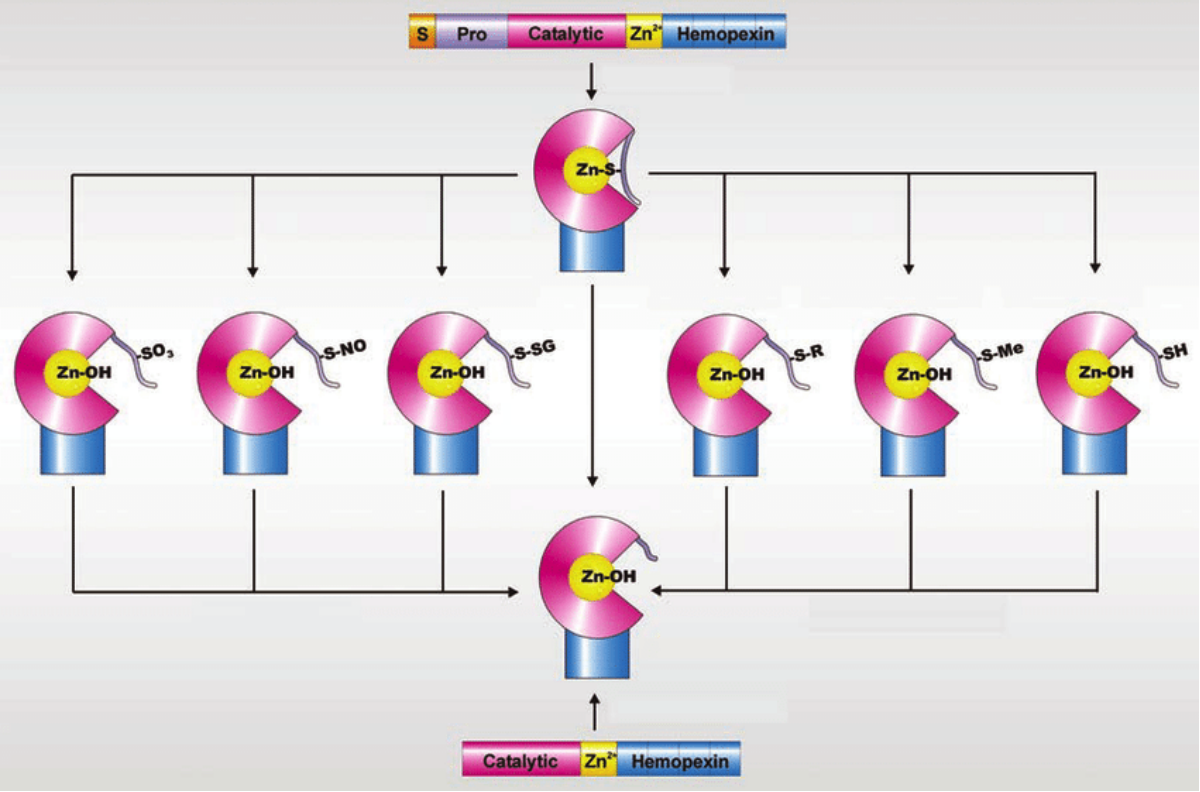

Figure 6 Mechansim of activation of MMPs. Typically MMP structure consists of a signal peptide (S), a pro-domain (Pro), a catalytic site that is protected by a Zn^{2+} domain and a hemopexin domain. The catalytic Zn^{2+} ion is connected by a thiol group to the cysteine residue on the pro-domain. Most often, the thiol-Zn^{2+} bond is hydrolysed to activate the MMP (-OH). Other physiological activation mechanism include disruption in the thiol-Zn^{2+} bond by reactive oxygen species ($-SO_2$), nitrosylation (S-NO) or glutathionation (S-SG) of the thiol group. Allosteric activation may also activate the MMP by binding of a receptor (-R).
Non physiologically, MMPs may be activated in vitro due to reagents such as organomercurials (-Me) or SDS (-SH). Figure adapted from [3]

3. PATHOPHYSIOLOGY OF BLADDER DYSFUNCTION

Lower Urinary tract symptoms (LUTS) include a wide range of symptoms that impact quality of life and emotional well-being in both men and women [83]. They include storage symptoms, such as overactive bladder (OAB) and incontinence (both stress and urge), as well as obstructive voiding symptoms, such as hesitancy and incomplete emptying [84]. There is an understanding of how LUTS arise due to obstruction or neurological disorders, but most storage symptoms in the absence of these causes are poorly understood. This section of the dissertation aims to review the pathophysiology of OAB and interstitial cystitis (IC) and discuss some of the inflammatory pathways within the bladder that may alter bladder wall biomechanics and lead to LUTS.

3.1 *Pathophysiology of overactive bladder (OAB)*

Overactive bladder encompasses storage symptoms such as urgency (sudden compelling desire to pass urine), frequency (frequent voiding by day) and nocturia (frequent voiding at night) that mostly present with detrusor overactivity (spontaneous or provoked involuntary non-voiding contractions during filling) [85]. These symptoms may occur with or without urge incontinence and are thus termed OAB wet or OAB dry subtypes, respectively [86]. Since the symptoms of bladder dysfunction are limited, their root cause is difficult to interpret through traditional urodynamic measurements [87]. For example, whether intravesical pressure is increased due to denervation of detrusor muscle or interstitial cystitis cannot be determined only by performing urodynamic studies on patients.

There are broadly two schools of thought on why OAB may occur. First, the “myogenic hypothesis” suggests that partial denervation of detrusor muscle fibers can morphologically change the electrical coupling in overactive bladders [88]. This hypothesis also proposes that coupling between detrusor muscle fibers may also contribute to maintenance of low intravesical

pressures. Increased coupling in OAB may lead to spontaneous spread of excitation through large areas of the bladder thereby increasing pressure [89]. Second, the "neurogenic hypothesis" suggests that changes in the central nervous system pathways or hypersensitization of the peripheral afferent terminals leads to premature activation of micturition reflexes, which induces unstable detrusor contractions [90]. There is also a newer "integrative hypothesis" that suggests there is no single basis responsible for bladder overactivity but the disruption in communications between different cell types leads to activation of many pathways listed in the myogenic and neurogenic hypotheses [91]. The findings supporting this hypothesis show that spontaneous localized contractions are actually normal and interstitial cells act as a pacemaker for these "micromotions". When alterations occur in crosstalk between the interstitial cell and detrusor muscle fibers, overactivity is seen [92]. None of these hypotheses are without limitations, a common one being an absence of consideration of the urothelium and its crosstalk with the detrusor and afferents that could alter bladder function. While we have hypotheses that outline the importance a single cell type, there is a major gap in knowledge about the interactions of these cells. There is no single hypothesis that explains how different origins of OAB can lead to the same outcome.

3.2 *Pathophysiology of interstitial cystitis/bladder pain syndrome (IC/BPS)*

Patients suffering from IC/BPS present with symptoms including those of OAB, but IC can be differentiated by presence of irritability and bladder pain. As described in Section 1, urothelial factors are released in a normal bladder to communicate with the underlying layers. Altered release of urothelial mediators are a marker of both OAB and IC [93-95]. The most common biomarkers associated with LUTS are nerve growth factor (NGF), brain-derived neurotrophic factor (BDNF), prostaglandin E2 (PGE2), ATP, and an increase in TRPV1 receptors [84]. For

example, signaling in the detrusor muscle fibers is predominantly cholinergic in healthy bladders but during inflammation, purinergic signaling is augmented. [96]. Another alteration in the urothelium during IC/BPS is the presence of Hunner's lesions which can be visualized as a typical inflammatory ulcer on the surface of the epithelial layer. IC patients with Hunner's lesions (5-10%) exhibit higher level of inflammation [97]. Similarly, alterations in central pain mechanisms are also implicated during IC/BPS. TRPV1 channel sensitization shifts sensory outflow from Aδ fibers to C fibers leading to irritability [98]. Pain due to C fiber sensitization is also associated with mast cell infiltration [99], a common cell-type that is implicated in IC/BPS. Offering treatments for IC/BPS is often difficult because actual etiology remains unclear. Most treatments only target the pathogenesis such as mast cell activation, urothelial dysfunction, and neurogenic inflammation [100].

3.3 *Inflammation in the bladder*

While there is an increase in pro-inflammatory mediators during LUTS, inflammation in most diseased bladders is measured differently hence, inflammatory basis of many bladder dysfunctions are not identified. This dissertation focuses on understanding LUTS arising from inflammatory pathways in the bladder wall that could lead to symptoms that don't traditionally arise from inflammation. Our hypotheses step away from studying LUTS resulting from known pathologies (e.g., bacterial infections, carcinomas, and diabetic neuropathy).

Pro-inflammatory mediators that are augmented in LUTS, including those released from mast cells, can directly sensitize afferent nerve fibers [101, 102]. Increased NGF levels in the bladder lead to hyper-innervation and increased mast cell counts [103]. This may explain the increased neuronal terminals and hyperexcitability arising from an inflammation in LUTS patients.

Many immune cells reside in the bladder and could act as a potential source of mediators upon inflammation. Out of the innate and adaptive resident immune cells in the bladder tissue, the most abundant are macrophages, mast cells, NK cells, and T cells [103, 104]. Historically, it was believed that all macrophages in soft tissue were monocyte-derived macrophages [105]. However, two sub-types of macrophages have since been identified by their specific spatial niches: the lamina propria and the detrusor layer [106]. While the monocyte-derived macrophages are more relevant in terms of fighting infection, the resident tissue macrophages resemble those present in the lung and dermis and play a larger role in tissue repair during homeostasis [107]. When we discuss effects of immune cell function alteration on detrusor contractility or bladder biomechanics, we are more interested in the resident macrophages than the monocyte-derived invading macrophages.

After macrophages, mast cells may be the most investigated immune cell in the bladder even though the specific role of mast cells in bladder dysfunction remains nebulous. Much like macrophages, their ontogeny has not been extensively studied in the bladder, but it is likely that they are both hematopoietic and yolk sac-derived in origin and similar to those observed in the intestine muscularis [108]. MCs are located just underneath the urothelium in the bladder where they can regulate both adaptive and innate immune responses by acting as histamine-releasing granulocytes [109]. The proximity of MCs to afferent nerve endings promotes the speculation that the bidirectional communication between MCs and afferents can be a basis for OAB [110]. Elevation of mast cell numbers and mast cell mediated urothelial permeabilization are also seen in IC patients [111]. MCs have been implicated in various disorders such as OAB [112], UTIs [102], cystitis [46, 113] due to alteration in their numbers, activation state or distribution. Many studies outline the degranulation of mast cells, the potential release of mediators, and their direct

effects on bladder function [114, 115]. Histamine is one of the most studied mast cell derived mediator that can alter contractile activity of urothelium and detrusor through H1 and H2 receptors [116-118]. Other agents released from MCs, such as proteases and cytokines can contribute to tissue remodeling and induce a state of inflammation and fibrosis.

Mast cells usually degranulate via activation of the IgE mediated FcεRI receptor [119] however it can also be activated by non-IgE mediated pathways via activation of the surface receptors on mast cells including toll-like receptors (TLRs) and protease-activated receptors (PARs) [120-122]. Degranulation due to activation of IgE dependent and non-IgE dependent pathways is different in that the former leads to release of smaller granules more rapidly [123].

3.4 *Bladder wall remodeling and bladder dysfunction*

LUTS as it relates to detrusor contractility and hyperactive neuronal firing has been discussed in detail; however, another important linchpin of proper bladder function is the extracellular matrix. Effects of inflammation on bladder ECM proteins are of great interest even in absence of a pathogen or injury. Since the ECM plays a role in maintaining a balance between bladder wall compliance and stiffness, temporary or permanent remodeling of these proteins in any way can change compliance and alter bladder function. The role of MMPs in degrading the components of ECM have been discussed in detail in section 2 of this chapter. MMPs can be modulated by various inflammatory pathways of interest. Recent studies show the role of ATP in rapidly activating MMPs that further degrade collagen fibers [76]. As it pertains to studies shown in this dissertation, we are interested in inflammatory mediators that can rapidly alter bladder biomechanics. While transcriptional and translational changes in MMP expression cannot be altered within minutes, changes in MMP activity levels are possible. Specific MMPs are

explored in chapter 3 of this dissertation that can remodel fibrillar and non-fibrillar collagen types and alter bladder biomechanics.

The other end of the spectrum for biomechanical balance of the bladder wall is an increase in expression of collagens. In case of chronic inflammation in the bladder wall due to injury or infection, fibroblasts can produce excess collagen [124] and its deposition causes a loss of bladder compliance. Matrix deposition is a tightly regulated process that is controlled by binding of polymerized collagen to an integrin receptor on the cell surface to suppress fibroblast production of excess collagen [125].

Not only does ECM provide structural support to the bladder but it also interacts with the detrusor to aid in its contraction. Hence, changes in ECM constitution can also alter muscle contractility. Myogenic symptoms of LUTS can arise from alterations that begin in the ECM structures. Although the chemical composition of ECM is important, mechanical stimuli alone may also be able to regulate integrin-mediated signaling events to the smooth muscle [126]. For example, microtubules are one element of the cytoskeleton that can alter muscle contractility after ECM reorganization due to chemical/mechanical stimuli [127]. Hence, the ECM is largely affected by LUTS and inflammation in the bladder due to interactions between the muscle and ECM and urothelium and ECM via adhesion receptors.

4. QUANTIFICATION OF WHOLE BLADDER BIOMECHANICS

4.1 *Clinical compliance vs. mechanical compliance*

As explained in the sections above, bladder compliance is an accurate and important measure of bladder function [128]. Urologists measure bladder compliance as change in volume per change in pressure ($\Delta V/\Delta P$) [129, 130] however this measurement comes from an incomplete understanding of the structures in the bladder and their contributions to bladder filling and storage. The traditional method of compliance measurements assumes that the ratio of cellular and acellular components in all bladder walls is the same. Therefore, it assumes that the mechanical properties of the material itself is same across all bladders and the contributions that bladder wall thickness and size can have on the biomechanics are inconsequential. To be able to understand the role of compliance in LUTS, a proper understanding of compliance in healthy bladders is necessary. Hence, new methods to measure compliance are needed that gives us a complete picture of mechanical properties of the wall and takes the non-linear nature of bladder filling into account. This can be done by including geometrical measurements of the bladder wall during filling along with increasing pressures [130]. Methods described in this dissertation focus on an engineer's perspective of bladder compliance. A new method to measure bladder compliance was devised in that, compliance was measured using the mechanical stress *vs.* spherical stretch curve instead of the pressure *vs*. volume curve. Obtaining geometrical measures required to plot these curves posed as one of the biggest obstacles in this process. The bladder was then modelled into a predictable shape in order to accurately measure changes in geometry as it fills. We assumed the bladder wall to be a homogenous material that undergoes isotropic deformation while filling because we are more interested in estimating the average stress experienced at any point on the bladder wall during bladder filling irrespective of its

directionality or regional variability. Hence, the bladder is modelled to be a spherical vessel that stretches uniformly in all directions.

4.2 *Biomechanics of hollow organs*

Visceral organs that contain an epithelium surrounded by a collagen rich matrix and one or more muscular layers can be termed as hollow organs of the human body [131]. These organs are often responsible for propelling or storing solids, fluids and air. Hence they undergo mechanical processes such as distention and contraction. Understanding the biomechanical characteristics of these materials is imperative to gain knowledge about their proper function. From a bioengineering perspective, their mechanical characteristics such as stress and strain are calculated to model their behavior in both health and disease. For example, most blood vessels are broadly modelled as pressurized hollow cylinders with a passive (collagens and elastin) and active layer (muscle) [132]. In this model, different stress tensors are used to describe stresses on the active layer and the passive layer since the directionality of force distribution as well as the linearity of length-tension relationship are different for both layers. This is only possible because stress calculations in a layered cylinder has been outlined in several studies. The bladder differs from these other hollow organs because of its unpredictable shape thus, mechanical stress calculation becomes a challenge. During the experiments outlined in chapters 2 and 3, we observed the empty bladder to be more spherical in shape but as it filled, it became elliptical. To our knowledge, there is very little information about measurements of Cauchy stress in elliptical vessels hence, our model of the bladder assumes sphericity and isotropy. While these assumptions maintain simplicity, they are not far from biomechanical assumptions previously made for the urinary bladder [133, 134] . One of the limitations of this system is our inability to manually calculate thickness of the empty bladder that is required for stress measurement due to

the opacity of an empty bladder. The initial thickness is calculated using the final thickness values and the assumption that the wall volume remains constant therefore, the assumption of incompressibility is made.

4.3 *Pentaplanar reflected image macroscopy system (PRIM)*

A new technique; pentaplanar reflected image macroscopy (PRIM) was developed and used to measure changes in bladder pressure, the volume as it fills, and bladder shape over the course of bladder filling. The components of the novel PRIM system (Figure 5) is explained in detail in Appendix 1. Briefly, it is a deep chamber with a curved cannula in the middle, four mirrors on all sides, and a camera on top of the system all run by an integrated control unit that has an in-line pressure transducer. When the bladder is cannulated in the chamber, and illuminated using the lightning shroud, five visual planes are recorded in a single frame. Each frame corresponds to a pressure and volume reading. The imaging data is then used to calculate changes in bladder shape as it fills and when combined with the pressure reading, mechanical stress on the bladder wall can be calculated as it stretches. Bladder mechanical compliance is then given as stress *vs.* stretch instead of change in volume per change in pressure. The linearized slope of stress-stretch curve gives the stiffness of the bladder.

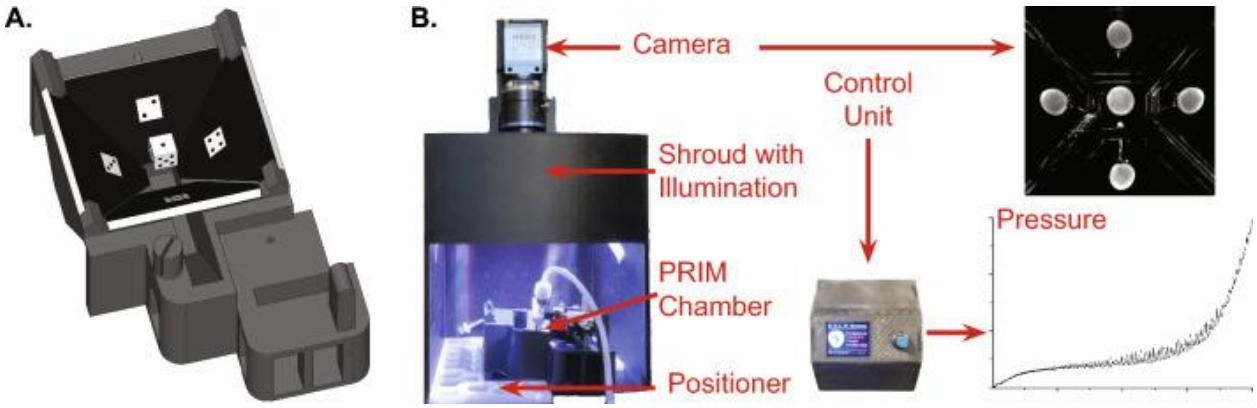

Figure 7 Parts of the PRIM system. (A) A model of the PRIM system, **(B)** The components of the system; camera, lightening shroud, PRIM chamber, and control unit. [1]

5. MAS-RELATED G PROTEIN-COUPLED RECEPTOR X2/B2

Mas-related G protein-coupled receptor X2 (MRGPRX2) is an orphan G protein coupled receptor (GPCR) that is most abundant on cutaneous mast cells. There is also evidence of MRGPRX2 mRNA expression in sensory neurons and keratinocytes [135]. The MRGPR family was discovered by screening several gene transcripts in small-diameter nociceptive neurons of the dorsal root ganglia (DRG). One of these transcripts closely resembled the protooncogene *Mas1*. Due to the resemblance to *Mas1*, the receptor family was named as such [136]. The human MRGPRX1 was the first primate-specific receptor to be classified from this family. Its agonist, bovine adrenal medulla 8-22 peptide (BAM8-22) was also identified but it has not yet been confirmed to be the actual physiological agonist for MRGPRX1 [137]. While several other synthetic and natural chemicals have been identified that bind to receptors from this family, it remains an orphan GPCR. There has been a controversy regarding the canonical signaling pathway of MRGPRs [138] however there is abundant evidence suggesting that it is $G\alpha_{Q/11}$-coupled. Hence MRGPRX1-4 structures have been elucidated based on complexes formed with G_q and the peptide Cortistatin-14 [139]. Among the many structural dissimilarities between MRGPRX2 and other GPCRs, one of the most interesting revelations was the wide-open extracellular ligand binding surface. Electrostatic potential calculations across the surface reveals that the MRGPRX2 pocket is highly negatively charged on one side and highly hydrophobic on the other giving it the potency to bind to many basic secretagogues [139].

McNeil et al. studied the mouse ortholog of MRGPRX2, Mrgprb2, and showed that Mrgprb2 activation produces rapid degranulation of mast cells in a landmark study [120]. Downstream of $G\alpha_{Q/11}$-coupled Mrgprb2 and MRGPRX2, the phospholipase-C pathway is activated to increase

release of intracellular calcium from the IP3-mediated SER stores [122]. Since MRGPRX2 is so important in the skin with reference to anaphylaxis reactions [140], it has been implicated in mediating itch, neurogenic inflammation, atopic dermatitis, and several other mast cell-mediated responses. However, there is also evidence of Mrgprb2/X2 mRNA in the urinary bladder [141]. Its exact functional role and location in the bladder remains elusive but many studies make the bladder an organ of interest for exploring MRGPRX2. MRGPRX2 has been found to be responsible for SP-induced mast cell degranulation in IC/BPS [142]. Chapter 2 of the dissertation explains the studies done in mice bladders to understand how bladder function can be altered via pseudo-inflammatory pathways mediated by Mrgprb2 even in mast cell-deficient mice. Being a transitional epithelium within the bladder, the urothelium is dissimilar from keratinocytes in the skin but just like keratinocytes, it is capable of responding to both chemical and mechanical stimuli to elicit downstream inflammatory pathways. The potential for urothelial cells in the bladder to act like keratinocytes in that they could express Mrgprb2 as a surface receptor and secrete mediators to alter bladder function is explored in this dissertation.

6. CONCLUSIONS

We reviewed the contributions of different components of the bladder wall to maintain proper function and how inflammation in the bladder can lead to alterations in bladder wall biomechanics via degradation/deposition of the ECM. We also learnt that an accurate method of measuring compliance is necessary, and the novel PRIM system fills that gap. The rest of this dissertation will outline two different aims: (1) to understand the effects of Mrgprb2 activation on bladder wall biomechanical properties; and (2) to hypothesize a pathway through which Mrgprb2 alters mechanical compliance of the bladder. These studies reveal new targets that can be explored for bladder dysfunction and outline the role of an important inflammatory receptor in the bladder that was previously unexplored. These studies will also show that the effects mediated via Mrgprb2 are mast cell independent and may be driving an increase in compliance through MMP activation. My final chapter will justify how my findings progresses the current knowledge of inflammatory bladder dysfunction, outline the pitfalls in our studies and identify future directions for bladder research.

QUANTIFYING WHOLE BLADDER BIOMECHANICS USING THE NOVEL PENTAPLANAR REFLECTED IMAGE MACROSCOPY SYSTEM

Modified from: Hennig G, Saxena P, Broemer E, Herrera GM, Roccabianca S & Tykocki NR. (2023). Quantifying whole bladder biomechanics using the novel pentaplanar reflected image macroscopy system. *Biomechanics and Modeling in Mechanobiology*. 2023 Oct; 22(5): 1685-1695. doi: 10.1007/s10237-023-01727-0. PMCID: PMC10511590.

Note: In the following manuscript, I contributed to developing the equations to infer wall thickness, performing ex vivo experiments to calculate wall compliance, and analyzing images that are used to measure compliance.

1. ABSTRACT

Optimal bladder compliance is essential to urinary bladder storage and voiding functions. Calculated as the change in filling volume per change in pressure, bladder compliance is used clinically to characterize changes in bladder wall biomechanical properties that associate with lower urinary tract dysfunction. But because this method calculates compliance without regard to wall structure or wall volume, it gives little insight into the mechanical properties of the bladder wall during filling. Thus, we developed Pentaplanar Reflected Image Macroscopy (PRIM): a novel ex vivo imaging method to accurately calculate bladder wall stress and stretch in real time during bladder filling. The PRIM system simultaneously records intravesical pressure, infused volume, and an image of the bladder in 5 distinct visual planes. Wall thickness and volume were then measured and used to calculate stress and stretch during filling. As predicted, wall stress was nonlinear; only when intravesical pressure exceeded ~15 mmHg did bladder wall stress rapidly increase with respect to stretch. This method of calculating compliance as stress vs stretch also showed that the mechanical properties of the bladder wall remain similar in bladders of varying capacity. This study demonstrates how wall tension, stress and stretch can be measured, quantified, and used to accurately define bladder wall biomechanics in terms of actual material properties and not pressure/volume changes. This method is especially useful for determining how changes in bladder biomechanics are altered in pathologies where profound bladder wall remodeling occurs, such as diabetes and spinal cord injury.

2. INTRODUCTION

Bladder compliance is measured clinically and experimentally as the change in volume for a given change in pressure during bladder filling, due in part to the inability to reliably calculate bladder wall volume without ultrasound imaging [143, 144]. Unfortunately, measuring compliance in this manner erroneously makes two key assumptions. First, it assumes that all healthy bladder walls are composed of cells and matrix components in similar proportions and thus have a similar elastic modulus. Second, it assumes that all healthy bladders have comparable total wall volume and gross geometry. These two assumptions mean that measuring compliance as $\Delta V/\Delta P$ is imprecise and easily skewed by the size and thickness of the bladder wall. For example: a large bladder with a thin, stiff wall could appear highly compliant if not filled to the point of engaging viscoelastic elements of the wall. One could then conclude erroneously that the bladder is extremely compliant when it is indeed not. These assumptions and omissions have resulted in immense variability in bladder compliance even in healthy individuals and made it extremely difficult to deduce "normal" compliance [128].

When considering the entirety of filling, the mechanical behavior of the bladder wall is nonlinear. Intravesical pressure changes very little for very large filling volumes but increases exponentially thereafter [145]. Measures of clinical compliance, however, are derived only from the low end of total bladder capacity [128] and thus do not give a complete picture of the mechanical properties of the bladder wall. By measuring pressure and bladder geometry over the entirety of filling, we could calculate the mechanical parameters of the bladder wall in the same way as mechanical engineers would measure the properties of any pressure vessel. This idea has been applied to human subjects by using ultrasound to take sagittal and transverse images (1 per minute) during cystometry [144]. However, the high cost and low resolution of this technique

makes it extremely difficult to implement in animal models and still only gives a partial view of bladder geometry during filling. In order to calculate the mechanical properties of the bladder wall, new methods are required by which bladder wall geometry and intravesical pressure can be measured inexpensively and in real time during filling.

Almost all biological imaging techniques have one major flaw: by their very nature, the images they collect only contain two-dimensional information for a given point in time. To overcome this limitation, advanced confocal and light sheet microscopy techniques were developed that take sequential images through the *z* plane of a sample to reconstruct tissue in three dimensions [146, 147]. However, even the fastest coded light-sheet array microscopes can only reach speeds of 6-10 volumes per second in very small, optically cleared tissue sections and with an absolute minimum amount of movement [148]. In order to image live tissue in 3 dimensions and at speeds greater than 10 Hz, new techniques must be developed. Thus, we invented "Pentaplanar Reflected Image Macroscopy" (PRIM), a new technique where a single camera and 4 fixed mirrors are used to record 5 imaging planes of a sample in a single camera frame. Because the camera, optics, light source, and the sample are stationary, all focal planes are taken at once and at high speeds (75 Hz or more, depending on the camera). Because the PRIM System allows rapid and accurate measurements of bladder shape, internal volume, and wall volume over the entirety of bladder filling while also capturing frame-locked intravesical pressure recordings, compliance can instead be reported as Cauchy stress/stretch instead of $\Delta V/\Delta P$. Because this equipment is scalable, inexpensive, and easy to use, it could potentially revolutionize imaging of any organ where dynamic movements occur in 3 dimensions simultaneously; this includes propagation of peristaltic movement in the gut, motility in the stomach or uterus, or even nutation of plant stems during growth.

In this study, we implement the PRIM System to measure bladder wall geometry and pressure and use this information to calculate bladder wall stress and stretch during *ex vivo* filling of normal mouse bladders. Our measurements were reproducible, robust, and consistent with those made using biaxial mechanical testing of bladder wall samples and other previously published measures of bladder biomechanics [149, 150]. Thus, the PRIM System can bring new insight into intact bladder wall biomechanics during filling.

3. MATERIALS AND METHODS

3.1 Animal Care and Use

All animal procedures followed institutional guidelines and were approved by the Institutional Animal Care and Use Committees of Michigan State University (NIH Assurance D16-0054). Male C57Bl/6 mice (9 – 12 weeks old; Jackson Laboratory, Bar Harbor, ME) were group housed in a temperature- and humidity-controlled environment with a 12 hr light/dark cycle. Mice were provided *ad libidum* access to standard chow and water. Mice were euthanized by injection of pentobarbital (>150 mg/kg i.p.) followed by decapitation.

3.2 Pentaplanar Reflected Image Macroscopy (PRIM) System

The PRIM System consists of four main sections: the PRIM imaging chamber, a digital camera with television lens, the lighting shroud, and the integrated control unit (Figs. 8A, B). Unless otherwise specified, all custom-designed pieces were three-dimensional printed from PETG plastic using a fused deposition modeling printer (Prusa i3 Mk3S; Prusa Research, Czech Republic). The PRIM chamber itself consists of a custom-designed ABS imaging chamber, 4 mirrors, the mounting cannula, and chamber positioner. The chamber is filled with liquid through a tube that enters in the center, below the sample. Fluid level is maintained using a peristaltic pump and suction tube (Warner Instruments, USA). Back-coated mirrors (3.18 mm thickness; The Home Depot, USA) were cut and shaped in house. Mirrors are fixed in position at 45° angles relative to the central specimen, which is placed on the cannula for *ex vivo* filling using a standard syringe pump. The monochrome digital camera (DMK33UX250, 5 megapixel, 3.45 μm^2 pixel size; The Imaging Source, USA) and television lens (TCL1616, 16 mm focal length, F1.6-16; The Imaging Source) were mounted atop the lighting shroud roughly 12 cm above the imaging chamber on a custom camera mount that allowed for focusing and centering of the

image. The camera sat atop the shroud, which was sized to allow full illumination of the sample without inclusion of the lights themselves in the reflected image. The integrated control unit consisted of an Arduino microcontroller, Wheatstone bridge amplifier shield (Robotshop.com), PicoBuck LED driver (COM-13705, Sparkfun), in-line pressure transducer (DYNJTRANSMF, Medline) and 12V DC power supply. As designed and assembled, the integrated control unit had a pressure resolution of 0.07 mmHg that remained linear across a range from 0 – 40 mmHg. Image pixel size was 64 μm^2. Pressure transducers were calibrated using a sphygmomanometer. Pixel size was confirmed in every image using the known width of the bottom of right-hand mirror, as measured by vernier caliper. Both pressure readings and camera triggering were regulated by the Arduino microcontroller to ensure a single pressure reading was matched with each image frame, and readings were collected at 10 Hz. Pressure data were collected using *VasoTracker-DataTracker* software (courtesy Dr. Calum Wilson, University of Strathclyde; UK) for later analysis. Video images were collected using *IC Capture* software (The Imaging Source; USA). When properly aligned, 5 visual planes are recorded in a single image and each image frame correlates to a single pressure and infused volume reading. These data are then used for measurement and analysis of bladder geometry and bladder compliance.

3.3 Ex Vivo Bladder Filling

Urinary bladders were isolated and cannulated using a modified version of our previously described protocol [151]. Briefly, the urinary bladder with ureters and urethra was removed and placed in ice-cold Ca^{2+}-free HEPES-buffered physiological saline solution (HB-PSS) containing [mM]: NaCl [134], KCl [6], MgCl2 [1.2], HEPES [10] and glucose [7]; pH=7.4. The bladder and urethra were cleaned of fat and connective tissue and ureters were tied proximal to the bladder wall with 4-0 suture. The tissue was then moved to the PRIM chamber (also containing Ca^{2+}-free

HB-PSS), cannulated, and affixed with 4-0 suture. HB-PSS was then exchanged for bicarbonate-buffered PSS containing [mM]: NaCl [119], $NaHCO_3$ [24], KCl [4.7], KH_2PO_4 [1.2], $MgCl_2$ [1.2], and $CaCl_2$ [2]. PSS buffer was bubbled externally with 5/20/75% $CO_2/O_2/N_2$ to maintain pH, recirculated by peristaltic pump, and heated to 37°C using an in-line heater (Warner Instruments). Ca^{2+}-replete PSS was infused into the bladder at a constant rate (30 µl/min) through the PRIM chamber's cannula using a calibrated syringe pump. *Ex vivo* filling commenced simultaneously with video and pressure recording. To increase the contrast between the lumen and bladder wall, infused buffer was mixed with dark food coloring. Bladders were filled until a maximum pressure of 20-25 mmHg was reached, at which time the infusion and video/pressure recordings were simultaneously stopped. Bladders were then emptied and allowed to re-equilibrate for 5-10 minutes before the next fill. To simulate preconditioning, fill-empty cycles were repeated at least 5 times for each bladder; the final fill-empty cycle was used for all calculations.

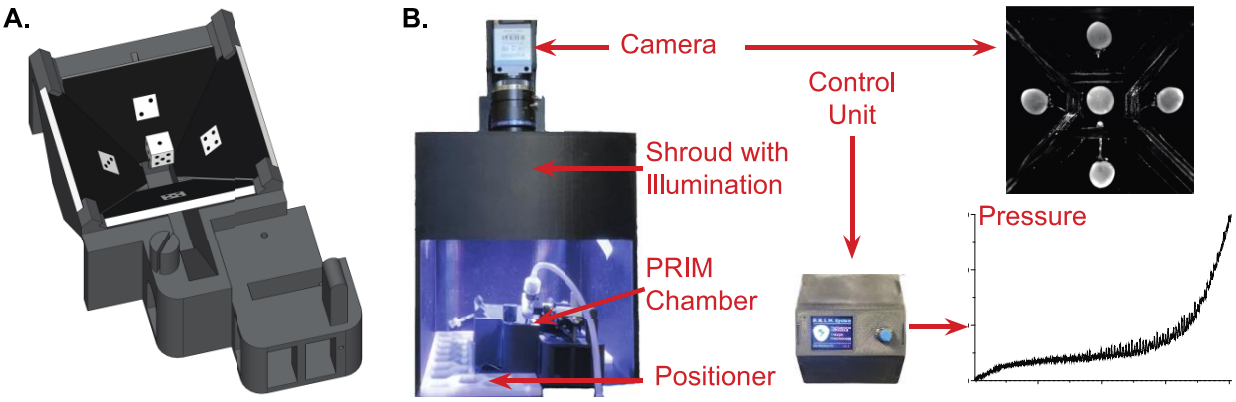

Figure 8 The Pentaplanar Reflected Image Macroscopy (PRIM) System. (A) Rendering of the PRIM chamber and mirrors, illustrating each of the 5 captured visual planes. (B) The entire system consists of the chamber, shroud, positioner, camera, and control unit. In addition to video images, other data (e.g., pressure) can be recorded. Time-linked pressure and imaging data can be combined to calculate the mechanical properties of the sample over time (e.g., Cauchy stress versus stretch of a mouse urinary bladder during filling).

3.4 Bladder Wall Thickness, Volume, and Residual Estimation

The urinary bladder was assumed to have an elastic wall of constant volume and uniform thickness, which deforms during filling and behaves as a nonlinear expanding vessel [133]. Here and in the following, lowercase letters will refer to the geometry of the bladder when full (deformed configuration at 20 mmHg) and uppercase letters will refer to the geometry of the bladder when empty (configuration at ~0 mmHg).

To measure all dimensions required to calculate the wall volume, the first and last frames of the filling video were extracted and areas of each image plane of the bladder was measured using ImageJ software (NIH) (Figure **9**). Perimeters were manually selected by the contrast between black background and white tissue. The average area of sections 1 – 4 (representing vertical planes of the bladder) and the area of section 5 (representing a plane perpendicular to the other sections) were first measured. These measurements were collected from images at 20 mmHg (Figure **9**A) and 0 mmHg (Figure **9**B). Bladder wall thickness in the full bladder (t) was first estimated by measuring the width of the brightest section of the edge of the bladder wall in the last frame of the filling video (Figure **9**A, inset). Calculated wall thickness was 107.83±19.11 μm (N = 6) at 20 mmHg.

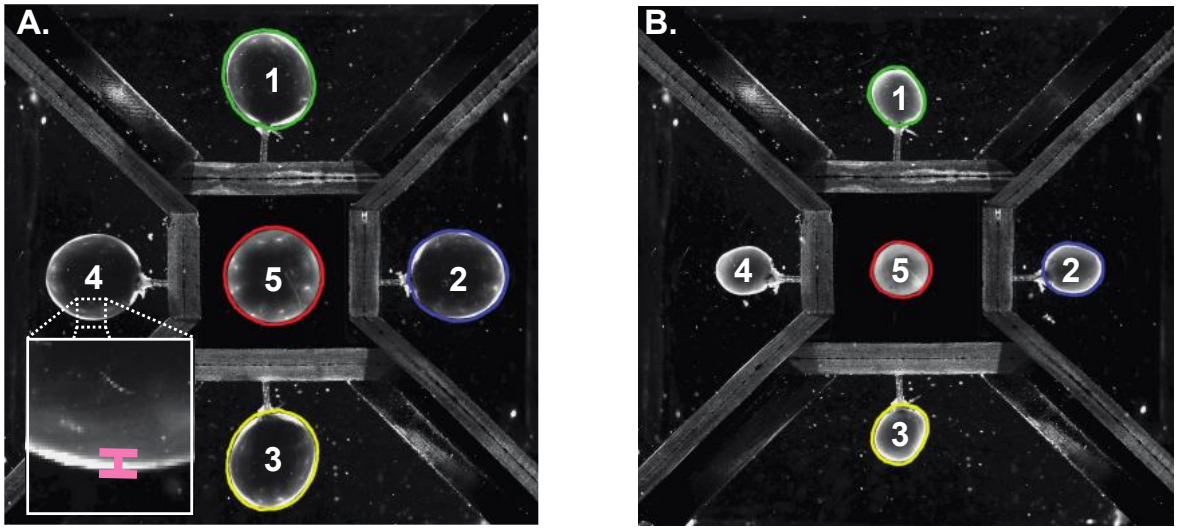

Figure 9 Measurement of planar areas and wall thickness from PRIM images of a full and empty urinary bladder. (A) Starting with the full bladder image, perimeters at the of each section were drawn and the enclosed area was calculated. Wall thickness was estimated as the area of highest contrast at the bladder edge (inset). (B) The area of each section was again calculated from the empty bladder image as filling began.

The bladder was next modeled as an ellipsoidal vessel. The area of section 5 was modeled as a circle of equivalent area with radius r_c. The average area of sections 1 – 4 were then modeled as an ellipse of equivalent area with radii r_c and r_e.The hollow ellipsoid model was formed by the intersection of the circle with radius r_c and an ellipse with radii r_c and r_e (Figure **10**A).

The outer volume of the full bladder (v_o) was calculated as the volume of an ellipsoid with radii r_c and r_e:

$$v_o = \frac{4}{3}\pi\, {r_c}^2 r_e \qquad \text{Eq. 1}$$

Inner full bladder volume (v_i) was calculated as the volume of an ellipsoid with radii less wall thickness, as*:*

$$v_i = \frac{4}{3}\pi(r_c - t)^2(r_e - t) \qquad \text{Eq. 2}$$

Thus, bladder wall volume (v_w) was the difference between outer and inner bladder volumes, calculated as:

$$v_w = v_o - v_i \qquad \text{Eq. 3}$$

Residual volume (v_{res}) was also calculated as the difference between inner volume of the full bladder and infused volume (v_{inf}):

$$v_{res} = v_i - v_{inf} \qquad \text{Eq. 4}$$

Note that the value of v_{res} is constant throughout the test as well as the analysis.

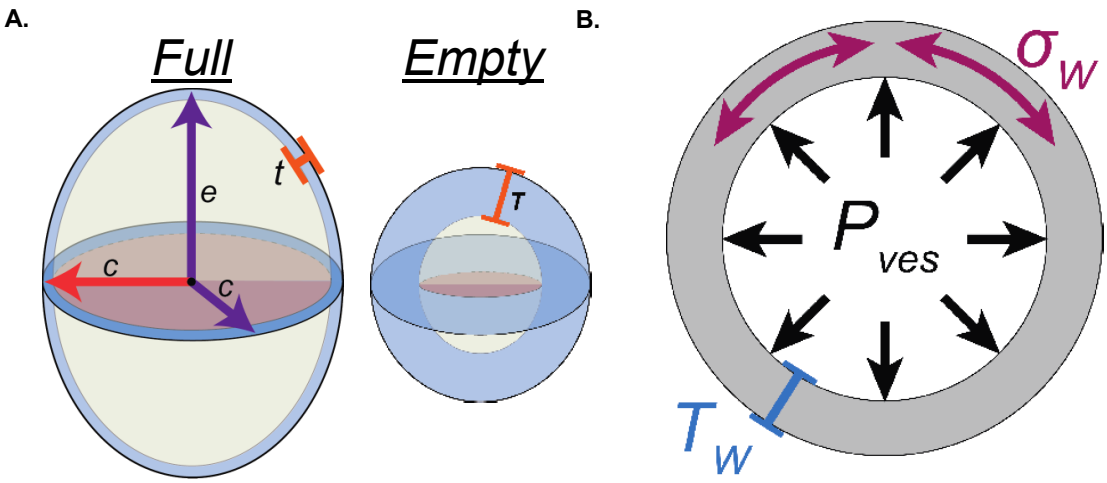

Figure 10 Urinary bladder internal volume, external volume, and wall volume for Cauchy stress calculations. (A, left) The internal and external volumes of the full bladder were modeled as ellipsoidal shells with thickness *t*, comprised of an intersecting circle (pink) of radius *c* (red) and an ellipse (yellow) with radii *c* and *e* (purple). The circle was equal in area to the area of section 5 (*See Figure 9*). The ellipse was equal in area to the average area of sections 1–4. Radii of internal volume were calculated by subtracting wall thickness. The difference between these two volumes was the volume of the bladder wall itself (blue). (A, right) Because wall volume is conserved, external volume of the empty bladder and the volume of the bladder wall were used to derive wall thickness when empty (*T*). (B) Wall stress (σ_W) was calculated by considering the bladder to be a thick-walled (T_W) isochoric sphere that undergoes isotropic deformation as intravesical pressure (P_{ves}) increases as the bladder fills.

This procedure could not be replicated to estimate the wall thickness in the empty bladder due to the opacity of the tissue. For this reason, wall thickness in an empty bladder was estimated by assuming that the bladder was undergoing isochoric deformation [133, 134, 144, 152]. Thus, bladder wall thickness when empty (T) was again calculated using equations 1 and 2. Circular (R_c) and elliptical (R_e) radii of the empty (0 mmHg) bladder were derived from sections 1 – 5 of PRIM images immediately prior to the start of filling (Figure 9B). Outer bladder wall volume when empty (V_o) was calculated as:

$$V_o = \frac{4}{3}\pi {R_c}^2 R_e \qquad \text{Eq. 5}$$

Due to the hypothesis of isochoric deformation, the volume of the bladder wall must be conserved throughout pressurization; therefore, $v_{wall} = V_{wall}$. The inner bladder volume can be calculated as:

$$V_o - v_{wall} = \frac{4}{3}\pi (R_c - T)^2 (R_e - T) \qquad \text{Eq. 6}$$

This allows us to calculate the thickness of the empty bladder t as the real, positive solution to the third-order quadratic equation:

$$T^3 + (-2R_c - R_e)T^2 + \left({R_c}^2 + 2R_c R_e\right)T - {R_c}^2 R_e + \frac{3}{4\pi}(V_o - v_{wall}) = 0 \qquad \text{Eq. 7}$$

As a means of validating the wall thickness measurements, the residual volume when empty (V_{res}) was calculated as above by subtracting V_o from v_{wall} and comparing this value to v_{res} calculated in Eq. 4. If these values were within ±10% of one another, we considered the wall thickness measurements valid. Two bladders were also used to validate thickness measurements using confocal microscopy (Figure **11**. After recording in the PRIM system to a maximum pressure of 25 mmHg, the bladder was emptied, removed from the cannula, and incubated with

10 µM wortmannin and 5µM Calcein stain (Thermo Fisher, USA). The bladder was then cannulated again, and Z stack images (1 µm thickness) were recorded using confocal microscopy. Error in bladder thickness was 1.57% and 3.25%, respectively.

The accuracy of our measurement methodology and mirror alignment was tested using two model spheres (10 mm diameter and 16 mm diameter). Spheres were placed on the cannula and imaged in both the presence and absence of buffer in the PRIM chamber. Dimensions were then calculated using the above methodology and compared to the known spherical volume. In the absence of buffer, the error in calculated volume was 3.43% and 3.38% for the 10 mm and 16 mm spheres, respectively. In the presence of liquid, the error in calculated volume was 1.41% and 0.98% for the 10 mm and 16 mm spheres, respectively.

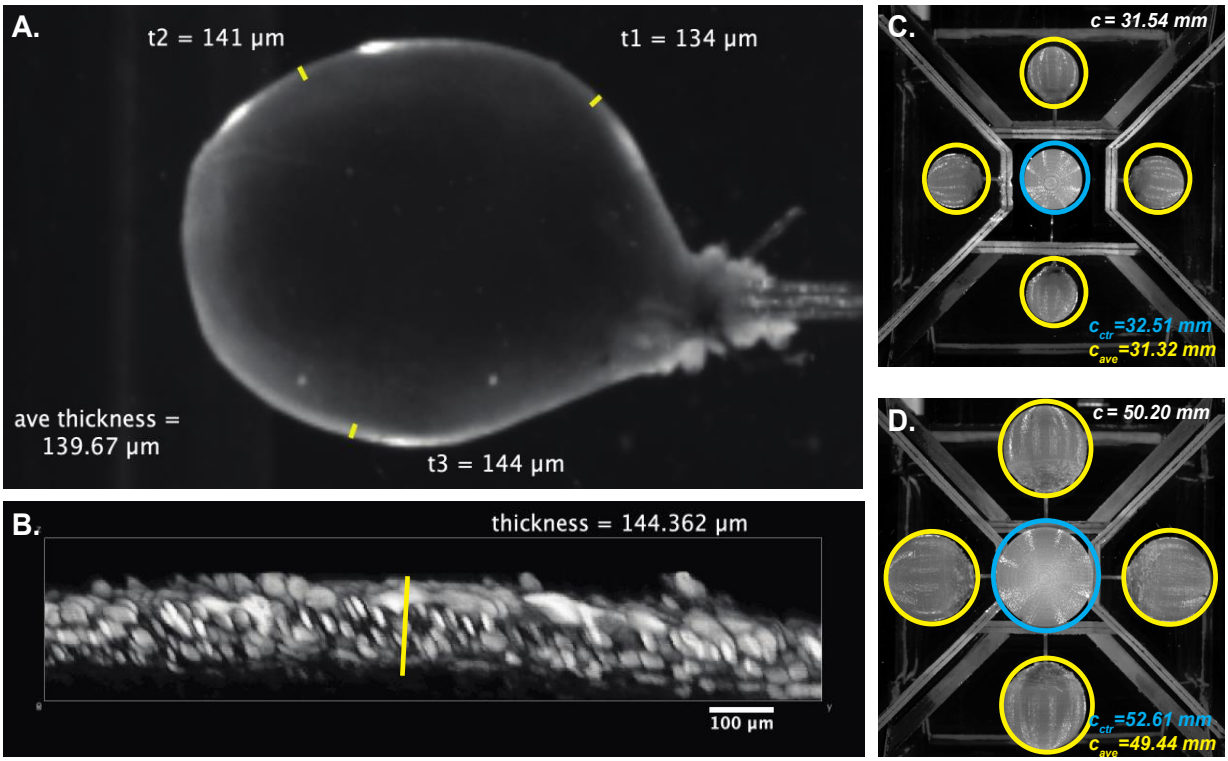

Figure 11 Validation of thickness measurements. (A) Representative PRIM image of a full bladder (25 mmHg). Wall thickness was measured as described at three places across the bladder wall. (B) 3D reconstruction of confocal Z stacks of the same bladder, again at 25 mmHg. (C and D) PRIM images of 3D printed spheres with diameter of 10 mm (C) or 16 mm (D). Actual (white) and calculated (yellow/cyan) circumferences are noted in each image.

3.5 Spherical Cauchy Stress Calculation

Mechanical forces acting on the bladder wall were calculated by first modeling the bladder to be a 3-dimensional pressurized spherical vessel made of elastic material (Figure 10B), similar to previous descriptions [144]. Radius (ρ) was calculated for any given value of pressure by modeling the bladder as a sphere equal in inner volume to the sum of the residual volume (v_{res}) and infused volume (V_{inf}) at each value of pressure. Thus, the radius (ρ) was calculated as:

$$\rho = \sqrt[3]{\frac{3(V_{inf}+V_{res})}{4\pi}} \quad \text{Eq. 8}$$

Stretch (λ) was used as a measure of deformation and was calculated as the ratio of the current radius by the undeformed (empty) radius:

$$\lambda = \rho / R \quad \text{Eq. 9}$$

Lastly, we used the measurements derived above to calculate Cauchy stress during bladder filling:

$$\sigma_W = \frac{p_{ves} \cdot \rho}{2 \cdot t'} \quad \text{Eq. 10}$$

Where p_{ves} is intravesical pressure, ρ is current spherical radius, and $t' = T/\lambda^2$ is wall thickness in the current configuration and how it relates to the initial thickness (T) due to the assumption of isochoricity. We assume that the thickness in the reference configuration is equal to that calculated using Eq. (7). Stress and stretch values were then plotted for each time point during *ex vivo* bladder filling.

3.6 Biomechanical Metrics

These data were also used to derive biomechanical metrics, as described previously [153, 154]. Briefly, we define E_{low} and E_{high} as the slope of the spherical stress-stretch curve for low and high values of pressure, respectively. We identified these values as the slope of the linear fitting

corresponding to the highest R^2, when fitting the first (E_{low}) or last (E_{high}) n points of the curves (where $5 \leq n \leq n_{tot}$). We also evaluated linearized stiffnesses as the slope of the stress-stretch curve for three physiologically relevant values of pressure: *in vivo* filling (5 mmHg), initiation of voiding (10 mmHg), and maximum filling (20 mmHg). The corresponding linearized stiffnesses (E_5, E_{10}, E_{20}) were calculated as follows: first, for each experimental dataset, we identified the specific pressure ± 2 mmHg, as well as the corresponding filling volumes (except for maximum filling pressure, where we considered the only the lower boundary of the interval). Then, we calculated the values of spherical stress and stretch using Eqns. (9-10) and, finally, we performed a linear fitting. The slope of the linear fitting represented the corresponding linearized stiffness.

3.7 Statistics

Statistical significance between groups was established using a two-tailed, paired Student's *t*-test ($\alpha = 0.05$). One-way ANOVA was used to determine if the means of three independent outcomes were significant when compared ($\alpha = 0.05$) followed by Tukey's post hoc analysis to compare individual means. Calculations were performed using Microsoft Excel or GraphPad Prism 9.5 (GraphPad Software, San Diego, CA). Values are expressed as means ± SEM. Differences with *P* values <0.05 were considered statistically significant.

4. RESULTS

4.1 Pressure-Volume Relationships

Generally, bladder filling consists of 4 phases, three of which are present in *ex vivo* bladder experiments [151, 155, 156]. An initial increase in pressure is then followed by a sustained period, during which pressure increases minimally as intravesical volume increases ("filling phase"). This is then followed by a rapid increase in pressure as maximum capacity was reached. Using C57Bl/6 mouse bladders, we measured the pressure-volume relationship during *ex vivo* filling (Figure 12). Each trace had a tri-phasic shape typical of *ex vivo* bladder filling (Figure 12 A). The pressures and volumes at which these phases occurred, however, varied substantially between bladders. This distorted the average pressure-volume relationship of these experiments (Figure 12 B). "Compliance" is also often considered clinically as a measure of bladder function, wherein the change in volume per change in pressure is noted during filling [156]. Because measures of pressure and volume alone cannot distinguish between geometric stiffness mechanical stiffness, differences in tissue composition, bladder size, or bladder wall thickness skew compliance calculations and are thus not representative of the actual mechanical properties of the bladder wall (Figure 12 C).

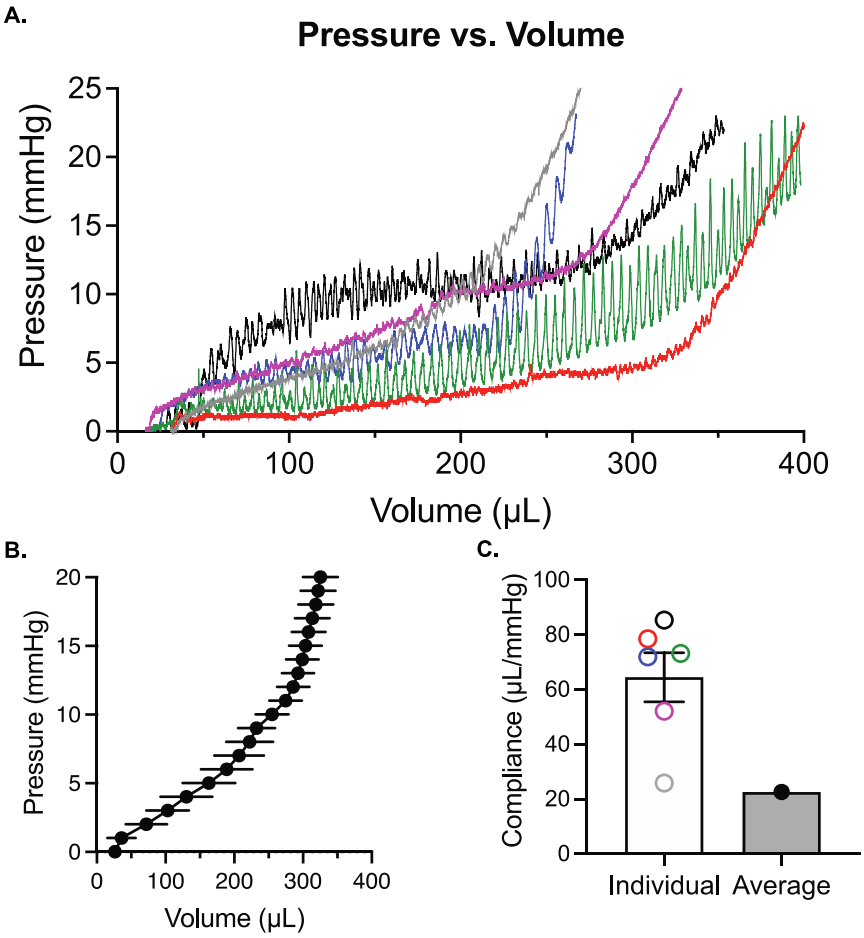

Figure 12 Pressure vs. volume comparisons between bladders is skewed by bladder wall geometry. (A) Graphs of pressure vs. volume for a group of male mouse urinary bladders of similar ages. (B) Summary graphs showing average pressure vs. volume. (C) Compliance measured in this way cannot distinguish between geometric stiffness and material stiffness; thus the compliance of the average curve appears almost 3 times stiffer than the mean of the individual curves. Circle color matches the trace from which it was calculated. Data shown as mean ± SEM. N=6.

4.2 Stress-Stretch Relationships

Using the PRIM System, we were able to use bladder geometry, infused volume, and intravesical pressure to measure the biomechanical characteristics of the bladder wall in terms of spherical stress *versus* stretch (Figure 13). Because changes in initial geometry and thickness of the bladder are included in calculations of stress and stretch, the mechanical properties of the bladder wall can be calculated and compared at any time during filling. Differences in compliance are indicated by rightward shifts in the stress-stretch curve. Thus, the least compliant bladder is shown in black whilst the most compliant bladder is in green.

4.3 Comparing Compliance Measurements from Pressure-Volume vs. Stress-Stretch

To exemplify the benefits of including bladder geometry when measuring bladder wall biomechanics, Figure 14 presents a data set where different conclusions regarding bladder wall compliance can be made when considering clinical compliance vs. mechanical compliance. In Figure 14A, clinical compliance ($\Delta V/\Delta P$) is measured as 28.83 µL/mmHg for bladder 1 *versus* 48.25 µL/mmHg for bladder 2. Thus, the conclusion would be that bladder 2 was more compliant than bladder 1 given the greater change in volume per increase in pressure. If geometric characteristics of the bladder are used to calculate mechanical stress and stretch during filling, it becomes apparent that bladder 2 is far more distensible than bladder 1. So, while the capacity of Bladder 2 is larger than Bladder 1, its wall is actually significantly stiffer. Thus, calculating bladder compliance in terms of stress and stretch considers not only bladder capacity, but also the thickness and makeup of the wall itself.

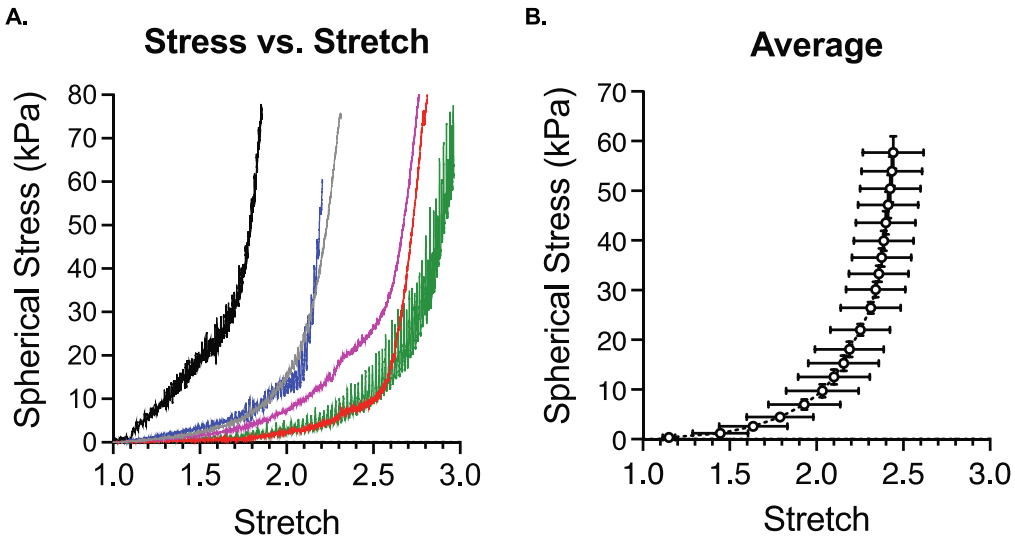

Figure 13 The stress vs. stretch relationship accurately models the biomechanical properties of the bladder wall during all stages of filling by accounting for bladder wall geometry. (A) Graphs of stress vs. stretch for the same group of male mouse urinary bladders as used in Figure 4. (B) Summary graphs showing average stress vs. stretch at each whole pressure value (1-20 mmHg). Bladders with the most spherical stress per stretch have the lowest compliance. Data are shown as mean ± SEM. N = 6.

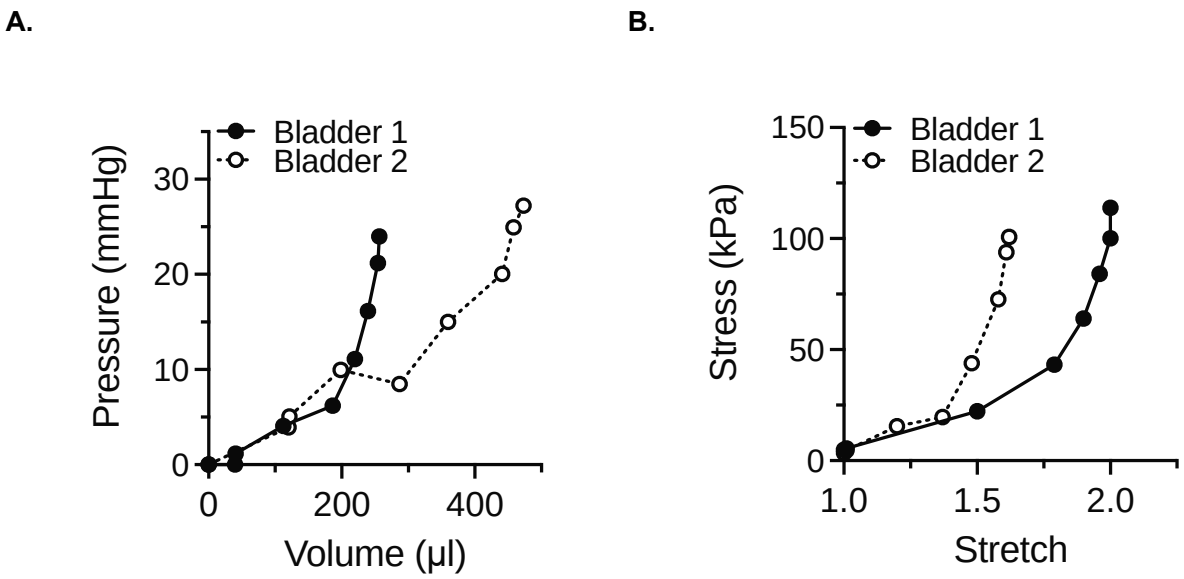

Figure 14 Pressure vs. volume curves can lead to false conclusions regarding bladder wall mechanical stiffness. Pressure-volume (A) and stress-stretch (B) curves for the same two bladders. After accounting for wall volume, bladder 1 is actually more compliant than Bladder 2.

4.4 Modeling Bladder Wall Biomechanics from PRIM Data

Stress is dominated by elastin and uncoiling of collagen fibers early in filling and by the mechanics of the straightened collagen fibers late in filling [151, 155]. In the transition region, tissue mechanics are dominated by the microstructure of uncoiling collagen fibers [154]. Biomechanical metrics can be derived from the slope of the linear fit of the stress-stretch relationship early in filling (E_{low}; low pressure stiffness) and late in filling (E_{high}; highest pressure stiffness), which quantify the purely elastic behavior of the bladder wall and its constituents. The intersection of the linear fits identified by E_{low} and E_{high}, described by the stretch λ_m, represents the mean recruitment stretch of collagen fibers within the bladder wall. When preforming a paired comparison between the values of stiffness evaluated at low and high pressures for each sample, we find that the bladder wall stiffness is significantly greater at high pressures vs. low (Figure 15).

We also evaluated localized stiffness for three values of pressure: 5 mmHg, 10 mmHg, and 20 mmHg. These three specific values were chosen because they represent three physiologically significant conditions in the micturition cycle, *in vivo* filling, initiation of voiding, and maximum filling, respectively. When performing a paired comparison, we find that the localized stiffness is significantly increasing at each pressure step we evaluated. This suggests the mechanical environment of the wall is progressively getting stiffer during filling. Taken together, these quantifications strengthen the proposition that a single parameter, such as clinical compliance, is not an accurate representation of the bladder wall mechanics due to the high non-linearity of the bladder tissue. Instead, measures like those presented here can accurately describe the mechanical behavior throughout the filling process.

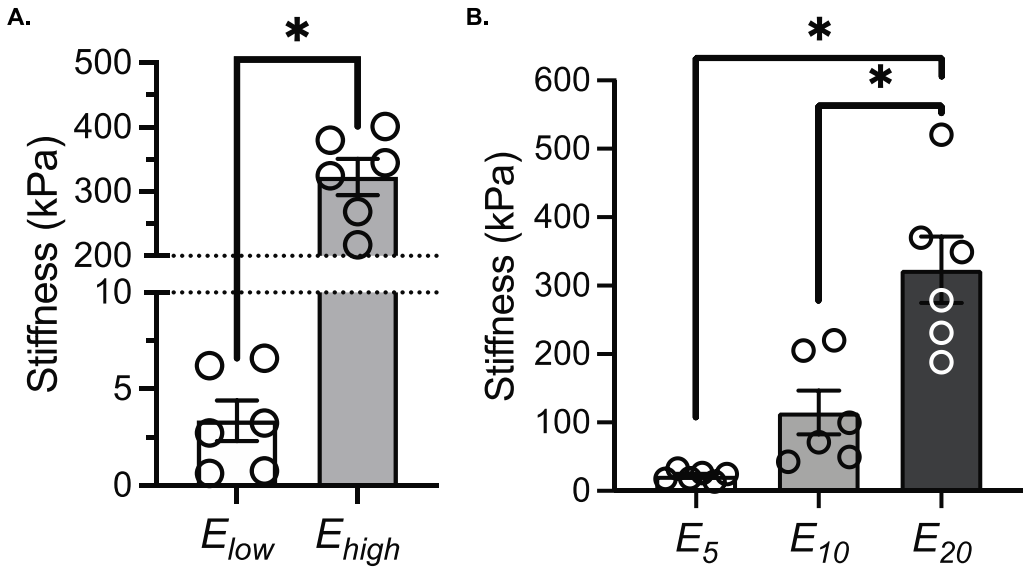

Figure 15 Bladder wall stiffness increases nonlinearly during bladder filling. (A) Average mechanical parameters at low and high pressures during filling. (B) Average mechanical parameters at 5 mmHg *(E_5)*, 10 mmHg *(E_{10})* and 20 mmHg *(E_{20})* during filling. Bladder stiffness significantly increases in a nonlinear fashion as pressure increases during *ex vivo* bladder filling. * = $p<0.05$ by paired t-test (A) or one-way repeated measures ANOVA (B). N=6.

5. DISCUSSION

Traditionally, bladder compliance was measured experimentally as the change in volume for a given change in infused pressure, due in part to the inability to reliably calculate the volume of the bladder wall without ultrasound imaging [143]. Measuring compliance in this manner erroneously makes two key assumptions: first, it assumes that all healthy bladders are the composed of similar proportions of cells and matrix and thus have a similar elastic modulus. Second, it assumes that the total volume and gross geometry of the bladder wall is the same. Because the measures of compliance are also taken at very low pressures as compared to total capacity, "compliance" is easily skewed by the size of the bladder overall. For example, a large bladder with a thin, stiff wall could appear to be highly compliant if only measuring at the lower portion of physiological filling pressures. Also, the mechanical behavior of the bladder wall clearly is nonlinear: intravesical pressure changes very little for very large filling volumes but increases exponentially thereafter [145]. To know the relationship between stress, stretch, and bladder filling, new methods are required that accurately measure the volume of the bladder wall itself to calculate stress and compliance. Because the PRIM System allows rapid and accurate measurements of bladder shape, internal volume, and wall volume over the entirety of bladder filling (See *Methods*) while also capturing frame-locked intravesical pressure recordings, compliance can instead be reported as actual engineering metrics (Cauchy stress/stretch) instead of $\Delta V/\Delta P$.

Previous work has used similar methods to identify bladder wall mechanical properties in humans *in vivo* using a combination of cystometry and ultrasound imaging [143, 157]. These studies highlight the value and importance that this new type of compliance measurement can have with regard to understanding urinary bladder function. *In vivo*, however, bladder wall

geometry was only captured in the sagittal plane due to limitations of ultrasound imaging and sampling rate. This required assumptions to be made with regard to the isotropy (or anisotropy) of the bladder during filling as changes to geometry in the transverse plane were unknown. This technique also has limited applicability to research models of bladder dysfunction due to the highly technical nature of ultrasound imaging, the expense of such devices, and the relative size of rodent bladders as compared to humans. The PRIM System is able to bridge this gap: our system can be used to make similar measurements quickly, accurately, and inexpensively in *ex vivo* rodent models that can be used to validate the measurements made in humans and the assumptions required therein. Our methods could also determine the ideal plane from which to measure human bladder mechanical properties using the aforementioned techniques. The *ex vivo* nature of the PRIM System also allows measurements beyond the physiological range of pressures and filling rates, as was conducted herein. Our intention in doing so was threefold: first it allowed us to correlate our mechanical findings to prior literature on *ex vivo* bladder filling and *in vivo* cystometry in mice [151]. Second, by moving to supraphysiological pressures we could also assess the previously proposed model of collagen fiber recruitment made from uniaxial stress/stretch measurements [153, 158] and apply it to the intact bladder configuration. Third, we can now address the interrelationship between ECM, bladder smooth muscle cell structure, and bladder muscle tone/contractility.

In terms of the calculations of the mechanical properties of the bladder wall, our methods do depart from those used to measure mechanical properties of the bladder *in vivo*. Previous calculations required that bladder wall thickness be accurately measured at every pressure value during filling [144, 159]. Our bladder wall stress calculations consider both the initial thickness and the relative change in radius during filling and not just the surface area of the vessel. Thus,

only a single measurement of wall volume is required to accurately calculate stress and stretch at all filling pressures. Due to technical limitations of older imaging techniques, previous investigations also determined the mechanical properties of the whole bladder by assuming that the cross-sectional area of a single plane is representative of all sections of a spherical vessel. While this may be true for some bladders, even a small deviation from the actual central planes can markedly skew the calculated Cauchy stress. With the development of the PRIM System, we are able to accurately measure and calculate the entire wall volume of the bladder without inference; thus, the radius and thickness we use to estimate Cauchy stress better describes the behavior of the entire bladder wall. We also believe this is more representative of the complete mechanical properties of the bladder wall over the entirety of filling and emptying given the marked change in wall thickness that occurs. This allowed us to quantify how the linearized stiffness is significantly different when evaluated for different values of pressure, even when performing a paired comparison for the same samples. This highlights how a single mechanical parameter such as compliance is inadequate to capture the complex mechanical behavior of the bladder wall.

Our calculations, however, are also not without their assumptions that must be considered. We, and others [144, 159], assumed the bladder wall to be a homogeneous material that undergoes and isotropic deformation during filling. The anatomical makeup of the bladder wall is clearly non-homogenous; smooth muscle cells, blood vessels, nerves, and urothelial cells exist heterogeneously throughout the bladder wall [160]. Multiple studies have examined the active and passive behavior of the bladder wall using similar calculations (reviewed in [134]), and it is important to consider that regional differences in mechanical properties do occur [158]. Nonetheless, given the paucity of information as the biomechanical properties of the intact

bladder wall during filling, the value of the measurements included here are not diminished and serve as a springboard for more in-depth measurements in the future. We also assume the bladder to be a spherical vessel undergoing isotropic deformation during filling. The first of these assumptions, sphericity, was made for simplicity: in this initial study, we were less curious as to the specific stresses relative to the angular deformation and more curious as to the average stresses experienced at any single point within the bladder wall at a given moment. While the spherical assumption made for the stress analysis is an approximation, it is a necessary one. This is due to the lack of automatized quantification of the geometry throughout the filling test, having manual quantification of all diameters would introduce an operator-dependent factor that the current analysis minimizes. Furthermore, the spherical assumption has been consistently used in the past when modeling the urinary bladder [144, 159, 161, 162]. Given the data collected, we are able to calculate stretch and stress as it varies with any polar angle during filling as done previously [133] and intend to do so in future studies. The second assumption, isotropy, is yet another current limitation we can overcome in future studies given the data we collect in the PRIM System. The bladder wall mechanical properties are most often measured using uniaxial testing paradigms best suited for isotropic materials, even though the wall itself is known to be anisotropic [152]. The results presented here are intended to serve as a comparator by which our methodologies and results can be related to those gleaned from uniaxial testing measurements. Because our samples are completely intact during the entirely of filling and 5 image planes are available for each data point, assessment of both anisotropy and angular deformation during filling is obtainable.

In conclusion, we developed the PRIM System in order to measure the mechanical properties of the bladder wall over the entirety of bladder filling since the information derived from pressure-

volume curves is incomplete. Using this relatively simple imaging technique, we are able to combine measurements of intravesical pressure and infused volume with wall geometry and wall thickness to calculate Cauchy stress and stretch during *ex vivo* bladder filling. Thus, the PRIM system offers unprecedented insights into the relationship between stress, stretch, and contractility that govern normal bladder function. Further, this technology can be used to measure the same properties in other hollow organs, such as uterus, gut, and stomach, and also be used to generate dynamic four-dimensional models of changes in shape of these organs with high temporal resolution. The PRIM System is thus a promising new tool for understanding how muscle contractions coordinate across an entire organ and the mechanical forces that accompany those contractions.

COMPOUND 48/80 INCREASES MURINE BLADDER WALL COMPLIANCE INDEPENDENT OF MAST CELLS

Modified from: Saxena P, Broemer E, Herrera GM, Mingin GC, Roccabianca S, Tykocki NR. Compound 48/80 increases murine bladder wall compliance independent of mast cells. Sci Rep. 2023 Jan 12;13(1):625. doi: 10.1038/s41598-023-27897-6. PMID: 36635439; PMCID: PMC9837046.

1. ABSTRACT

A balance between stiffness and compliance is essential to normal bladder function, and changes in the mechanical properties of the bladder wall occur in many bladder pathologies. These changes are often associated with the release of basic secretagogues that in turn drive the release of inflammatory mediators from mast cells. Mast cell degranulation by basic secretagogues is thought to occur by activating an orphan receptor, Mas-related G protein-coupled receptor B2 (Mrgprb2). We explored the effects of the putative mast cell degranulator and Mrgprb2 agonist Compound 48/80 on urinary bladder wall mechanical compliance, smooth muscle contractility, and urodynamics, and if these effects were mast cell dependent. In wild-type mice, Mrgprb2 receptor mRNA was expressed in both the urothelium and smooth muscle layers. Intravesical instillation of Compound 48/80 decreased intermicturition interval and void volume, indicative of bladder overactivity. Compound 48/80 also increased bladder compliance while simultaneously increasing the amplitude and leading slope of transient pressure events during *ex vivo* filling and these effects were inhibited by the Mrgprb2 antagonist QWF. Surprisingly, all effects of Compound 48/80 persisted in mast cell-deficient mice, suggesting these effects were independent of mast cells. These findings suggest that Compound 48/80 degrades extracellular matrix and increases urinary bladder smooth muscle excitability through activation of Mrgprb2 receptors located outside of mast cells. Thus, the pharmacology and physiology of Mrgprb2 in the urinary bladder is of potential interest and importance in terms of treating lower urinary tract dysfunction.

2. INTRODUCTION

The urinary bladder is a highly distensible organ and is typically capable of holding a relatively large amount of urine as it undergoes deformation during filling [163, 164]. Proper bladder function (i.e., storage and periodic expulsion of urine) is attributed to a balance between two mechanical properties of bladder tissue itself: stiffness and elasticity [92, 165]. Bladder wall stiffness refers to the extent to which bladder wall can resist deformation as it fills [166], while bladder wall elasticity refers to the ability of the wall to return to its original shape and size after deformation [167]. Both properties depend on the expression, interaction, and interconnection between extracellular matrix (ECM) and urinary bladder smooth muscle (UBSM) cells within the bladder wall [69, 168, 169].

The bladder ECM consists primarily of collagen and elastin fibers, which change in orientation and conformation to accommodate increasing urine volumes during filling [5, 71]. Both Type I and Type III collagen fibers are widely distributed in the bladder where they surround the smooth muscle cells and provide tensile strength to the bladder wall through complex coiling [5, 68]. Elastic fibers present in all layers of the bladder wall allow the bladder to recoil to its original shape after emptying [170, 171]. Interactions between the UBSM and the ECM control both basal smooth muscle tone as well as non-voiding transient pressure events that drive the majority of sensory outflow to the central nervous system [35]. Because the stiffness and elasticity of the bladder wall tissue is imparted by properties of both UBSM and ECM, altered muscle tone and collagen content are present in many bladder pathologies.

Lower urinary tract symptoms (LUTS), including frequency, urgency and urge incontinence, are often associated with both an alteration in clinical compliance as well as bladder inflammation [83, 172, 173]. The pathogenesis of inflammatory bladder remodeling is also associated with the

degranulation of mast cells present within the bladder wall [27, 174]. Basic secretagogues, such as Substance P and Compound 48/80, can rapidly degranulate these mast cells to secrete inflammatory mediators [175]. These cationic compounds are thought to initiate IgE-independent mast cell degranulation by binding to the orphan receptor Mas-related G protein-coupled receptor-B2 (Mrgprb2) [176]. Mouse Mrgprb2 receptors and their human ortholog (MRGPRX2) are implicated in nociception and inflammation in other organ systems [177]. However, function of Mrgprb2 in the bladder is unexplored.

In this study, we used Compound 48/80 to determine if bladder mast cell activation altered bladder wall mechanical compliance during filling. We discovered that Compound 48/80 increases smooth muscle contractility while paradoxically increasing compliance in C57Bl/6J mice. The effects of Compound 48/80 on wall compliance and contractility were inhibited by the Mrgprb2 antagonist QWF, suggesting the effects are indeed mediated by Mrgprb2 activation. Surprisingly, these effects also persisted in mast cell-deficient (*C-kit*$^{W\text{-}sh}$) mice, suggesting Mrgprb2 is expressed outside of mast cells in the urinary bladder. This conclusion is further reinforced by our finding that Mrgprb2 mRNA expression was similar in bladders from mast cell deficient as well as wild-type mice. Collectively, our results suggest that Compound 48/80 increases bladder wall compliance and UBSM excitability through activation of Mrgprb2 receptors expressed outside of mast cells. Mrgprb2 receptors may thus have an important physiological and pathological function in the urinary bladder.

3. MATERIALS AND METHODS

3.1. Animal Care and Use

All animal procedures followed institutional guidelines and were approved by the Institutional Animal Care and Use Committees (IACUC) of Michigan State University (NIH Assurance D16-0054). All procedures followed the recommendations in the ARRIVE guidelines. Male C57Bl/6 mice and male mast cell-deficient (*C-kit$^{W\text{-}sh}$*) mice (9-12 weeks old; Jackson Laboratory, Bar Harbor, ME USA) were group housed in a temperature- and humidity-controlled environment with a 12-hour light/dark cycle and *ad libitum* access to standard chow and water. Mice were euthanized by intraperitoneal injection of pentobarbital (>150mg/kg) followed by decapitation prior to all experimental procedures.

3.2. Ex vivo whole bladder filling using the Pentaplanar Reflected Image Macroscopy (PRIM) System

Urinary bladders were dissected and placed in ice-cold Ca^{2+}-free HEPES dissection buffer containing (in mM): NaCl (134), KCl (6), $MgCl_2$ (1.2), HEPES (10) and glucose (7); pH=7.4. Tissues were cleaned of connective tissue, pinned in a dissecting dish, and ureters tied off with 4-0 suture. The bladder was then cannulated through the urethra in the Pentaplanar Reflected Image Macroscopy (PRIM) chamber. The PRIM system consists of an imaging chamber (Figure 6A) with a curved cannula and 4 mirrors fixed at 45° angles. A digital camera (DMK33UX250; The Imaging Source, Charlotte NC USA) was mounted above the chamber along with LED lighting to illuminate the sample. When properly aligned, 5 visual planes were in focus and able to be recorded in a single image (Figure 6B). Images and pressure readings were recorded simultaneously at a rate of 10 Hz. Intravesical pressure was recorded *via* an inline pressure transducer (DYNJTRANSMF; Medline, Northfield, IL, USA) connected to the cannula.

Throughout the experiment, the PRIM chamber was recirculated with warm (37°C) bicarbonate-buffered physiological salt solution (PSS) consisting of (mM): NaCl (119), $NaHCO_3$ (24), KCl (4.7), KH_2PO_4 (1.2), $MgCl_2$ (1.2), and $CaCl_2$ (2) using a recirculating peristaltic pump. PSS was bubbled throughout the duration of the experiment with biological atmosphere gas (25% O_2, 5% CO_2, 70% N_2) to maintain pH and tissue oxygenation. Bladders were then filled through the cannula at a rate of 30 µL/min using a syringe pump until a maximum pressure of 25 mmHg was reached. To increase contrast, the infused PSS was mixed with purple food coloring. After reaching 25 mmHg, the bladder was then emptied and allowed to re-equilibrate at atmospheric pressure for 5-10 minutes before the next fill. Each bladder underwent 3 equilibration fills prior to 3 experimental fills. To account for variability, comparisons were made between the same three consecutive fills in each bladder: (1) the antepenultimate fill and empty cycle (control); (2) the penultimate fill and empty cycle in presence of vehicle or inhibitor; and (3) the final fill and empty cycle after the addition of agonist. As previously described, all drugs and their respective vehicles were incubated for 30 min prior to filling cycles.[35]

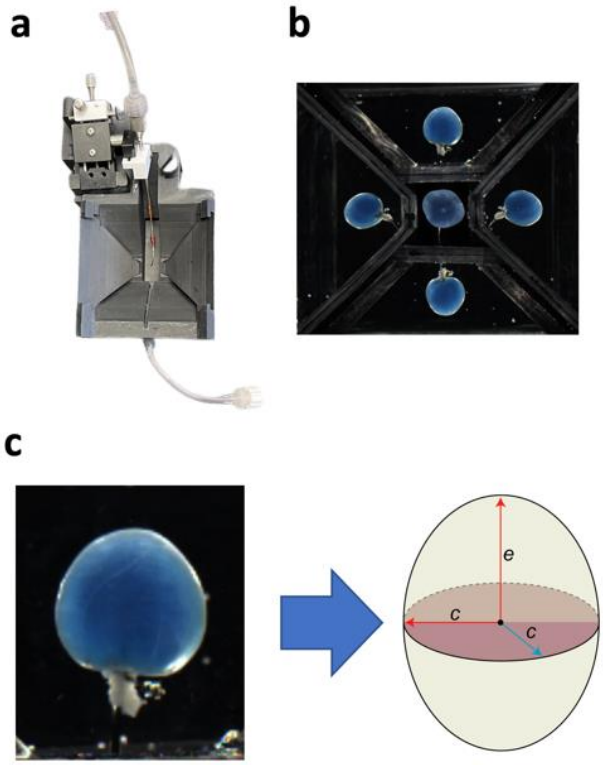

Figure 16 Pentaplanar Reflected Image Macroscopy system. **A**, Top view of Novel pentaplanar reflected image macroscopy (PRIM) system chamber. The mirrors were removed to make the cannula visible. **B**, Single frame of *ex vivo* bladder filling video recording, showing all 5 visual planes recorded in the PRIM chamber. These images were used to calculate area and thickness of the bladder wall. **C**, the bladder was modeled as an ellipsoid with radii c and e. This assumption was made to accurately calculate the geometrical parameters and bladder wall volume used for later determination of stress and stretch during filling.

3.3. Calculation of True Wall Compliance

Wall stress is defined as the force per unit cross-sectional area exerted tangential to the wall in response to the outward pressure exerted by the fluid inside the bladder [178]. Wall stretch is defined as a measure of deformation that can be given as change in size of the bladder with reference to its original size [178]. The urinary bladder wall was assumed to be a 3-dimensional elastic system; thus, bladder wall compliance was quantified as wall stress *versus* stretch. Bladder wall area and thickness were derived from the PRIM system images using ImageJ (NIH). These measurements were then used to model the bladder as an ellipsoid of radii c and e (Figure 14C), with constant wall volume and uniform thickness, that behaves as a non-linearly expanding deformable vessel as described previously [133]. For each value of pressure, we evaluated the radius of the sphere of equivalent wall volume to the ellipsoid, and employed the Laplace equation to evaluate the spherical Cauchy stress as:

$$\sigma_w = \frac{P_{\text{ves}} \cdot r}{2 \cdot t}$$

Where P_{ves} is intravesical pressure, and r and t are the radius and thickness of the equivalent sphere in the current configuration (i.e., for $P = P_{\text{ves}}$).

The stretch was used as a measure of deformation and was calculated as:

$$\lambda = \frac{r}{R_i}$$

Where R_i is defined as the radius of the equivalent sphere in the initial configuration (i.e., for $P \leq 1\ mmHg$). Under the assumption of incompressibility [179], we can substitute for the current thickness t with the initial wall thickness (T_i) as:

$$t = \frac{T_i}{\lambda^2}$$

Both stress and stretch were plotted for each time point during *ex vivo* bladder filling. To summarize data from multiple experiments, stress and stretch recordings were first plotted at each corresponding pressure value in 5 mmHg increments (0 – 25 mmHg) using a custom MATLAB (MathWorks; Natick, MA USA) program. The program was also used to calculate wall stiffness (defined as the slope of stress/stretch curve) at 5, 10, and 25 mmHg. All curves belonging to the same group were then averaged for both stress and stretch using GraphPad Prism (GraphPad Software; San Diego, CA USA). Clinical compliance for all groups was also calculated as described previously [128].

3.4. Analysis of Transient Pressure Events

Transient pressure events were measured and analyzed using LabChart Pro (ADInstruments; Sydney, Australia). The transient pressure event amplitude and leading slope were measured for all events occurring over the range of physiological voiding pressures (1-11 mmHg), as described previously [35]. To represent the effects of drug and vehicle, ΔPeak Amplitude and ΔLeading slope were calculated by subtracting their average values after exposure to drug from average control values prior to exposure to drug.

3.5. Quantitative RT-PCR

Unless otherwise noted, all qRT-PCR primers, reagents, and equipment were obtained from Thermo-Fisher Scientific (Waltham, MA USA). Urinary bladders were dissected, cut longitudinally from urethera to dome, pinned *en face*, and denuded of urothelium by blunt dissection. Both urothelium and UBSM layers were saved separately in *RNA Later* for RNA isolation. Total RNA was isolated and purified using RNAeasy Mini Kit for whole tissues (Qiagen; Hilden, Germany) according to the manufacturer's instructions. The yield and purity of the RNA was measured photometrically using a Nanodrop 2000c. A High-Capacity cDNA

Reverse Transcription kit was used to reverse transcribe RNA to first-strand cDNA in a 96-well thermocycler (Applied Biosystems). The yield and purity of resultant cDNA was also measured photometrically using a Nanodrop 2000c. Expression of target mRNAs was measured from each sample by qPCR in the QuantStudio 6 Flex Real-Time PCR System with Taqman Universal PCR Mastermix. Cycle conditions were as follows: 2 minutes at 50°C, 10 minutes at 95°C, 40 cycles of 15 seconds at 95°C and 1 minute at 60°C. Each PCR procedure included a no-template negative control reaction. Expression of *Actb* (Mm02619580_g1), *Acta2* (Mm00725412_s1), *Upk2* (Mm00447665_m1), and *Mrgprb2* (Mm01956240_s1) were measured, using *Actb* as a reference gene.

3.6. Conscious Cystometry

Conscious cystometry was performed as described previously [34]. Briefly, mice were anaesthetized with inhaled isoflurane (1–3% in O_2) and a lower midline abdominal incision was made to expose the urinary bladder. A polyethylene catheter (PE-10) was inserted into the dome of the urinary bladder and secured in place using a purse string suture. The bladder catheter was sealed and routed subcutaneously to the back of the neck, where it was coiled and stored in a skin pouch. Following a 3-day recovery period, the bladder catheter was exteriorized and opened. The animal was placed in a Small Animal Cystometry Lab Station (MED Associates, Georgia, VT USA) for urodynamic measurements. An in-line pressure transducer was connected between the catheter and a syringe pump. Sterile isotonic saline (0.9 % NaCl; room temperature) was continuously infused into the bladder at a rate of 30 μL/min. An analytical balance beneath the wire-bottom animal cage measured void volumes during continuous cystometry. A single cystometrogram (CMG) was defined as the simultaneous recording of intravesical pressure, infused volume, and voided volume during a single filling-voiding cycle. Cystometrograms were

recorded before and after intravesical infusion of Compound 48/80 (50 µg/mL). Data analysis was performed by averaging CMGs recorded from separate mice under the same conditions.

3.7. Drugs and Chemicals

QWF was obtained from Tocris Bioscience (Bristol, UK). Unless otherwise specified, Compound 48/80 and all other reagents were obtained from Sigma-Aldrich (Cleveland, OH, USA).

3.8. Statistical Analysis

For comparison of two samples of equal variance, statistical significance between groups were assessed using two-tailed, paired Student's *t* tests ($\alpha = 0.05$). For multiple sample comparisons of equal variance, ordinary one-way ANOVA was used followed by Tukey's post-hoc analysis to compare individual means. Calculations were performed using Excel (Microsoft Corporation; Redmond, WA, USA) or GraphPad Prism. Values are expressed as mean ± SEM. For clarity, data points from C57Bl/6 mice are represented by circles and *C-Kit*$^{W\text{-}Sh}$ mice are represented by squares in all figures. Comparisons with *P* values <0.05 were considered statistically significant. Asterisks were used to express statistical significance in figures: **P*<0.05 and ***P*<0.01. Exact *P* values are stated in the results. For clarity, "N" represents the number of animals in each group. Multiple replicates from a single animal are not used or reported in this study.

4. RESULTS

4.1. Mas-Related G Protein-Coupled Receptor B2 (Mrgprb2) receptor mRNA is expressed in urinary bladder smooth muscle and urothelium

Quantitative RT-PCR was used to determine *Mrgprb2* mRNA expression in isolated urothelium and smooth muscle tissues from wild-type and *C-kit*$^{W\text{-}sh}$ mice. Both layers expressed *Mrgprb2* mRNA in both animal models. mRNA expression was normalized to β-actin (*Actb*) expression. No significant changes were observed in the mRNA expression of Mrgprb2 in both animal models ($P = 0.44$ and $P = 0.06$ for detrusor and urothelium respectively, N=10, Figure 7) suggesting that Mrgprb2 receptor is present outside of mast cells in the urinary bladder wall. However, *Mrgprb2* mRNA expression is significantly higher in the urothelium in both mouse models ($P = 0.0028$ and $P= 0.0061$ for C57Bl/6 and *C-kit*$^{W\text{-}sh}$ mice respectively).

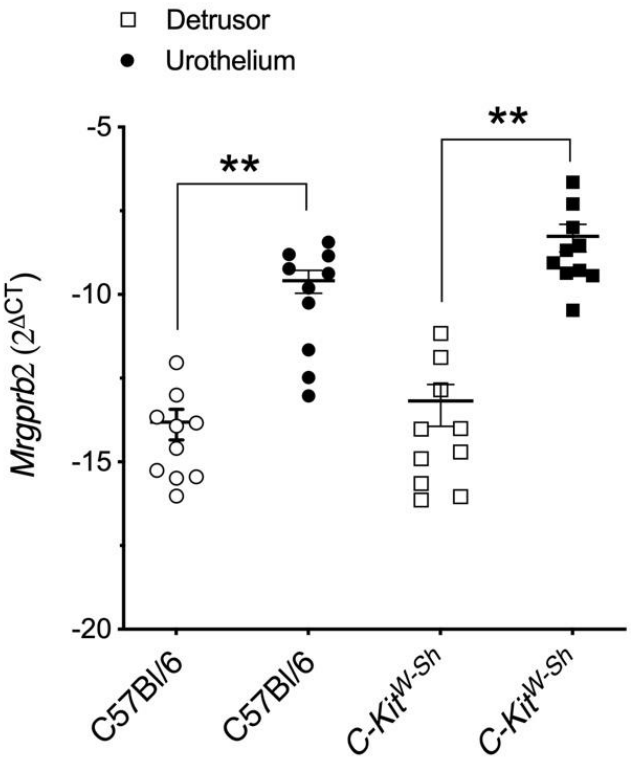

Figure 17 Isolated bladder tissue from both wild-type and mast cell-deficient mice express Mrgprb2 mRNA. Mrgprb2 mRNA expression in the urinary bladder smooth muscle layer and urothelial layer from both C57Bl/6 (N=10) and *C-Kit*$^{W\text{-}Sh}$ mice (N=10), as measured by qRT-PCR. Both mouse models express Mrgprb2 in the bladder in both layers and to a similar extent [$P = 0.442$ and $P = 0.0555$ for detrusor and urothelium respectively (C57Bl/6 *vs.* *C-Kit*$^{W\text{-}Sh}$)]. Mrgprb2 mRNA expression in the urothelium is significantly higher in both mouse models [($P = 0.0028$ and $P = 0.0061$ for C57Bl/6 and *C-Kit*$^{W\text{-}Sh}$ respectively (Detrusor vs. Urothelium)]. Data shown as Mrgprb2 expression relative to the housekeeping gene, ß-actin.

4.2. Effects of Compound 48/80 are Mediated through Mrgprb2

The orphan receptor Mrgprb2 is traditionally believed to be expressed on mast cells, nerve fibers, and keratinocytes, where it mediates pseudo-inflammatory pathways [180]. While traditionally described as an ambiguous mast cell activator, responses to Compound 48/80 and its endogenous analogue Substance P are both mediated by the Mrgprb2 receptor [175, 181]. To investigate the effects of Compound 48/80 on wall compliance, we recorded intravesical pressure and pentaplanar images (Figure 8A) during *ex vivo* whole bladder filling using the Pentaplanar Reflected Image Macroscopy (PRIM) System. These data were then used to calculate bladder wall stress and stretch during filling. Wall compliance rapidly increased after exposure to Compound 48/80 (10 µg/mL), as demonstrated by a rightward shift of the stress-stretch curve (Figure 8B, N=6) and by the significant increase in stretch at 10 mmHg ($P = 0.011$) and 25 mmHg ($P = 0.01$; Figure 8C). Wall stiffness remained unchanged after exposure to Compound 48/80 ($P = 0.91$, $P = 0.58$ and $P = 0.09$ for 5, 10 and 25 mmHg respectively; Figure 8D). To determine if the increase in compliance caused by Compound 48/80 was mediated by Mrgprb2, *ex vivo* bladder filling was next performed in the absence or presence of the Mrgprb2 antagonist QWF (10 µM) (N=6, Figure 8E). Compound 48/80 did not increase wall compliance in the presence of QWF (Figure 8F), nor did it significantly alter stretch ($P = 0.40$, $P = 0.140$ and $P = 0.070$ for 5, 10 and 25 mmHg respectively; Figure 8G) or stiffness ($P = 0.110$, $P = 0.130$ and $P = 0.140$ for 5, 10 and 25 mmHg respectively; Figure 8H) at 5, 10 and 25 mmHg. Neither vehicle nor QWF significantly affected the mechanical properties of the bladder wall in the absence of Compound 48/80. This suggests that increased wall compliance caused by Compound 48/80 is due to Mrgprb2 activation.

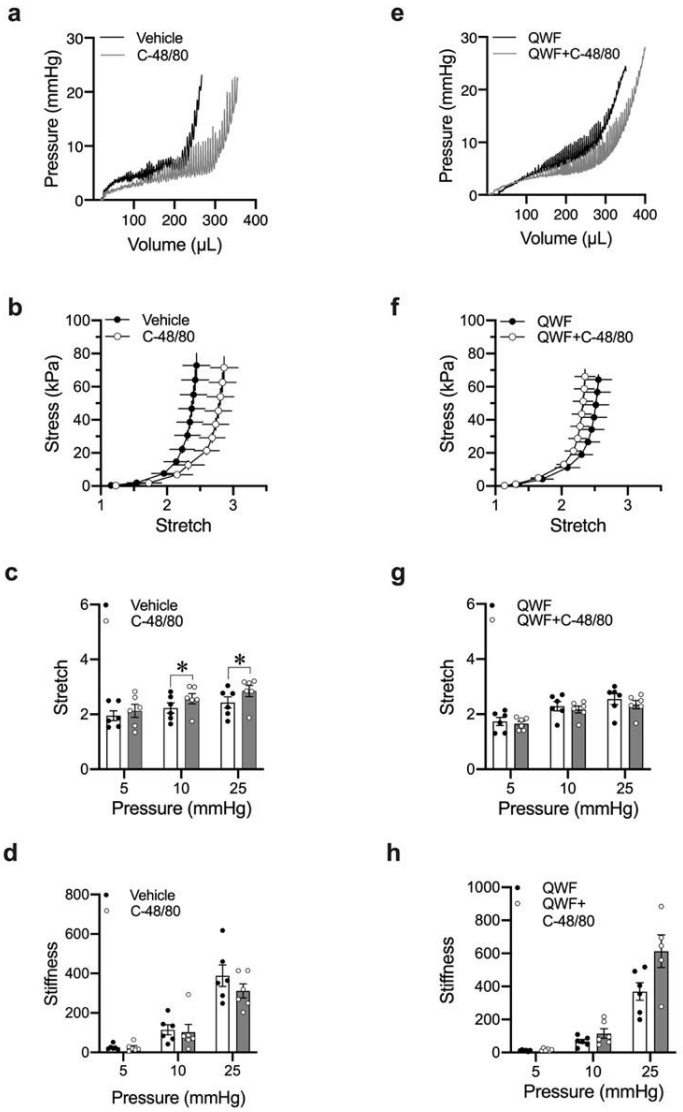

Figure 18 Compound 48/80 increases bladder wall compliance through Mrgprb2 activation. A, Representative pressure-volume trace of ex vivo filling of C57Bl/6 mouse bladders in the absence and presence of the Mrgprb2 agonist Compound 48/80 alone (10 µg/mL). **E**, representative pressure-volume trace after prior exposure to the Mrgprb2 antagonist QWF (10 µM). **B-C**, compliance is increased in the presence of C-48/80 (N=6) signified by the rightward shift of the stress-stretch curve and a significant increase in stretch at 10 (P = 0.01 vehicle *vs.* C-48/80) and 25 mmHg (P = 0.01 vehicle *vs.* C-48/80). **F-G**, the increase in compliance by C-48/80 is blocked by QWF (N=6) signified by the absence of rightward shift of the stress-stretch curve and increase in stretch (P = 0.4, P = 0.14 and P = 0.07 for 5, 10 and 25 mmHg respectively; QWF *vs.* QWF + C-48/80). **D and H**, stiffness is unchanged in both groups. Within the group comparisons were made via two-tailed, paired Student's t-test. "C-48/80": 10 µg/mL Compound 48/80; "QWF": 10 µM QWF.

4.3. Effects of Compound 48/80 on Bladder Compliance are Mast Cell Independent

Mice with the *C-kit*$^{W\text{-}sh}$ mutation do not express mast cells [182]. To determine if Compound 48/80 increases bladder compliance in a mast cell-mediated manner, *ex vivo* filling was again performed in the PRIM system using bladders from mast cell-deficient *C-kit*$^{W\text{-}sh}$ mice (N=6). *C-kit*$^{W\text{-}sh}$ mice showed no significant differences compared to wild-type mice in mechanical compliance, stretch, or stiffness in the absence of Compound 48/80. Compound 48/80 still caused a rightward shift in the stress/stretch curve and increased bladder wall stretch at 5 mmHg (P = 0.010), 10 mmHg (P = 0.006) and 25 mmHg (P = 0.008) (Figure 9A-C). Similar to wild-type mice, stiffness was also unchanged at all pressures (P = 0.960, P = 0.183 and P = 0.958 for 5, 10 and 25 mmHg respectively; Figure 9D). The increase in stretch was prevented by QWF (P = 0.343, P = 0.255 and P = 0.282 at 5, 10 and 25 mmHg respectively, N=4, Figure 9E-G). There was no change in stiffness after prior exposure to QWF (P = 0.124, P = 0.340 and P = 0.293 at 5, 10 and 25 mmHg respectively, N=4, Figure 9H). Similar to wild-type mice, neither vehicle nor QWF significantly affected the mechanical properties of the bladder wall in the absence of Compound 48/80. Together, these results suggest that the effects of Compound 48/80 on urinary bladder wall compliance are independent of mast cells but dependent on Mrgprb2.

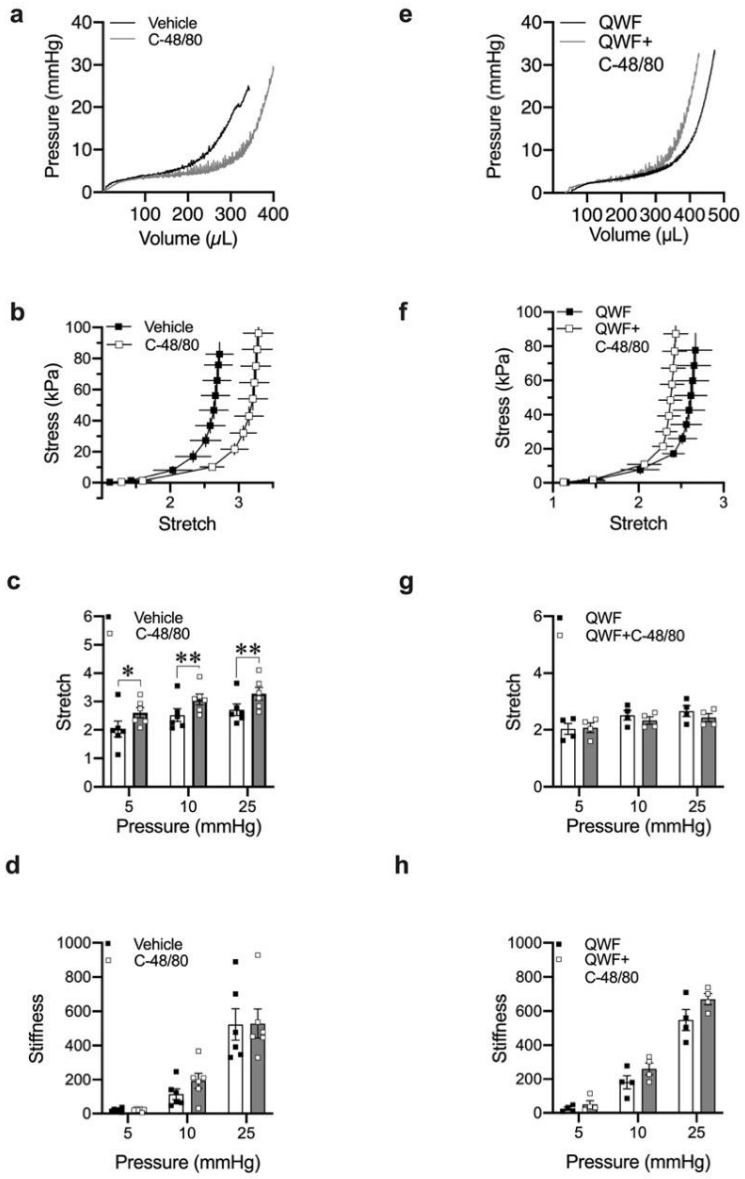

Figure 19 Compound 48/80 increases bladder wall compliance independent of mast cells. **A,** Representative pressure-volume trace of ex vivo filling of *C-Kit*$^{W\text{-}Sh}$ mouse bladders in the absence and presence of the Mrgprb2 agonist Compound 48/80 alone (10 μg/mL) **E**, representative pressure-volume trace after prior exposure to the Mrgprb2 antagonist QWF (10 μM). **B-C**, As with C57Bl/6 mice, compliance is increased in the presence of C-48/80 in mast cell-deficient *C-Kit*$^{W\text{-}Sh}$ mice (N=6) signified by the increase in stretch (P = 0.01, P = 0.006 and P = 0.008 for vehicle *vs.* C-48/80) at 5, 10, and 25 mmHg respectively. **F and G**, the increase in compliance by C-48/80 was again blocked by QWF (N=4) signified by the overlapping stress-stretch curves and no increase in stretch (P = 0.343, P = 0.255 and P = 0.282 for 5, 10 and 25 mmHg respectively for QWF *vs.* QWF + C-48/80). **D and H**, similar to wild-type, stiffness remains unchanged. Within the group comparisons were made via two-tailed, paired Student's t-test. "C-48/80": 10 μg/mL Compound 48/80; "QWF": 10 μM QWF.

4.4. Compound 48/80 increases Clinical Compliance

As a comparator to our measures of stretch and stress, we also calculated clinical compliance in terms of the change in volume per change in pressure during the quasi-linear portion of bladder filling. In the absence of Compound 48/80, no differences in clinical compliance were seen between C57Bl/6 and *C-Kit*$^{W\text{-}Sh}$ mice. Compound 48/80 increased clinical compliance in wild-type (P = 0.01, N=6, Vehicle *vs.* C-48/80; Figure 10A) and *C-Kit*$^{W\text{-}Sh}$ mice (P = 0.034, N=6, Vehicle *vs.* C-48/80; Fig 10C). In both mouse models, the increase was blocked by QWF (P = 0.206, N=6, Figure 10B and P = 0.209, N=4, Figure 10D).

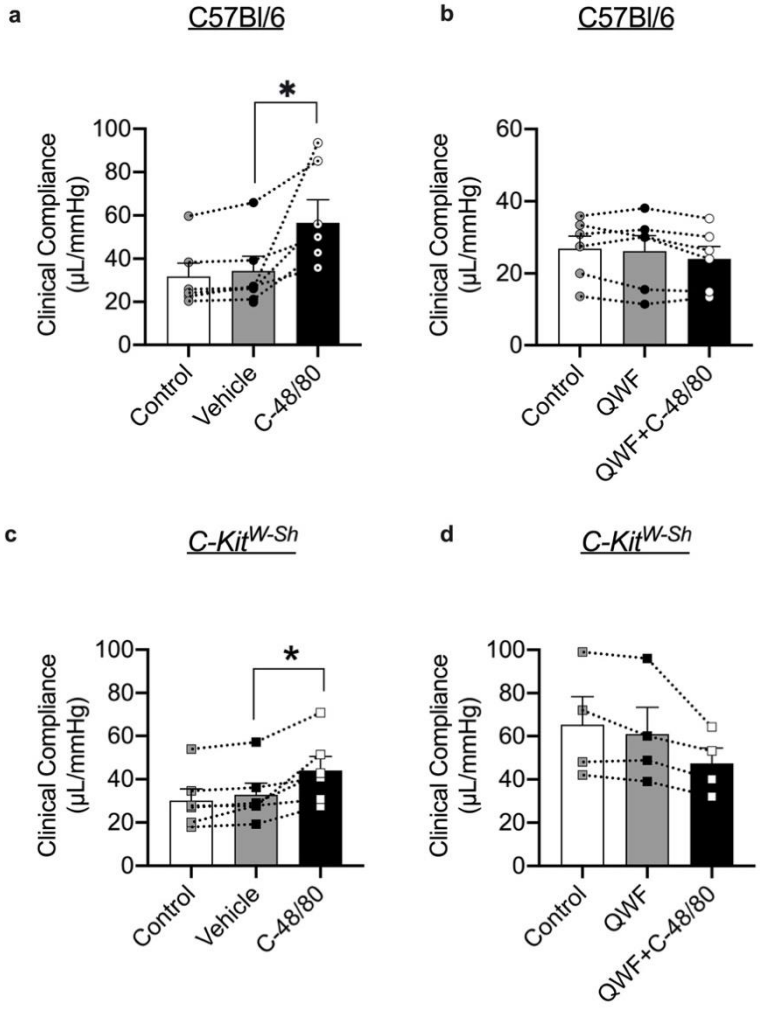

Figure 20 Compound 48/80 significantly increases clinical compliance independent of mast cell activation. A-B, Clinical compliance was increased after exposure to 10 µg/mL Compound 48/80 in both C57Bl/6 (P = 0.01; N=6, C-48/80 *vs.* Vehicle) and *C-kit*$^{W\text{-}Sh}$ mice (P = 0.034; N=6, C-48/80 *vs.* Vehicle). **C-D**, this increase was blocked by 10 µM QWF in both C57Bl/6 (P = 0.206; N=6, QWF *vs.* QWF+C-48/80) and *C-kit*$^{W\text{-}Sh}$ mice (P = 0.209; N=4, QWF *vs.* QWF+C-48/80). No significant differences were seen between control and vehicle in all groups. Within the group comparisons were made via one-way ANOVA followed by Tukey's *post-hoc* analysis. "C-48/80": 10 µg/mL Compound 48/80; "QWF": 10 µM QWF.

4.5. Activation of Mrgprb2 by Compound 48/80 increases UBSM Excitability

Transient pressure events are responsible for driving sensory outflow to the central nervous system during filling, and their rate of rise directly correlates with the amplitude of afferent bursts [35]. Thus, we analyzed the amplitude and rate of rise of transient pressure events as a measure of UBSM excitability as well as a surrogate measure of associated sensory outflow. Compound 48/80 significantly increased the amplitude and the rate of rise of transient contractions as compared to vehicle in both mouse models (Figure 11A and Figure 12A). The effect of Compound 48/80 on peak amplitude and leading slope was reduced by QWF in wild-type mice ($P = 0.024$ and $P = 0.010$ for 11C and 11D respectively, QWF+C-48/80 *vs.* C-48/80, N=6). There was an increase in peak amplitude due to Compound 48/80 even in the presence of QWF, but it was significantly smaller than Compound 48/80 alone ($P = 0.014$ Vehicle *vs.* QWF+C-48/80). Similar to wild-type mice, effects of Compound 48/80 were reduced by QWF in mast cell deficient mice ($P = 0.048$; N=6 and $P = 0.03$ for 12C and 12D respectively, QWF+C-48/80 vs. C-48/80). Collectively, these findings indicate that while the bladder is more compliant after exposure to Compound 48/80, UBSM excitability (and possibly afferent outflow) are also increased. These findings also suggested that the effects of Compound 48/80 on bladder wall compliance and transient pressure event leading slope are mediated by Mrgprb2.

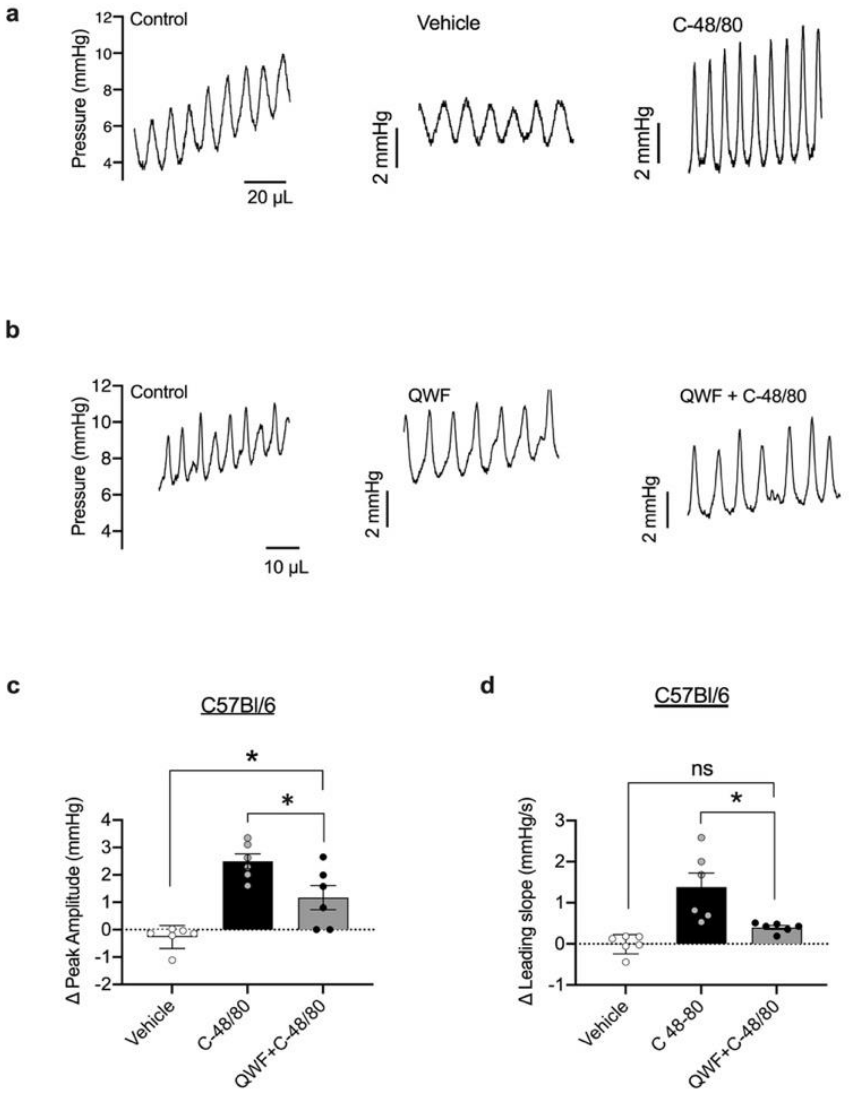

Figure 21 Compound 48/80 increases the amplitude and leading slope of transient contractions through Mrgprb2 activation. A, Representative trace of transient pressure events during *ex vivo* filling of a C57Bl/6 mouse bladder during control fill, fill in presence of vehicle or **(B)** 10 µM QWF (N=6), and after exposure to 10 µg/mL Compound 48/80 (N=6). **C-D**, the increase in both leading slope (P = 0.014, N=6, C-48/80 *vs.* QWF+C-48/80) and peak amplitude (P = 0.024, N=6, C-48/80 *vs.* QWF+C-48/80) by Compound 48/80 was blocked by QWF. There was an increase in peak amplitude due to Compound 48/80 even in the presence of QWF (P = 0.014 Vehicle *vs.* QWF+C-48/80, Figure 6c). No significant differences in leading slope and peak amplitude were seen in the presence of QWF alone. Between group comparisons were made via one-way ANOVA followed by Tukey's *post-hoc* analysis. "C-48/80": 10 µg/mL Compound 48/80; "QWF": 10 µM QWF.

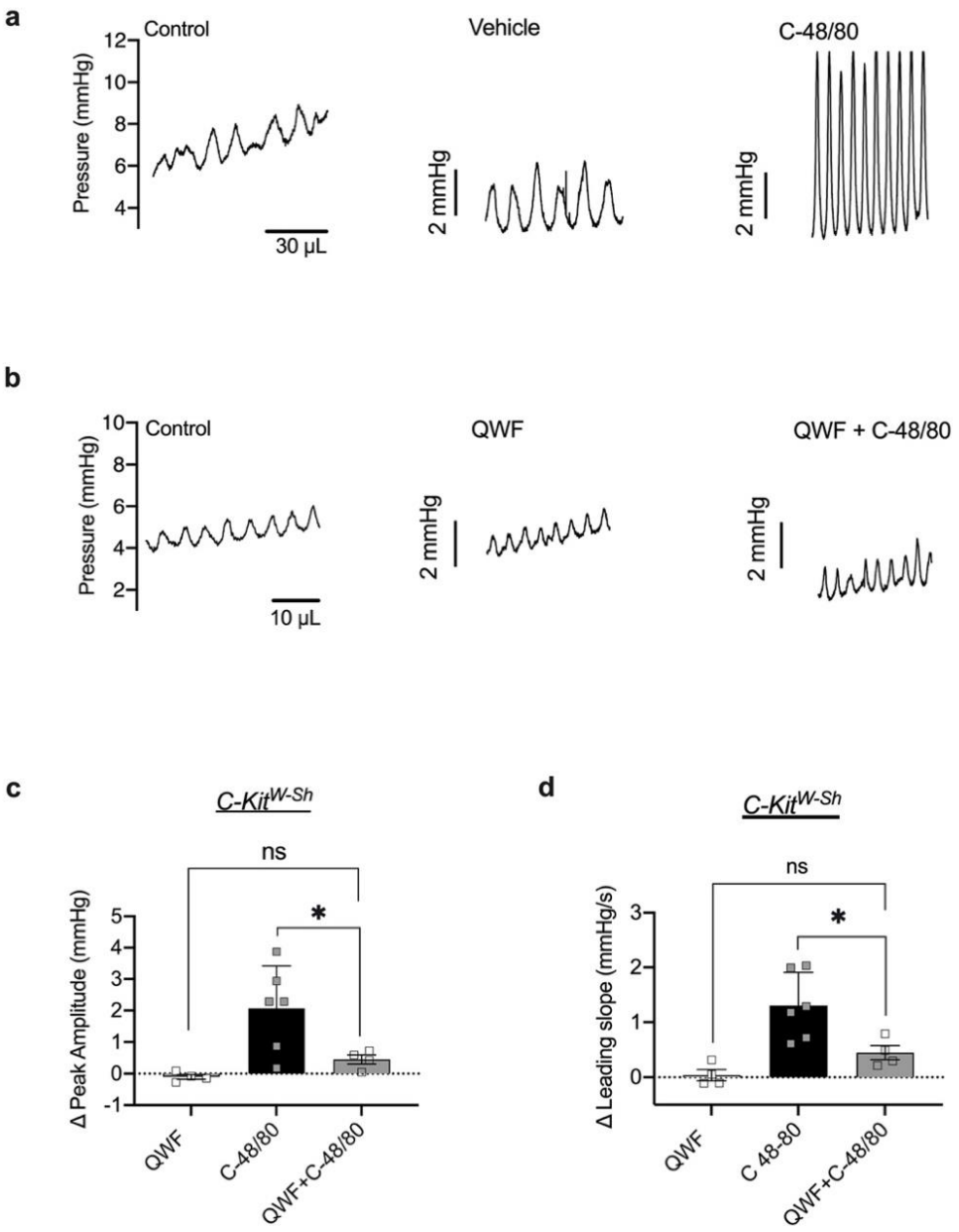

Figure 22 Compound 48/80 increases the amplitude and leading slope of transient contractions independent of mast cell activation. A, Representative trace of transient pressure events during *ex vivo* filling of a *C-kit*$^{W\text{-}Sh}$ mouse bladder during control fill, fill in presence of vehicle or **(B)** 10 µM QWF (N=4) and after exposure to 10 mg/mL Compound 48/80 (N=6). **C, D** The increase in both leading slope (P = 0.030) and peak amplitude (P = 0.048) by Compound 48/80 was blocked by QWF. No significant differences in leading slope and peak amplitude were seen in the presence of QWF alone. . Between group comparisons were made via one-way ANOVA followed by Tukey's *post-hoc* analysis. "C-48/80": 10 µg/mL Compound 48/80; "QWF": 10 µM QWF.

4.6. Treatment with Compound 48/80 causes bladder overactivity

We next determined if the *ex vivo* effects of Compound 48/80 translated into *in vivo* changes in urodynamics. In order to prevent systemic activation of mast cells, conscious cystometry was performed before and after intravesical infusion of Compound 48/80. In order to overcome the permeability barrier formed by umbrella cells lining the bladder without inducing inflammation or destroying the integrity of the urothelium , a higher concentration of Compound 48/80 (50 µg/mL) was used in these experiments. Compound 48/80 decreased intermicturition interval and void volume in C57Bl/6 mice, indicative of bladder overactivity ($P = 0.005$ and $P = 0.002$ for IMI and void volume respectively, N=8, Figure13A-B). These findings were recapitulated in *C-kit*$^{W\text{-}Sh}$ mice, again suggesting that the effects of Compound 48/80 were mast cell-independent ($P = 0.005$ and $P = 0.040$ for IMI and void volume respectively, N=4, Figure 13C-D).

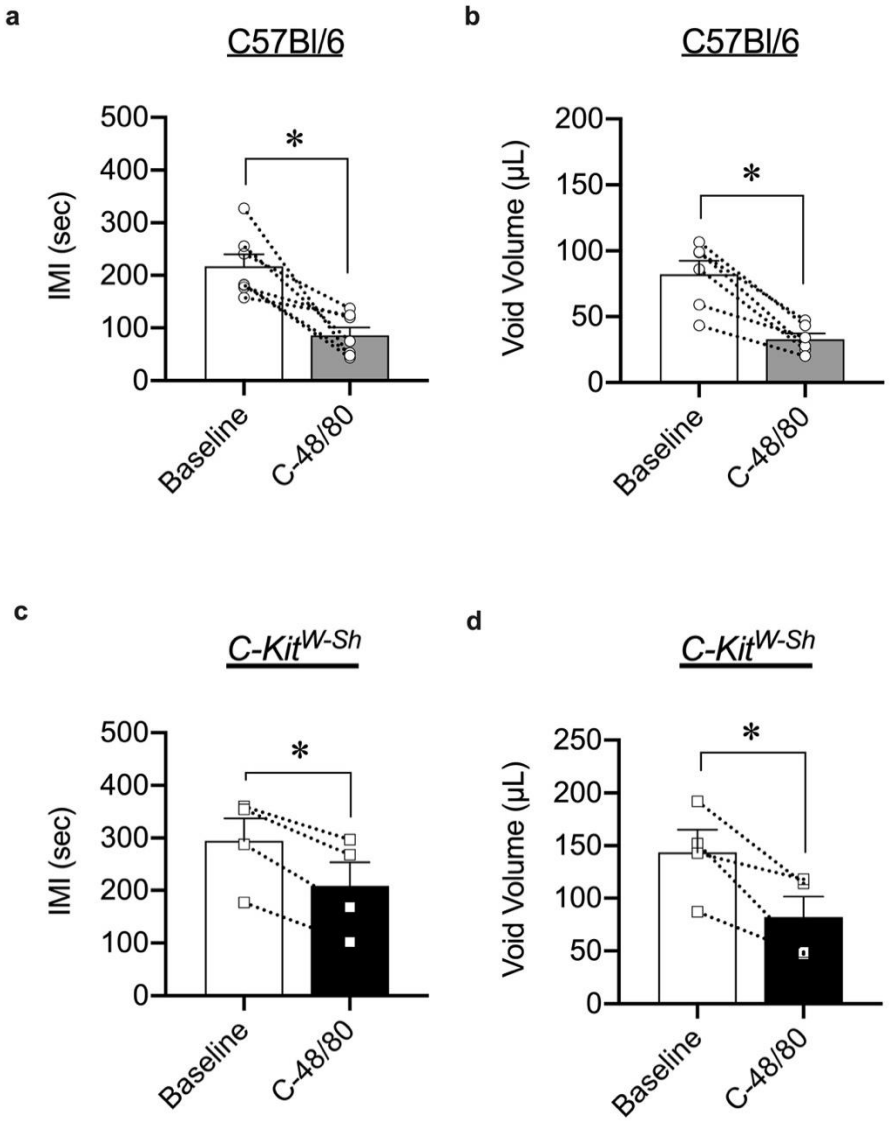

Figure 23 Compound 48/80 causes bladder overactivity in wild-type and mast cell-deficient mice. A, Intravesical instillation of Compound 48/80 (50 µg/mL) significantly decreased intermicturition interval (P = 0.005) and **(B)** void volume (P = 0.002) in C57Bl/6 mice (N=8) during conscious cystometry. **C-D**, Compound 48/80 had the same effect on intermicturition interval and void volume in mast cell-deficient *C-kit*$^{W\text{-}Sh}$ mice (P = 0.005 and P = 0.04, N=4). Within the group comparisons were made via paired Student's t-test.

5. DISCUSSION

Using cystometry, knockout mouse models, gene expression assays, and the novel pentaplanar reflected image macroscopy (PRIM) system, we comprehensively assessed how the mast cell activator Compound 48/80 alters urinary bladder function. While Compound 48/80 increased urination frequency *in vivo* and increased transient pressure events and mechanical compliance *ex vivo*, it did so in a mast cell-independent manner. The effects of Compound 48/80 were instead mediated by Mrgprb2 receptors presumably expressed in other cells within the urinary bladder wall itself. One interesting finding of this study was the speed at which Compound 48/80 can cause profound increases in urinary bladder compliance: within 30 minutes of exposure, both bladder wall mechanical compliance and UBSM excitability were augmented. These data suggest that: (1) basic secretagogues can alter bladder function independent of traditional mast cell-mediated and nerve-mediated pathways; and (2) rapid increases in bladder compliance correlate with bladder overactivity, likely related to increased sensory outflow during transient contractions of the bladder wall. Our findings also suggest that the Mrgprb2 receptor is an important linchpin in regulating bladder wall remodeling and changes to UBSM excitability caused by inflammation.

5.1. Clinical versus Mechanical Compliance

Many previous studies use "compliance" as a measure of stiffness and elasticity during filling [183]. However, the term "compliance" is often inaccurately defined [184]. Clinically, bladder compliance is calculated as the change in volume per change in intravesical pressure [185]. This definition, however, is incomplete as it disregards any variations in wall structure and thickness that occur during filling. As such, the traditional measure of clinical compliance would only be accurate if every bladder is the same size and thickness. By omitting the amount of bladder wall

present and the contribution of each constituent of the bladder wall's structure, this definition significantly skews our understanding of how the bladder wall remodels in disease. Clinical compliance also gives incomplete information about changes is the bladder wall structure and content itself, as it cannot differentiate between geometric stiffness (stiffness imparted due to the shape of the bladder) and mechanical stiffness (stiffness intrinsic to the material properties of the bladder wall). Instead, it only considers how both of these together influence the static second phase of bladder filling where pressure increases the least [156]. In this study, we instead measure bladder compliance as the relationship between wall stress and stretch. These factors consider the distribution of force across the total amount of bladder wall as it fills [167] and account for the volume of wall present in each bladder. Thus, accurate and appropriate comparisons of bladder wall mechanical properties can be made between subjects. We also included measures of clinical compliance as a means of comparing "traditional" measures of compliance with our calculations of stress, stretch, and stiffness. Even though our conclusions from our experiments were similar in each methodology, the ability to determine changes in stretch and stiffness at multiple points during filling brings information impossible to glean from pressure and volume alone.

5.2. Effects of Compound 48/80 on the Urinary Bladder function

Compound 48/80 has been extensively studied as a mast cell degranulating compound in the bladder as well as other organ systems [186-188]. Previous work utilizing Compound 48/80 to study the effects of mast cell-driven inflammation showed heightened UBSM excitability indirectly due to effects on peripheral endings of primary afferent neurons [189]. None of these studies considered the effects Compound 48/80 may have on the mechanical properties of the bladder wall and if changes to these properties are mast cell dependent. This study is the first of

its kind to show that an increase in mechanical compliance accompanies increased UBSM contractility after exposure to Compound 48/80. These effects suggest that the immediate response to inflammation in the bladder is both an increase in contractility along with a paradoxical increase in compliance, which can happen within minutes and lead to bladder overactivity. These results were counterintuitive since bladder overactivity is most often associated with a decrease in wall compliance and an increased muscle tone [169, 190]. Our findings instead suggest that the first step in bladder wall remodeling is an initial loss of ECM interconnectivity that increases distensibility, which is perhaps then followed by deposition of improperly arranged collagen that leads to remodeling. Such deposition is noted in rat models of overactive bladder due to spinal cord injury, where changes in collagen tortuosity and morphology increase bladder distensibility [153].

Interestingly, the change in compliance is almost entirely due to increased bladder wall stretch. Wall stiffness remained unchanged, implying that while the arrangement and interconnections of the ECM change acutely in response to Compound 48/80, the mechanical properties of the constituent elements remain the same. These findings also suggest that the effect of muscle tone on wall compliance may have been overestimated in the past [191]. Thus, the structural arrangement of the extracellular matrix may have a stronger influence on wall mechanics than muscle tone when considering the distribution of forces during the entirety of bladder filling.

The most interesting and surprising finding in this study was that effects of Compound 48/80 persisted in the absence of mast cells. Compound 48/80, a prototypical mast cell activator, degranulates mast cells by acting on the orphan Mrgprb2 receptor present in the mast cell membrane [140]. Our findings support the idea that Mrgprb2 is not mast cell specific, but instead is expressed throughout the bladder with the highest expression being in the urothelial layer.

Furthermore, the effects of Compound 48/80 on both compliance and UBSM contractility imply that activation of Mrgprb2 may cause release of inflammatory mediators normally attributed to mast cell degranulation irrespective of whether mast cells are present or not. When released from mast cells, mediators alter both the organization of the extracellular matrix and UBSM activity [192] and lead to effects on wall compliance and transient contractions. Thus, it appears that the presence of Mrgprb2 in other bladder cells causes them to behave like quasi-immune cells to drive remodeling and UBSM hyperexcitability.

5.3. Function and Pharmacology of Mas-related G protein-coupled receptor B2

Mrgprb2 (the mouse ortholog of human MRGPRX2) is an orphan receptor primarily studied in the context of non-IgE mediated mast cell degranulation and inflammation [193, 194]. Activation of MRGPRX2 and Mrgprb2 using basic secretagogues and neurokinins brings about IgE-independent anaphylaxis [120]. Transcripts from both MRGPRX2 and Mrgprb2 were detected in skin, sensory neurons, urinary bladder, and adipose tissue, though the presence of mast cells in these tissues was not ruled out as the source of Mrgprb2/X2 mRNA [135, 195-197]. While prior research has primarily focused on the skin in context with MRGPRX2-dependent reactions, adult urinary bladder has the third highest level of Mrgprb2/X2 mRNA of all tissues surveyed [141]. Therefore, effects of Mrgprb2 on the components of the bladder wall (urothelial cells, UBSM, extracellular matrix, etc.) are of potential interest in terms of lower urinary tract dysfunction. Our study piques this interest even more, as it is the first to demonstrate the mast cell-independent effects of Mrgprb2 activation specifically in the bladder *ex vivo* and *in vivo*. Our findings also suggest that *Mrgprb2* mRNA is predominantly expressed in the urothelium. This was not completely surprising since the urothelium is also a transitional epithelium that may act like secretory cells upon activation of inflammatory pathways, very much like keratinocytes [198]

which are an identified cell type that express Mrgprb2 receptors. Thus, Mrgprb2 receptors may be key in the development of bladder dysfunction associated with inflammatory insult and fibrosis.

Due to the dual nature of its actions, the pathway (or pathways) that Compound 48/80 activates may be two-fold and parallel to each other. Hypothetically, Mrgprb2 receptors present on urothelial cells could make them respond to basic secretagogues like immune cells – specifically mast cells. This is not unprecedented, since urothelial cells produce and release multiple products common to mast cell degranulation that increase UBSM contractility [199]. At the same time, activation of Mrgprb2 could also release mediators that activate downstream pro-inflammatory pathways, including the release and activation of matrix metalloproteases, that alter the structure and organization of the extracellular matrix [71, 77]. The nature of this dual effect may make the pathway of Mrgprb2 activation in the bladder extremely significant in both health and disease. Based on our findings and assuming similar expression patterns in humans, targeting human MRGPRX2 receptors could alleviate both the increased excitability and remodeling intrinsic to LUTS without preventing UBSM contractions in response to parasympathetic stimuli.

The lack of specific compounds that activate or inhibit Mrgprb2, however, poses an obstacle in receptor specificity studies. Some cationic peptides similar to Compound 48/80 activate Mrgprb2 and produce a local edema accompanied by itch when given subcutaneously [120]. Neurokinin-1 (NK_1) receptor antagonists show efficacy in animal models, but are inactive on human MRGPRX2 except QWF [176]. Compound 48/80 remains the only diagnostic compound that is a highly potent Mrgprb2/X2 agonist. Similarly for antagonists, QWF is the only compound that purports to be an antagonist for both Mrgprb2 and MRGPRX2. The generation of more selective

and potent drugs will markedly aid in our understanding of how and where these receptors drive physiology.

Our initial hypothesis stated that the increase in UBSM activity and wall compliance is brought about by activation of Mrgprb2 since the effects of Compound 48/80 were inhibited by the Mrgprb2 antagonist QWF. QWF also inhibits NK_1 receptors, thus the activation of NK_1 receptors by Compound 48/80 was still a possibility. Itch responses evoked by Mrgprb2 activation are inhibited by QWF even in the absence of NK_1 receptors [176], suggesting that although QWF antagonizes both receptors, the effects of Compound 48/80 are likely only mediated by Mrgprb2. This complexity means that specific actions of Compound 48/80 associated with Mrgprb2 activation cannot be clearly delineated by pharmacology alone in whole bladder tissue. Future projects will focus on developing specific and potent modulators of Mrgprb2. Alternatively, NK_1 receptor knockout mice could be used to perform similar stress-stretch analysis studies to confirm the effects of both Compound 48/80 and QWF in the bladder depend on Mrgprb2.

5.4. Conclusions

In conclusion, activation of the orphan receptor Mrgprb2 by Compound 48/80 alters the true mechanical properties of the bladder wall independent of mast cells by rapid rearrangement of the bladder wall matrix without changing the inherent mechanical stiffness of the constituent elements of the wall. The present study also demonstrates that muscle tone and excitability have surprisingly little influence on wall compliance, as Compound 48/80 increased wall compliance even in the face of an increase in UBSM excitability. This suggests that bladder wall structure and mechanical properties are more labile than originally thought, and rapidly influenced by the

actions of basic secretagogues acting on Mrgprb2. Future studies will determine the exact location of Mrgprb2 in the urinary bladder and assess the mediators released upon its activation.

MECHANISM OF INCREASED BLADDER COMPLIANCE INDUCED BY MRGPRB2 ACTIVATION IN MURINE BLADDER

Modified from: Pragya Saxena[1], Ashika Goel[1], Eli Broemer[2], Emma Flood[1], Osvaldo Jose Vega-Rodriguez[1], Gerald Mingin[4], Sara Roccabianca[3], Nathan R. Tykocki[1]

Manuscript in prep.

1. ABSTRACT

Bladder wall ECM structure and components influence the biomechanical behavior of the bladder. Matrix metalloproteases (MMP) are a family of Zinc-dependent enzymes that degrade components of the ECM and lead to ECM remodeling. Disruption in arrangement of the ECM can lead to alterations in mechanical compliance and stiffness, both of which are associated with lower urinary tract symptoms (LUTS). LUTS can arise due to many underlying pathways in the bladder, but we are particularly interested in pseudo-inflammation caused by activation of orphan G protein-coupled receptor, Mrgprb2 (Mas-related G protein-coupled receptor B2). Activation of Mrgprb2 using basic secretagogue, compound 48/80 increases mechanical compliance and the amplitude and leading slope of transient pressure events implying that even when compliance is increased afferent activity that relays fullness to the brain is also increased. This study explores how compound 48/80 increases compliance and its effects on collagen fibers in the ECM. In wild type C57Bl/6 mice, compound 48/80 alone significantly increased mechanical compliance which was inhibited by broad spectrum MMP inhibitor, doxycycline and specific MMP-2 inhibitor, ARP100. Z-stack recording of pressurized bladders also showed that compound 48/80 reduced bladder wall thickness when administered intravesically. Surprisingly, no change in urothelial permeabilization was observed. MMP-2 activity was increased, and TIMP-2 activity was reduced upon incubation with compound 48/80 prior to protein isolation. Together these findings suggest that Mrgprb2 activation rapidly leads to activation of MMP-2 and inhibition of TIMP-2 that cumulatively alter collagen fiber arrangement in the wall to increase mechanical compliance. Thus, the mechanism of altered compliance downstream of Mrgprb2 is important and should be explored to fill the gaps in understanding of inflammation leading to LUTS.

2. INTRODUCTION

Normal bladder function is contingent upon the bladder's ability to maintain a balance between mechanical compliance and stiffness, and alteration of this balance can lead to bladder dysfunction [92, 165]. Mechanical properties of the bladder wall are influenced greatly by the acellular components that reside in and comprise the extracellular matrix (ECM) [37, 69, 168]. Bladder ECM contains fibrillar proteins (e.g., collagens and elastins [5]), adhesive proteins (e.g., fibronectins and laminins [59]), ECM receptors [60], cross-linking proteins, and matrix metalloproteases responsible for ECM degradation [5, 200]. For urinary bladder smooth muscle cells to contract adequately during emptying, the bladder wall can neither be too stiff nor too compliant; hence ECM cross-linking needs to be constantly regulated [201].Only recently was bladder ECM identified as more than the structure that holds the cells together. It is a continuously dynamic structure that can respond to cellular signals [51, 52]. Cellular behavior and cell-to-cell interactions can be mediated by altering the mechanical integrity of the ECM [71]. The ECM is also vital in maintaining the integrity of the bladder wall during storage and filling, and inflammatory conditions could lead to disturbances in the ECM [202]. Hence, the components of the ECM represent a novel target to understand how inflammation in the bladder wall affects bladder wall biomechanics.

Matrix metalloproteases (MMPs) are a family of Zinc-dependent endopeptidases that are secreted in their "pro" form by many cells, including smooth muscle cells and fibroblasts [74, 203]. These proteases play a role in ECM turnover by degrading components of the ECM, including the fibrillar collagens I and III, elastins, and the non-fibrillar collagens II and IV [77]. In the bladder, MMP1, MMP2, MMP7, MMP9, MMP11, MMP14, and MMP28 have been identified, but very few studies show their role in bladder dysfunction outside of bladder cancer [5]. MMPs can be activated by

serine proteases, tryptases, ATP and other inflammatory mediators [75, 76]. The catalytic activity of MMP is controlled at the transcriptional level, during pro-peptide cleavage from tissue inhibitors of matrix metalloproteases (TIMPs) and by specific inhibitors such as tetracycline derivatives [78]. MMPs are activated in several ways through removal of the pro-domain to expose the active site that is protected by a cysteine residue [80]. Removal of the cysteine residue takes place in the pericellular space and is triggered by multiple mediators including but not limited to TIMPs, other activated endoproteinases, and reactive oxygen species [78]. Allosteric activation of MMPs may also occur through the disruption of the thiol-Zn^{2+} bond that protects the active site [78]. This can happen *in vivo* due to interactions with integrins and proteoglycans and *in vitro* due to SDS. Once activated, MMPs can degrade specific substrates based on their specific proteolytic sites [74]. Some overlap is observed, but different ECM components are degraded by their respective MMPs. Due to their effects on structural ECM proteins, activation of specific MMPs either directly or by relief of TIMP inhibition can alter the biomechanics of soft tissue [204, 205].

Previously, we uncovered that the prototypical mast cell activator Compound 48/80 increased both bladder mechanical compliance and detrusor contractility via activation of the orphan Mas-related G- protein-coupled receptor type B2 (Mrgprb2) receptor [26, 206]. Furthermore, these effects were completely independent of mast cells. While the increase in mechanical compliance is profound and rapid, the mechanism regulating it is unknown. This study tests the hypothesis that Mrgprb2 agonism activates MMPs to increase bladder compliance via rapid collagen remodeling.

3. MATERIALS AND METHODS

3.1. Animal Care and Use

All animal procedures followed institutional Animal Care and Use Committees (IACUC) of Michigan State University (NIH Assurance D16-0054). All procedures followed the recommendations in the Animal Research: Reporting of In Vivo Experiments (ARRIVE) guidelines. Male C57Bl/6 mice (8-12 weeks old; Jackson Laboratory, Bar Harbor, ME USA) were housed in a temperature- and humidity-controlled environment with a 12-hour light/dark cycle and *ad libitum* access to standard chow and water. Mice were euthanized by intraperitoneal injection of pentobarbital (>150 mg/kg) followed by decapitation prior to all experimental procedures.

3.2. Calculating mechanical bladder compliance using Pentaplanar Reflected Image Macroscopy (PRIM) System

As previously described [1, 206], bladder wall compliance was quantified as wall stress *versus* stretch using the measurements obtained via *ex vivo* filling in the PRIM system [1]. Briefly, whole mouse bladders were dissected, placed in ice-cold Ca^{2+} free HEPES buffer, cleaned of connective tissue and cannulated through the urethra in the PRIM chamber for *ex vivo* filling. Throughout the experiment, the PRIM chamber was recirculated with bicarbonate buffered physiological salt solution consisting of the following [in mM]: NaCl [119], KCl [4.7], $NaHCO_3$ [24], KH_2PO_4 [1.2], EDTA (0.023), and glucose [7]; pH=7.4. Buffer was warmed to 37°C and aerated with biological atmosphere gas (20% O_2, 5% CO_2, and 75% N_2) to maintain pH and tissue oxygenation. Bladders were then filled through the cannula at a rate of 30 µl/min until a maximum pressure of 25 mmHg was reached at which point they were emptied. Each bladder underwent 3 equilibration control fills prior to a fill in the presence of vehicle/antagonist

followed by a fill in presence of 10 µg/mL Compound 48/80. All drugs and chemicals were allowed to incubate in the recirculating bath for 10-20 minutes before filling was recorded. Bladder wall thickness and area in empty and full configurations were derived from the PRIM system images using ImageJ (NIH). Bladder was then modelled as an ellipsoid that expands non-linearly with a constant wall volume as described previously [207]. Bladder wall stress and stretch were calculated for each time point during the *ex vivo* fill. To summarize data from multiple experiments, stress and stretch from all curves of the same group were averaged with reference to pressure using MATLAB R2022a (MathWorks).

3.3. Bladder Protein Isolation

Whole mouse bladders were dissected, cut in half transversely from the urethra to the dome, and placed in separate tubes with Ca^{2+} containing HEPES buffer at 37°C. One half of each bladder was exposed to 10 µg/mL Compound 48/80 for 30 minutes. Bladder tissue was then flash frozen in liquid N_2 and homogenized in NP-40 lysis buffer (125 mM NaCl, 30 mM TrisHCl and 10% NP-40) using a Bead Ruptor (Omni Inc.). Homogenized tissue was then centrifuged for 20 minutes at 12,000 *g* and supernatant was collected and stored at -80°C. Total protein content for each sample was estimated using a bicinchoninic acid assay.

3.4. Gelatin Zymography

Bladder protein isolates (30 µg) were loaded into 1% gelatin zymogram gels (Thermo Fisher) and placed in an electrophoresis mini-gel tank (Invitrogen) filled with SDS-PAGE running buffer. In addition to bladder protein isolates, gels included recombinant MMP-1, MMP-2, and MMP-9 (R&D Systems) as positive controls. Gels were run for 2.5 h at 115 V and then transferred to renaturing buffer (2.5% Triton X-100) on a rocker for 30 minutes. Gels were then rinsed with developing buffer [in mM]: $ZnCl_2$ [5], $CaCl_2$ [10], Tris HCl [50], NaCl [50], and

0.2% Brij-35. Gels were next incubated in developing buffer for 30 h at 37°C. After rinsing with distilled water, gels were stained using Coomassie blue for 1 h and destained for 2 h. Finally, destained gels were imaged using the Licor Odyssey Clx imaging system. MMP activity was visualized as light bands against the dark background.

3.5. Collagen Zymography

Samples were prepared as described above. To prepare collagen zymogram gels, 0.3 mg/mL Collagen type I and III were added to Surecast resolving and stacking buffer packs (Thermo Fisher). Resolving and stacking gel solutions were prepared as described in Supplementary table 1. Once the gels polymerized, samples were run and gels were developed, incubated, stained, destained, and imaged as described above. MMP activity was visualized as light bands against the dark background.

3.6. Reverse Zymography

Samples were prepared as described above. Resolving buffer solution containing 0.3 mg/mL collagen type I and III and 5 ng MMP-2 was prepared as described in Supplementary table 1. Gels were run, developed, incubated, stained, and destained as described above. TIMP-dependent inhibition of MMP-2 was visualized as dark bands against a light background.

3.7. Ex vivo imaging of bladder wall permeability and thickness

Whole bladders were dissected, cannulated, and mounted in a custom-designed imaging chamber. Ca^{2+}-replete HEPES buffer containing 10 µM Wortmannin was recirculated through the chamber and warmed to 37°C. Bladders were filled to an intravesical pressure of 25 mmHg with Ca^{2+} containing HEPES buffer mixed with FITC-dextran (4 kDa) to identify the lumen and additionally assess urothelial permeability. Full thickness Z stacks were captured at two randomized locations on the surface across the bladder wall using 2-photon laser microscopy

(Zeiss). In addition to FITC signal, second harmonic generation (SHG) of collagen was also recorded for each Z stack and served to demarcate the bladder wall [114]. Images were taken before and 10 minutes after intravesical installation of Compound 48/80 (50 μg/mL). As a positive control for permeabilization of the bladder wall, 1% Triton X-100 was infused in the bladder at the end of the experiment and the bladder wall was imaged again. To calculate wall thickness, width of the SHG signal was measured. To calculate permeabilization, average FITC intensity was recorded inside the lumen and within the wall. For analysis of images obtained via two-photon microscopy, each Z-stack was rotated perpendicularly to avoid the interference of bladder's curvature for accurate calculation of SHG signal width.

3.8. Drugs and Chemicals

ARP100 and JNJ0966 were obtained from Tocris (Bristol, UK). Doxycycline, Compound 48/80, and all other salts and reagents were obtained from Sigma Aldrich (Cleveland, OH).

3.9. Statistical Analysis

For comparison of two samples of equal variance, statistical significance between groups was assessed using two-tailed, paired Student's *t* tests ($\alpha = 0.05$). For analysis of images gathered from two-photon microscopy, 10 random images from each stack belonging to the same group were chosen. All 20 images were averaged and compared with other groups using a Wilcoxon paired sign-rank test ($\alpha = 0.05$). Calculations were performed using Excel (Microsoft Corporation) or GraphPad Prism (GraphPad Software). Comparisons with P values <0.05 were considered statistically significant. Asterisks were used to express statistical significance in figures: $*P<0.05$ and $**P<0.01$. Exact P values are stated in the figure legends. For clarity, "N" represents the number of animals in each group.

4. RESULTS

4.1. *Compound 48/80 decreases bladder wall thickness without increasing urothelial permeability*

Inflammatory mediators activate MMPs degrade the basal lamina propria and alter permeability in blood vessels [208, 209]. To test if Compound 48/80 released inflammatory mediators that elicited a similar response in the bladder, we tested its effects on urothelial barrier function using a 4 kDa FITC dextran and on bladder wall collagen fibers via the SHG signal (Figure 14). In *ex vivo* pressurized bladders exposed to 50 µg/mL Compound 48/80, no increase in FITC fluorescence intensity within the bladder wall was noted, indicative of maintained barrier function (Figure 15A-B). As a positive control, the surfactant Triton X-100 was able to permeabilize the bladder wall (Figure 15C) Interestingly, pressurized bladders exposed to Compound 48/80 had a significant decrease in bladder wall thickness that was not recapitulated by Triton X-100 (Figure 14D - F and 15D).

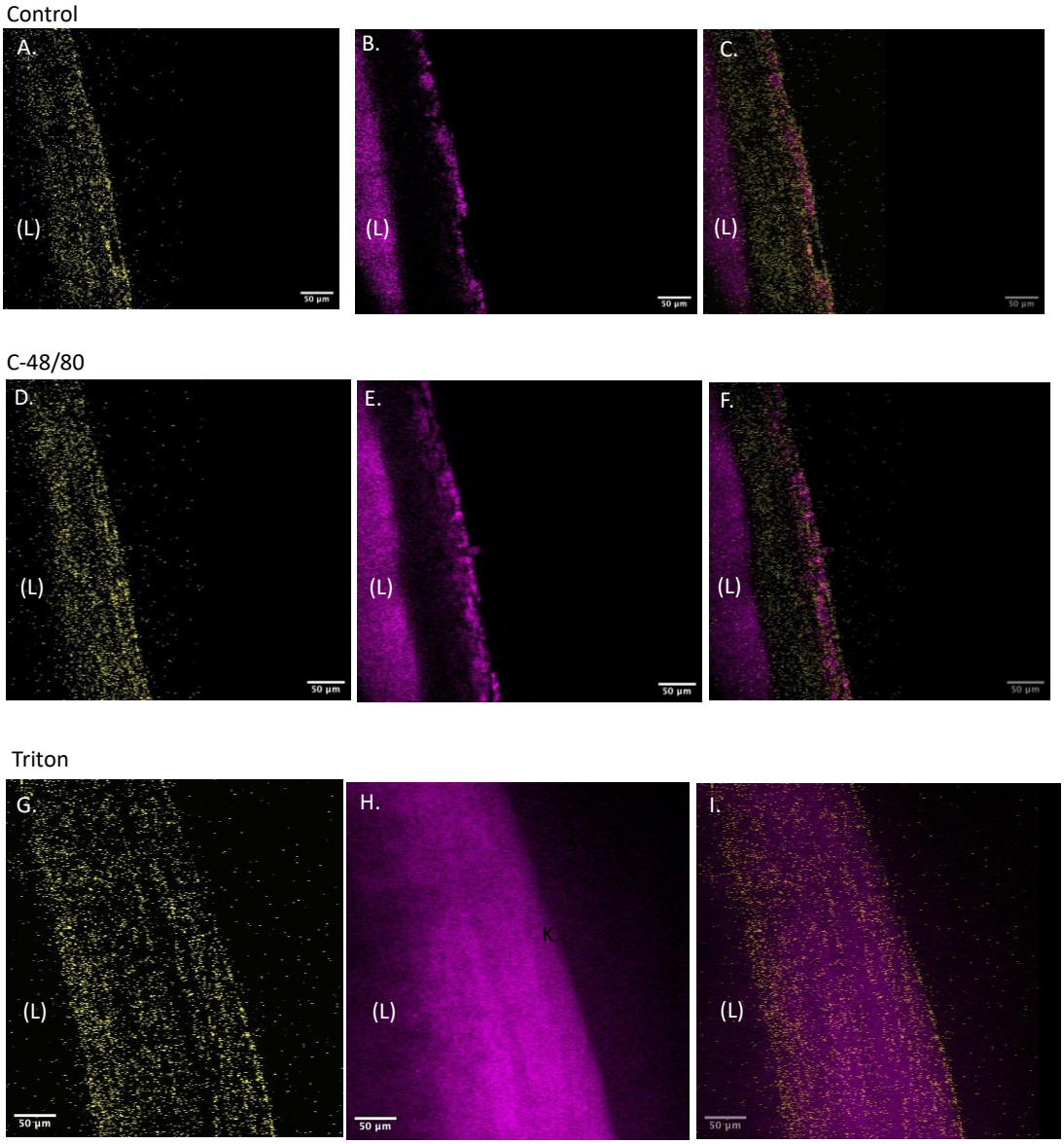

Figure 24 Permeability of the bladder wall to FITC-Dextran. Representative images of urothelial permeabilization and bladder wall thickness using FITC Dextran (4 kDa; purple) and second harmonic generation (SHG; yellow), respectively. Each panel shows collagen alone (left), FITC-Dextran alone (middle), and overlay of both channels (right). **(A-C)** intact bladders pressurized to 25 mmHg in the absence of any drug. **(D-F)** The Mrgprb2 receptor agonist compound 48/80 (50 µg/mL) administered intravesically for 10 minutes did not permeabilize the urothelium, signified by an absence of FITC signal in the bladder wall. **(G-I)** Intravesical infusion of 1% Triton X-100 for 10 minutes permeabilized the urothelium, signified by the colocalization of FITC and SHG signal and a loss if FITC-Dextran from the lumen. Images represent a total N=4 experiments. L: bladder lumen.

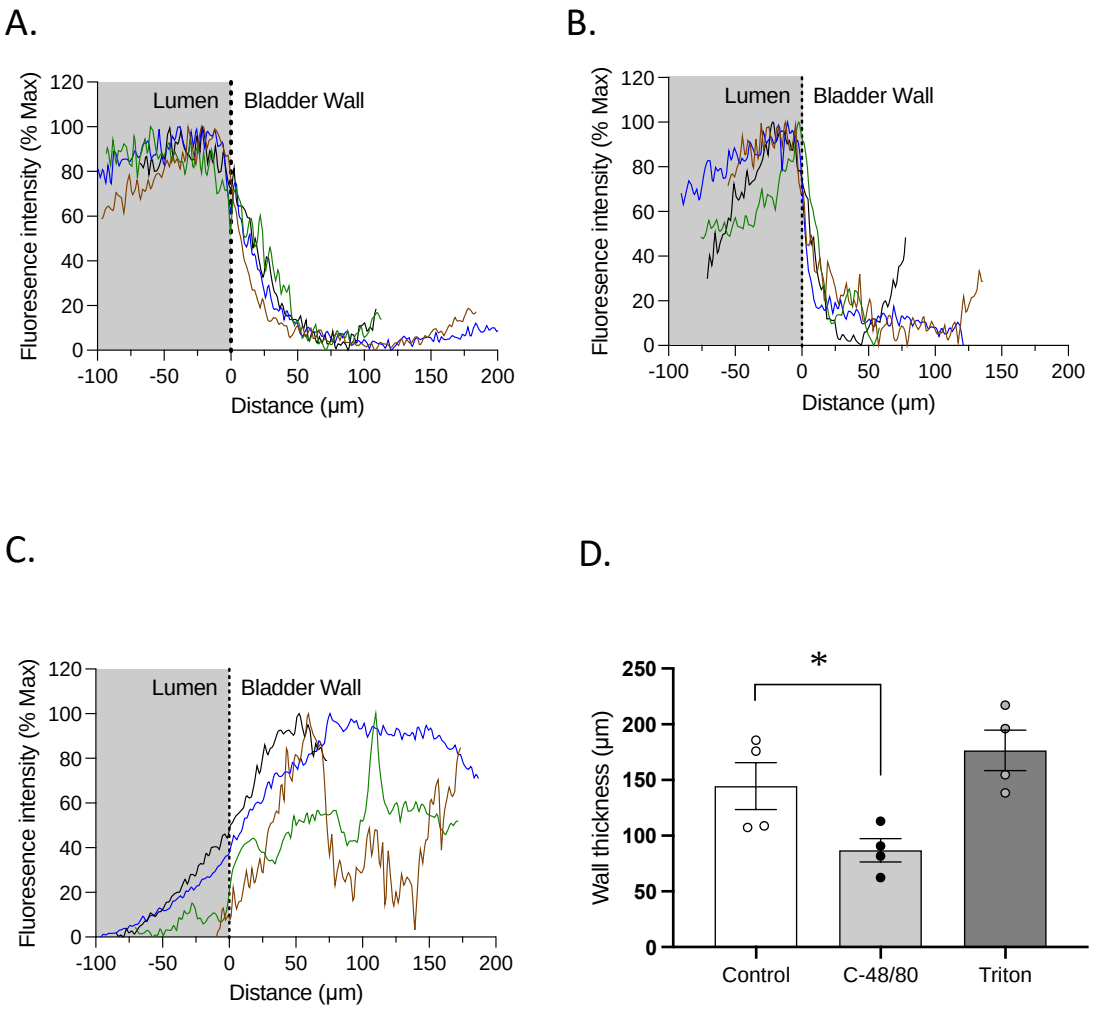

Figure 25 Compound 48/80 reduces bladder wall thickness without permeabilizing the wall. (A-C) Plots of FITC-Dextran fluorescence intensity as a function of distance across the bladder wall for bladders exposed to vehicle, the Mrgprb2 receptor agonist compound 48/80 (10 µg/mL), and 1% Triton X-100. Neither vehicle **(A)** nor 50 µg/mL compound 48/80 **(B)** permeabilized the bladder, as shown by the stark drop in fluorescence intensity at the transition from bladder lumen to bladder wall. Triton was used as positive control and it permeabilized the urothelium to let FITC into the wall **(C).** The different colors of the curves represent the Ns. **(D)** Quantification of bladder wall thickness after being exposed to vehicle, compound 48/80 and triton**.** 50 µg/mL compound 48/80 significantly reduced the thickness of bladder wall collagen whereas 1% Triton had no effect on wall thickness (P=0.022 for Control *vs.* C-48/80 and P=0.333 for Control *vs.* Triton, N=4). Between group comparisons were made *via* two-tailed, paired, Student's *t* test.

4.2. Compound 48/80 alters bladder wall mechanical compliance by activating MMP-2

Previously, we uncovered that compound 48/80 increased mechanical compliance while simultaneously increasing the amplitude and leading slope of transient pressure events [206]. To confirm the effects of compound 48/80, *ex vivo* bladder filling was performed in the presence of 10 µg/mL compound 48/80 (Figure 16). Compound 48/80 increases mechanical compliance suggested by a rightward shift in the stress-stretch curve and a significant increase in stretch at 10 and 25 mmHg (Figure 16B-C). Additionally, stiffness is also significantly lowered at 25 mmHg (Figure 16D). To determine if the increase in bladder wall mechanical compliance caused by Compound 48/80 was due to MMP activation, *ex vivo* bladder filling was performed in the presence of the broad spectrum MMP antagonist doxycycline (20 µM) before exposure to Compound 48/80 (10 µg/mL) (Figure 17). Doxycycline prevented the increase in compliance (Figure 17A, B) and stretch (Figure 17C), as well as the decrease in stiffness (Figure 17D), caused by Compound 48/80. To explore which MMPs may be responsible for effects of Compound 48/80, this experiment was repeated using the specific MMP-2 inhibitor ARP100 (200 nM) (Fig 17). Compound 48/80 did not increase wall compliance in the presence of ARP100 (Figure 4A, B), nor did it alter stretch (Figure 17C) or stiffness (Figure 17D).

Surprisingly, Compound 48/80's effects on amplitude and leading slope of transient pressure events persisted in the presence of doxycycline (Figure 19A-C) and ARP100 (Figure 19D-F). This suggests that while compound 48/80 activates MMP-2 to degrade collagen in the bladder ECM and increase mechanical compliance, the effects of Compound 48/80 on spontaneous detrusor activity occur due to other parallel mechanisms.

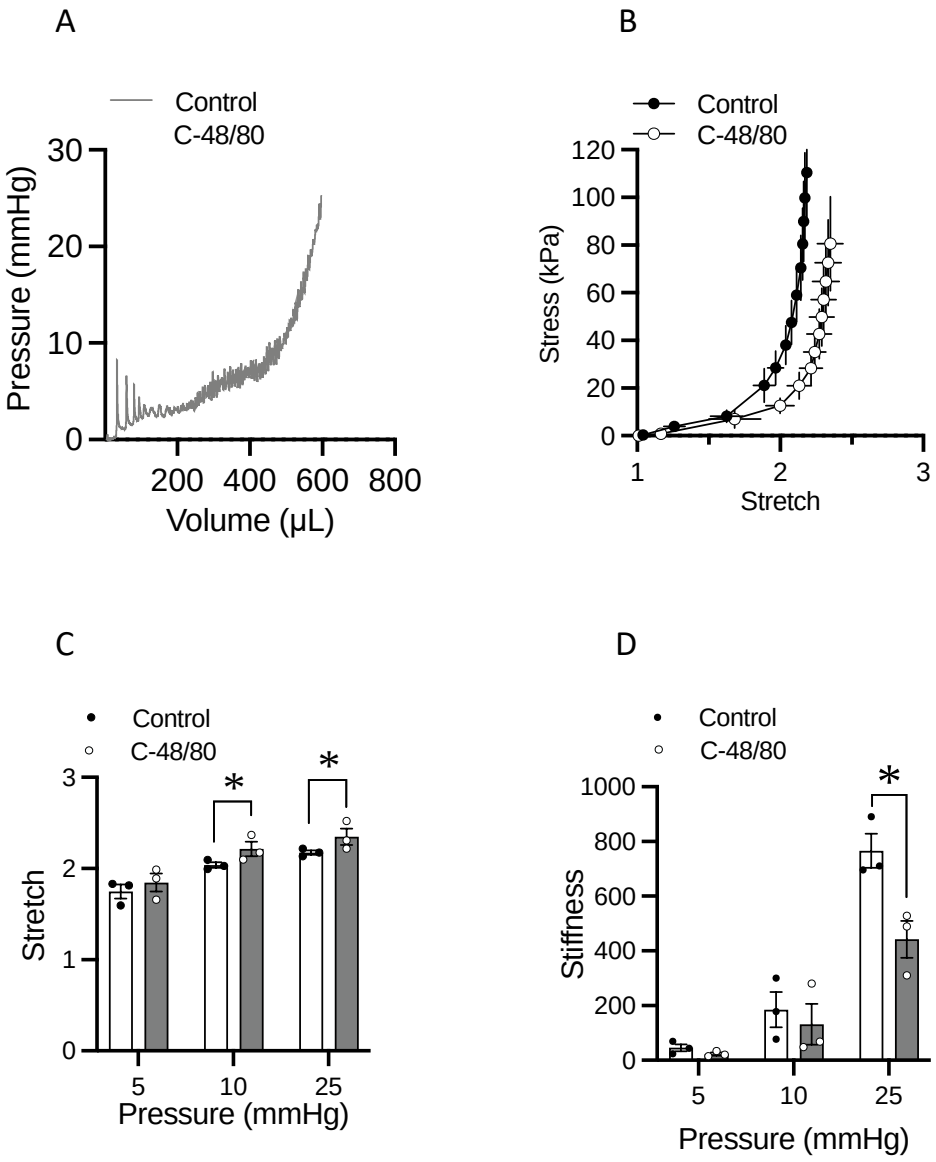

Figure 26 Compound 48/80 increases bladder wall mechanical compliance. (A) Representative pressure-volume trace of ex vivo filling of C57Bl/6 mouse bladders in presence of the Mrgprb2 receptor agonist compound 48/80 (10 µg/mL). Compound 48/80 increases mechanical compliance, signified by the rightward shift in stress-stretch curve **(B)** and a significant increase in stretch at 10, and 25 mmHg (**C,** P=0.027). Stiffness is decreased at 25 mmHg **(D,** P=0.031). *: $P \leq 0.05$. N = 3.

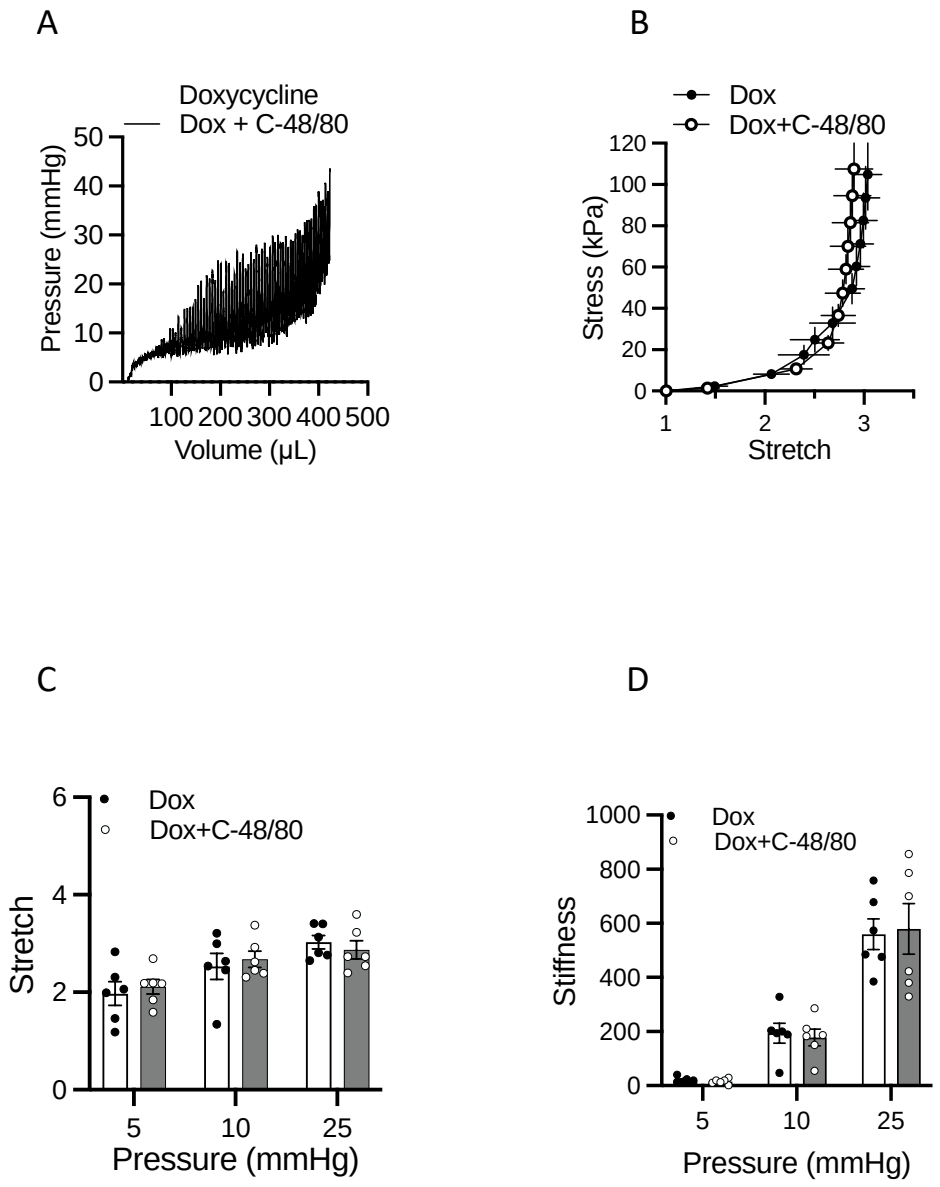

Figure 27 The effects of Compound 48/80 on bladder wall compliance are mediated by matrix metalloproteases. (A) Representative pressure-volume trace of *ex vivo* filling of C57Bl/6 mouse bladders in presence of the MMP inhibitor doxycycline (20 µM) alone and after addition of the Mrgprb2 receptor agonist compound 48/80 (10 µg/mL). Doxycycline blocks the increase in compliance driven by compound 48/80 signified by the absence of rightward shift of stress-stretch curve **(B)** and no significant increase in stretch at 5, 10, and 25 mmHg **(C,** P=0.706). Stiffness remains unchanged in both groups **(D).** N = 6

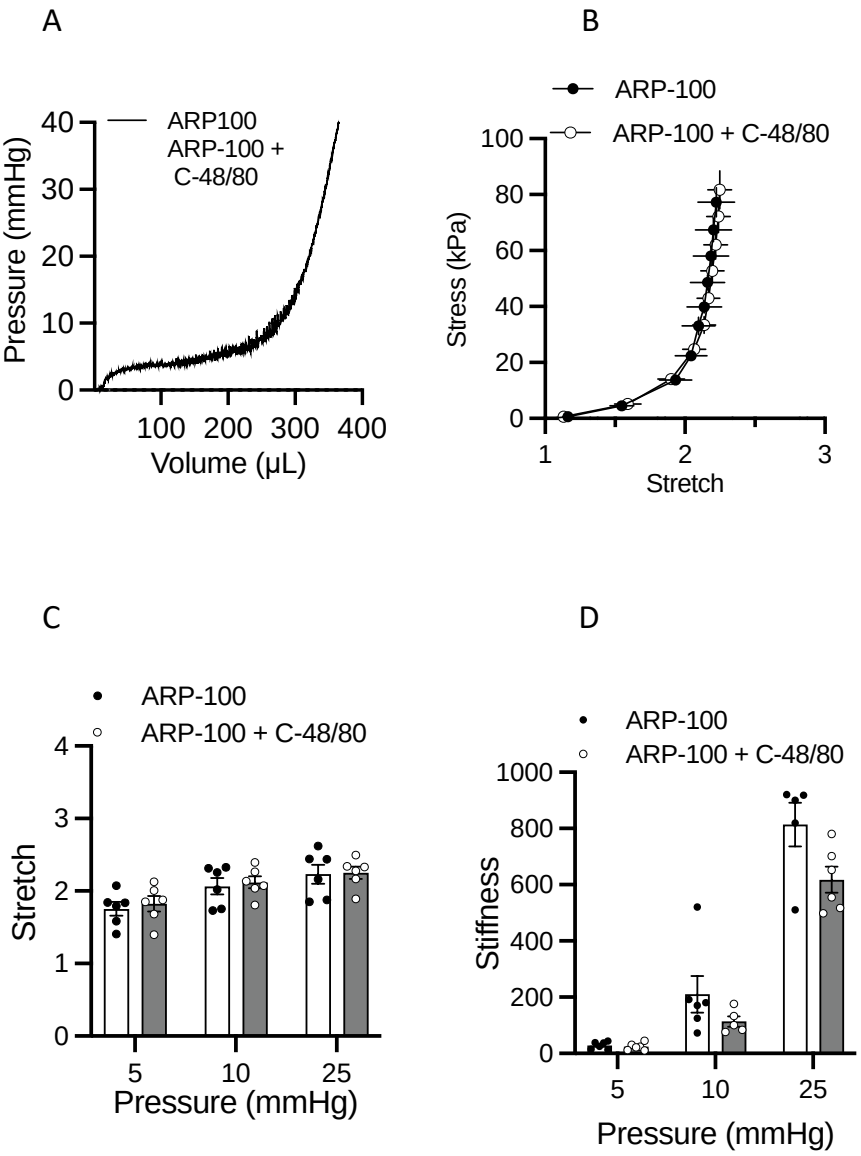

Figure 28 The MMP-2 inhibitor ARP100 blocks the increase in mechanical compliance driven by compound 48/80. (A) Representative pressure-volume trace of *ex vivo* filling of C57Bl/6 mouse bladders in presence of the selective MMP-2 inhibitor ARP100 (200 nM) alone and after addition of the Mrgprb2 receptor agonist compound 48/80 (10 µg/mL). ARP100 blocks the increase in compliance caused by compound 48/80, signified by the absence of rightward shift of stress-stretch curve **(B)** and no significant increase in stretch at 5, 10, and 25 mmHg **(C,** P=0.093). Stiffness remains unchanged in both groups **(D).** N = 6.

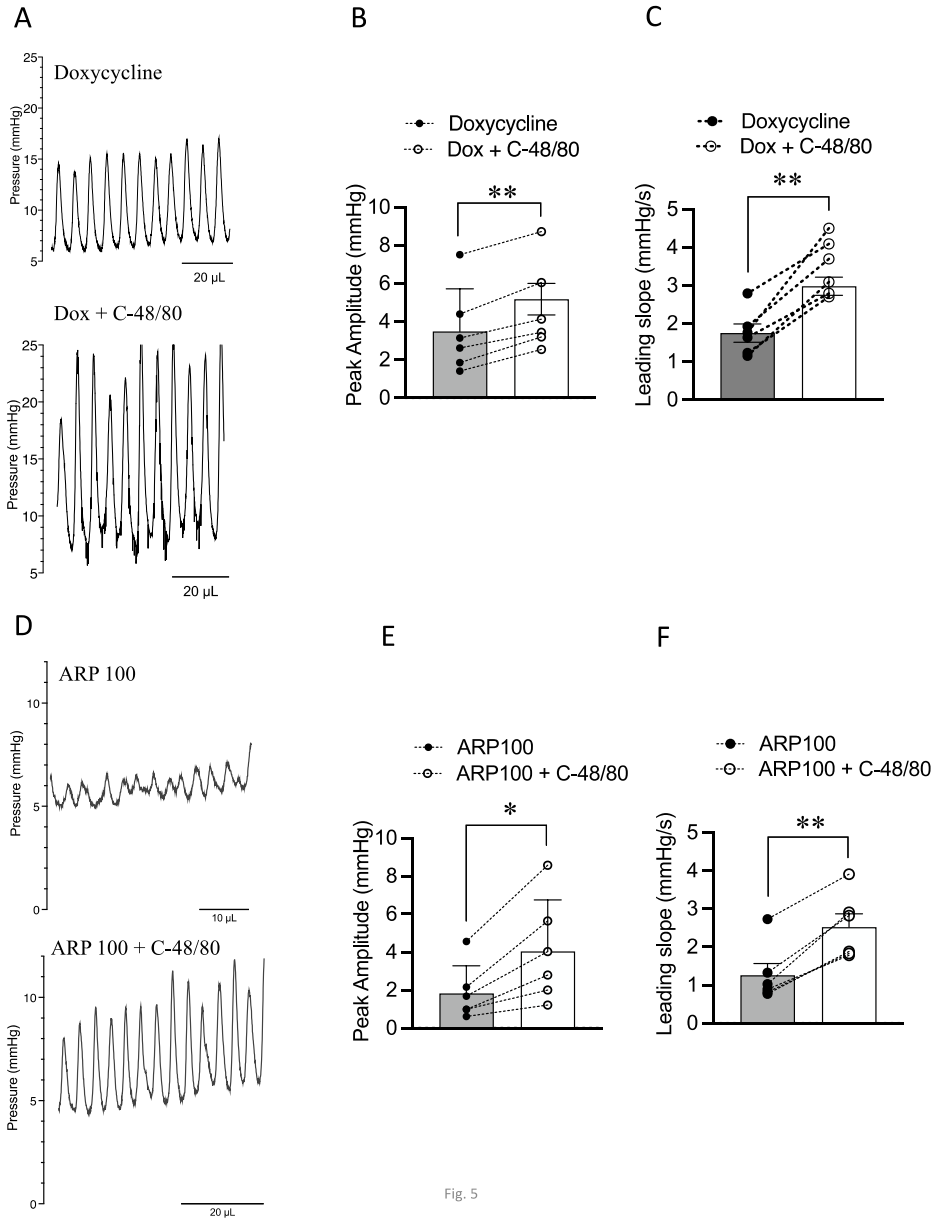

Figure 29 Figure 6 Compound 48/80 increases in the amplitude and leading slope of transient pressure events independent of MMP inhibition. (A) Representative traces of transient pressure events in presence of the MMP inhibitor doxycycline alone and after addition of the Mrgprb2 receptor agonist compound 48/80 (10 µg/mL). The increase in peak amplitude **(B)** and leading slope **(C)** were unaffected by doxycycline **(**P=0.0002 for peak amplitude and P=0.003 for leading slope). **(D-F)** The selective MMP-2 inhibitor ARP100 also had no effect (P=0.010 for peak amplitude and P=0.0004 for leading slope**).** *: $P \leq 0.05$. **: $P \leq 0.01$. N = 6.

4.3. MMP-2 is basally active in the bladder wall

MMP-1 is the primary collagenase that is expressed in the bladder to denature fibrillar collagens (type I and III) while MMP-2 and MMP-9 are gelatinases that also break down collagen type I along with their canonical substrates; collagen type II and IV [5]. Thus, the enzymatic activity of MMP-1, -2, and -9 was assessed using gelatin and collagen zymography (Figure 6). Gelatin zymography showed that MMP-2 was basally active in all tissues, as shown by the light bands at a similar molecular weight as recombinant MMP-2 (Fig 20A). Additionally, MMP-2 activity was significantly increased in samples exposed to compound 48/80 prior to protein isolation (Fig 20B). Likewise, collagen zymography showed MMP activity, at bands of a distinct molecular weight from recombinant MMP-1 but similar in weight to MMP-2 (Fig 20C). Further, compound 48/80 significantly increased MMP activity in collagen zymography (Fig 20D). Together, these data suggest that MMP-2 is basally active in the bladder and this activity can be augmented by compound 48/80.

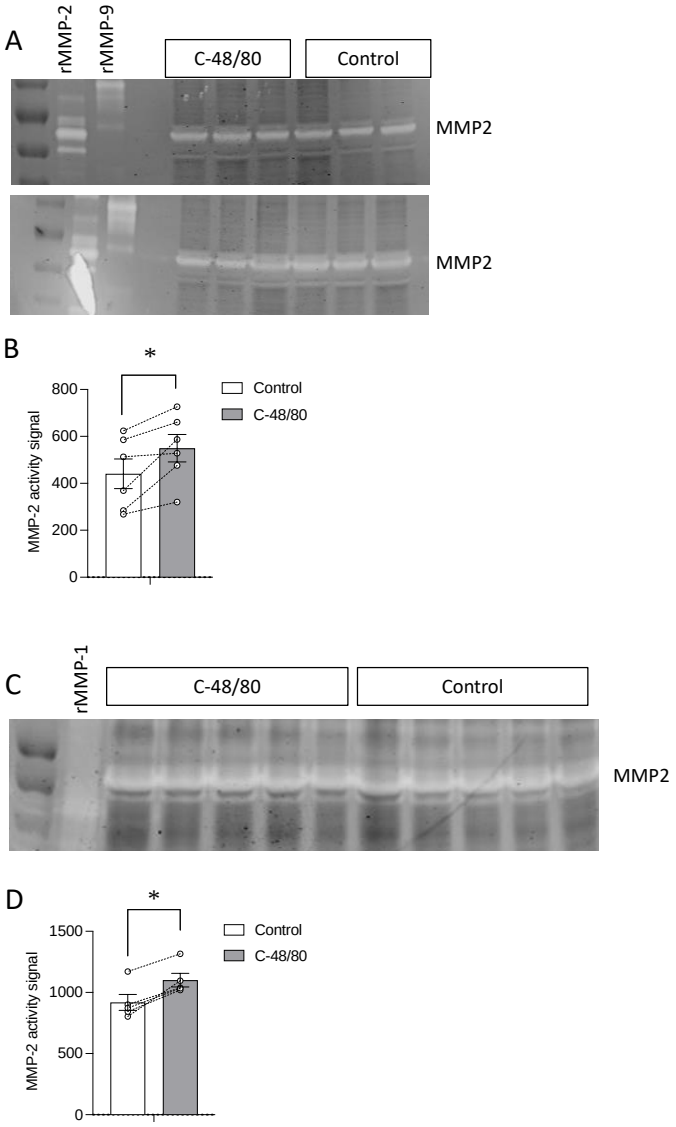

Figure 30 Compound 48/80 increases gelatinolytic and collagenolytic activity of MMP-2. (A) Gelatin zymograms showing MMP-2 activity of whole bladder protein exposed to vehicle or 10 µg/mL of compound 48/80 prior to protein isolation. Recombinant MMP-2 and MMP-9 were used as positive controls. MMP-2 active band is seen at 68 kDa. **(B)** Compound 48/80 significantly increases MMP-2 activity (P=0.0208, N=6). **(C)** Collagen zymograms showing MMP-2 activity of whole bladder protein exposed to vehicle or 10 µg/mL of compound 48/80 prior to protein isolation. Recombinant MMP-1 was used as a positive control. **D**, Compound 48/80 increased MMP activity with a band at a molecular weight consistent with MMP-2 but different than MMP-1 (P=0.002) *: $P \leq 0.05$. N=5.

4.4. Compound 48/80 significantly reduces TIMP activity

MMPs are endogenously regulated by their inhibitors, tissue inhibitors of metalloproteases (TIMPs) [82]. Specifically, TIMP-2 is primarily responsible for inhibiting MMP-2 [210]. We next explored compound 48/80's effects on TIMP-2-mediated inhibition of MMP-2 activity using reverse zymography (Figure 21A). In samples exposed to compound 48/80 prior to protein isolation, TIMP-2-mediated inhibition of MMP-2 activity was significantly reduced (Fig 21B). These data suggest that the effects of compound 48/80 on bladder compliance are due to a cumulative effect of increased MMP-2 activation and a relief of MMP-2 inhibition by TIMP-2.

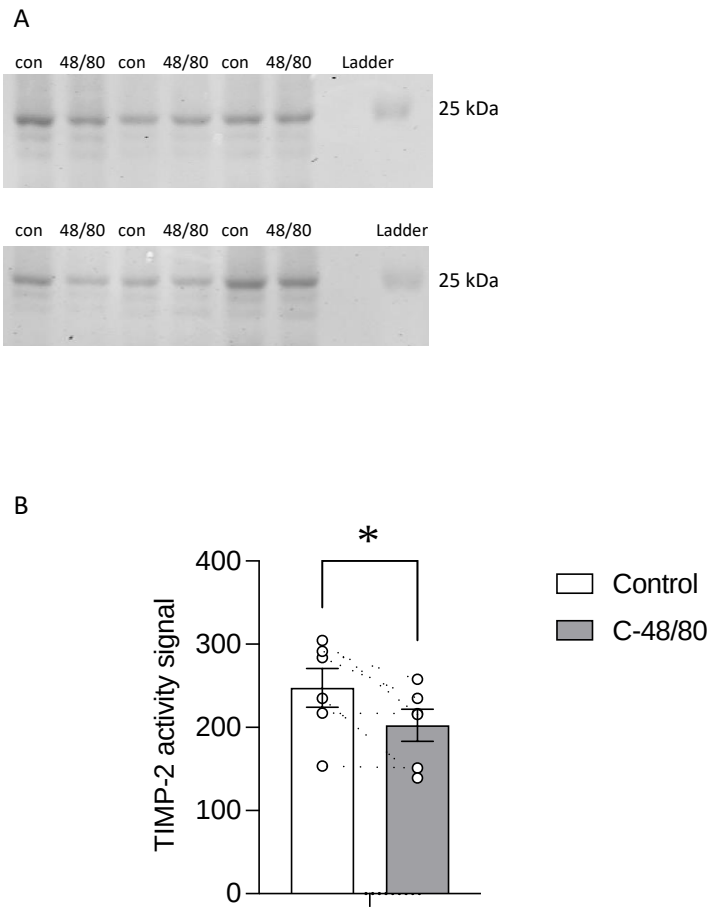

Figure 31 Compound 48/80 decreases TIMP-2 activity. (A) Reverse zymograms containing 0.3 mg/mL collagen type I and III and 5 ng MMP-2 as substrate to assess activity of TIMP-2 in whole bladder proteins exposed to either vehicle or 10 µg/mL compound 48/80 prior to protein isolation. TIMP-2 activity was observed at 24 kDa. **(B)** Compound 48/80 significantly reduced TIMP-2 activity thereby relieving the inhibition of MMP-2 (P=0.043). *: $P \leq 0.05$. N=6.

5. DISCUSSION

In this study, we used multi-photon microscopy, biomechanical measurements, and zymography to explore the mechanisms by which the Mrgprb2 receptor agonist compound 48/80 increases mechanical compliance of the bladder. We found that compound 48/80 administered intravesically reduces the thickness of bladder wall without increasing urothelial permeability. This effect of compound 48/80 aligns perfectly with its alteration of mechanical compliance due to increases in MMP activity, as a more compliant wall would experience increased stretch when held at constant pressure. An interesting finding of these studies is that the effects of Mrgprb2 agonism on MMP activity is a cumulation of both MMP-2 activation and TIMP inhibition. Together, these data suggest that: (1) the MMP-TIMP balance is altered downstream of Mrgprb2 activation; and (2) rapid and profound remodeling of bladder wall collagen due to Mrgprb2 activation does not affect urothelial permeability. Thus, the effects of compound 48/80 resemble an acute inflammatory state that profoundly alters the biomechanical behavior of the bladder wall and causes bladder overactivity [206] but does so while still maintaining the urothelial barrier.

5.1. *Collagen degradation and bladder wall biomechanics*

The deposition, degradation, and crosslinking of ECM components contribute greatly to the stiffness, dimensionality, and geometry of the extracellular space [211]. Since bladder ECM can also provide biochemical signals to cells and modulate cell behavior [212], its remodeling and composition have been examined for associations with inflammatory lower urinary tract symptoms (LUTS). Previous studies utilized fixed tissue samples of urinary bladder to evaluate changes in collagen expression and arrangement over periods of days to months [213]. Our study is the first of its kind to discover profound collagen remodeling in the bladder in fewer than 30

minutes. While gaps in knowledge about collagen turnover in healthy bladder tissue exist, detailed studies about how fast collagen is formed and degraded in other soft tissues (e.g., blood vessels) suggest that the two primary structural components of the bladder have very different turnover rates. In the vasculature, the turnover rate for elastin is less than 1% per year, whereas collagen fibers are degraded and synthesized continuously [205]. New procollagen can be synthesized in 1-2 hours but the aggregation of existing soluble collagens into collagen fibers takes as little as 20 minutes [214]. 3-10% of normal collagen type I fibrils are degraded every day by enzymes present in the extracellular matrix (MMPs, serine proteases etc.) [215, 216]. Thus, the arrangement and rearrangement of collagen fibers can be altered within minutes, but their actual degradation and synthesis may take longer. Since blood vessels show a similar ability to distend and respond to mechanical stimuli, similar rates of turnover and synthesis are likely occurring in the bladder as well. Our study provides new mechanistic evidence for rapid collagen rearrangement in the bladder wall being responsible for changes in compliance seen after Mrgprb2 receptor activation. After only ~20 minutes incubation with compound 48/80, bladder compliance increases, MMP-2 activity increases, and bladder wall thickness decreases. Together, these findings suggest that collagen remodeling is taking place.

The reduction of bladder wall thickness could arise due to two reasons: (1) mediators released downstream of Mrgprb2 agonism, such as ATP and prostaglandins [26], rapidly activate MMPs, and degrade both fibrillar and non-fibrillar collagens into smaller fragments that are then disposed away. This would imply that the increased compliance is due to a physical reduction in the ECM contents of the wall. (2) Collagen content is the same, but the fibers may have realigned themselves from their load-bearing alignment leading to increased stretch at a constant pressure. This would show an apparent reduction in wall thickness only because the bladder is

more stretched at constant pressure and the radius to thickness ratio is increased. Both scenarios would lead to an increased compliance thereby aligning with our findings in *ex vivo* experiments on the PRIM system. Through these findings we reveal how bladder function is not just by virtue of myogenic and neurogenic contributions, but the structural arrangement of ECM components is also critical.

5.2. MMPs and TIMPs in the bladder wall

While MMPs have been extensively studied as regulators of ECM turnover in physiological states of other soft tissues, studies exploring their pathological role in the bladder are largely limited to urothelial cancer and only focus on the transcriptional regulation of MMPs [217]. Our study is one of the first that outlines the pathophysiological role of rapid activation of bladder MMPs and their ability to alter the biomechanical properties of the bladder wall. Additionally, our study also shows both constitutive activity of MMPs (specifically MMP-2) as well as post-translational regulation of MMP-2 by TIMPs.

Spatial aspects of MMP-TIMP interaction play an important role in understanding their activity [77]. Out of the eight structural groups of MMPs, five of them are secreted into the pericellular space and three of them are membrane-bound [218, 219]. TIMPs are present in the ECM in a soluble form where they reversibly bind to MMPs in a 1:1 stoichiometric ratio to block their active site [220]. However, zymography assays are limiting in that they can assess gross changes in the amount of MMPs/TIMPs expressed in a sample but cannot assess the spatiotemporal characteristics of MMP-TIMP interactions because TIMPs dissociate from MMPs during electrophoresis. As such, the MMP activity noted in our experiments may be an over-estimation of *in vivo* activity and instead represent "potential" activity. Nonetheless, MMP activity was significantly increased by compound 48/80, with a parallel decrease in TIMP-mediated

inhibition. It is likely that these differences would be even more pronounced if better spatiotemporal analyses were possible. This conclusion is further supported by biomechanical assays, where pharmacological inhibition of MMP-2 blocked the *ex vivo* effects of compound 48/80 on mechanical compliance. During homeostasis, TIMP activity is inversely related to MMP activity to maintain the balance of ECM components [210]. Interestingly, our findings show the opposite effect; the resulting increase in mechanical compliance after exposure to compound 48/80 is not due to increased MMP-2 activity alone but also due to a relief of TIMP-2-mediated MMP inhibition. These results suggest that the effects on collagen fibers by the MMP-TIMP family are cumulative.

What is most surprising about our findings is compound 48/80 drives bladder wall remodeling without affecting urothelial permeability. Bladder inflammation is often caused experimentally by intravesical infusion of chemicals that specifically degrade the urothelial barrier, including protamine sulfate and acetic acid [221]. In our experiments, intravesical infusion of compound 48/80 had no effect on permeability; yet this same concentration was able to cause bladder overactivity in mice [206]. Given the relative impermeability of the urothelium to pharmacological agents [222], our findings also suggest that compound 48/80 is activating a receptor-mediated signaling cascade, possibly through Mrgprb2 receptors in umbrella cells. This in turn drives the release of ATP and prostaglandins to activate MMPs and initiate bladder wall remodeling. Our previous studies support this hypothesis, as both removal of the urothelium and purinergic receptor inhibition mitigated the effects of compound 48/80, as did inhibition of Mrgprb2 receptors by QWF [26, 206]. Further experiments will explore the expression of Mrgprb2 receptors throughout the bladder wall and will determine if this orphan receptor may be

a key player in transducing pro-inflammatory signals from within the urine into the bladder wall itself.

5.3. *MMP-2 independent effects of Mrgprb2 activation*

Results from our biomechanical assays show that inhibition of MMP-2 blocks the effects of compound 48/80 on compliance but not the effects on transient pressure events. Compound 48/80 alone significantly increases the amplitude and leading slope of transient pressure events, which are the primary drivers of sensory outflow to the central nervous system during bladder filling [35]. This effect persists in the presence of doxycycline and ARP100, implying that Mrgprb2 activation elicits a dual effect and both pathways are most likely independent of each other. It is possible that the effects of compound 48/80 on detrusor excitability are mediated by ATP, since inhibiting purinergic receptors prevented the increases in detrusor contractility caused by compound 48/80 [26]. Future experiments will determine the mediators released after Mrgprb2 activation that may trigger both or either pathway.

5.4. *Limitations*

Our study is not without limitations. While our method of analysis of the Z-stack images gives us an accurate representation of the thickness of collagen within the wall, the exact nature of the changes in collagen arrangement remain to be explored. Imaging of collagen arrangement in live tissue without sectioning or fixing is also necessary since fixation and embedding techniques changes the native arrangement of collagen thereby making it impossible to understand the dynamic nature of collagen cross-linking that affects compliance [223]. Future studies will focus on staining collagen in live tissue to accurately image its remodeling during filling in the presence or absence of compound 48/80. Additionally, actual measurements of afferent nerve activity are required to determine if bladder overactivity caused by compound 48/80 coincides

with increased sensory outflow and not due to rearrangement of the mechanosensory mechanisms present within the bladder wall.

5.5. Conclusions

In conclusion, activation of the orphan G protein-coupled receptor Mrgprb2 by compound 48/80 increases bladder wall mechanical compliance and increased the amplitude and leading slope of transient pressure events that drive sensory outflow during filling. Alterations in compliance occur due to collagen remodeling and degradation that are driven by MMP-2 activation and TIMP-2 inhibition. These processes also lead to a reduction of bladder wall thickness. Interestingly, despite this profound remodeling, the urothelial barrier remains intact. Together, these data suggest that the mechanical properties of the bladder wall can be influenced rapidly and profoundly by activation of Mrgprb2 receptors and that Mrgprb2 receptors represent an important linchpin between inflammatory signaling and mechanical behavior in the bladder wall.

OVERALL SUMMARY AND PERSPECTIVES

1. CONCLUSIONS

Lower urinary tract symptoms, such as overactivity and incontinence, have been observed in nature since the beginning of mankind; yet the scientific studies that originated to understand their mechanism from a biomechanical perspective are relatively new [224]. A vigorous analysis of bladder function at all structural levels is required to completely understand the intricate mechanisms of bladder dysfunction. Urodynamic studies that measure compliance, capacity, and overactivity are used to understand the biological aspects of bladder function [225], but the inherent mechanical characteristics of bladder tissue are not explored to the same extent. In the last decade, considerable progress has been made in our ability to model parts of the lower urinary tract [226] to understand the biomechanics of the bladder. Yet, a plethora of questions remain unanswered. Thus, the goal of this dissertation was to understand measures of bladder function, such as compliance and stiffness, with the help of a mathematical model of the murine urinary bladder in the absence of any disease. Additionally, we explored target proteins that alter the biomechanical properties of the bladder and their mechanisms. Results from the experiments outlined in chapters 2 and 3 show that a receptor that is part of known inflammatory pathways can be activated to rapidly and profoundly alter mechanical compliance via matrix metalloproteases.

1.1 Mas-related G protein-coupled receptor B2/X2

The orphan G protein-coupled receptor Mrgprb2, the mouse ortholog of the human MRGPRX2 receptor, is primarily characterized by its role in IgE-independent mast cell activation [227]. Mrgprb2/X2 was traditionally assumed to be expressed on mast cells, as well as keratinocytes in the skin, in some adipose tissue, and on cell bodies of some sensory neurons [136]. While prior research on the receptor has focused on the skin in context of MRGPRX2-dependent

anaphylactic reactions [228], urinary bladder has the third highest Mrgprb2/X2 mRNA of all tissues studied [141]. Therefore, effects of Mrgprb2 activation on bladder function piqued my interest and formed a basis for the experiments outlined in chapter 2.

The first aim of this dissertation was to determine the effects of the mast cell activator and basic secretagogue compound 48/80 on mechanical compliance and detrusor contractility. The research design consisted of a series of *ex vivo* experiments that provided a quantifiable measure of compliance as a representation of mechanical stress *vs.* spherical stretch using our mathematical model of the bladder shape. These experiments were combined with *in vivo* urodynamic measurements to assess the effects of compound 48/80 on voiding behavior. To confirm that the effects were due to Mrgprb2 receptors expressed on mast cells, two approaches were used: (1) *Ex vivo* filling of whole bladders in the presence of the Mrgprb2 antagonist QWF and compound 48/80; and (2) *ex vivo* filling of whole bladders and *in vivo* urodynamic studies using mice deficient in mast cells. We discovered not only the presence of Mrgprb2 in the bladder but also that it is functional in altering biomechanics independent of mast cells both *in vivo* and *ex vivo*.

The data presented in this dissertation outline the role of Mrgprb2 activation in the bladder and show that Mrgprb2 receptors may be key in the development of bladder dysfunction associated with inflammation. Overall, my findings makes two things clear: (1) Exploring the cell types that express Mrgprb2 is important because these cells must then be capable of inducing a signaling cascade that leads to increased compliance and excitability. (2) The dual nature of compound 48/80's actions makes this pathway extremely significant since targeting Mrgprb2/X2 could reduce both increased excitability and compliance associated with LUTS.

The mast cell independent effects of compound 48/80 also makes one question if the urothelial cell type that expresses Mrgprb2 does more than just act like a barrier. Much like keratinocytes, the stratified epithelial layer of the bladder may act as a proxy immune cell once this receptor is activated. This is not completely unprecedented, since urothelial signaling is increased during metabolic stress and inflammatory conditions [17]. Therefore, it is possible that the Mrgprb2 receptor expression within the urothelium is activated upon exposure to compound 48/80 leading to alteration of bladder biomechanics via increased urothelial signaling. My aims try to confirm this hypothesis by preliminary studies that can be carried forward in the future.

1.2 Mrgprb2 mediated remodeling of the extracellular matrix

The second and third aims of the dissertation focused on the effects of Mrgprb2 activation on the components of the ECM and how they are elicited. Specifically, for my second aim, experiments were designed to make sure collagen fibers can be visualized in pressurized live bladders to avoid any tampering with the native state of collagen introduced by cutting and fixing of tissue. Collagen was imaged using second harmonic generation with multi-photon microscopy. Since compound 48/80 driven inflammatory signaling occurs in vascular tissue due to permeabilization of the endothelium [229], it is possible that effects of compound 48/80 on the bladder were also due to urothelial damage and permeabilization. Hence, this aim also tested if intravesical administration of compound 48/80 altered collagen fiber arrangement due to increased urothelial permeability. FITC penetration through the wall was used as a measure of permeabilization [230] and 1% Triton X-100 was used as a positive control because of its ability to insert a detergent monomer into the lipid membrane leading to its permeabilization [231]. Surprisingly, compound 48/80 the thickness of the wall without altering urothelial permeability, suggesting that the

effects of compound 48/80 were not due to any physical damage to the urothelium but due to a pharmacological effect on Mrgprb2.

The third aim of this project was to determine the mechanistic pathway by which Mrgprb2 activation leads to remodeling of collagen fibers and the subsequent increase in mechanical compliance, a range of pharmacological evaluations were conducted. It was hypothesized that urothelial signaling increased after compound 48/80 activated Mrgprb2. Previous studies done in my lab had explored the effects of inhibiting COX and P2X receptors on Mrgprb2 mediated effects on bladder tissue strips [26], but no work was done on whole bladders. Thus, purinergic signaling and prostaglandin synthesis were explored as modulators of detrusor contractility [95, 232]. My experimental design was based on classic pathways associated with chemical-mediated urothelial activation and mediator release [233, 234]. Because of the alterations in mechanical compliance I observed, the MMP-TIMP family was also explored as being an integral part of the pathway that leads to ECM remodeling. Broad spectrum MMP inhibitor doxycycline and specific MMP-2 inhibitor ARP100 blocked the increase in mechanical compliance caused by compound 48/80 but did not prevent the increased detrusor contractility. Additionally, compound 48/80 increased MMP-2 activity and reduced TIMP-2 activity after 30 minutes. Overall, my results suggested that Mrgprb2 activation has a cumulative effect on activities of MMP-2 and TIMP-2 in that, it simultaneously increases MMP-2 activity and relieves TIMP-2 inhibition of MMP-2 implying a net increase of MMP activity. These results indicate that the balance of MMP-TIMP activity can be altered within minutes and Mrgprb2 is likely a modulator of that balance.

1.3 Proposed pathway for the dual effects of Mrgprb2

Overall, results outlined in chapter 3 suggest that compound 48/80 activates Mrgprb2 in the urothelium to trigger release of mediators (including ATP and prostaglandins) that signal downstream to activate MMPs while simultaneously increasing detrusor contractility. My hypothetical pathway is based on several studies: First, previous experiments including those done in my lab show that it is perhaps an entourage effect of multiple prostaglandins (Prostaglandin E_2, Prostaglandin F_2, and thromboxane) that drive effects of compound 48/80 on contractility [26, 232]. Second, studies on rodent and human bladders that characterize the role of all seven P2X receptors and several P2Y receptors are well established [235, 236]. It is also implied that urothelium-derived ATP could directly or indirectly (via interstitial cells) alter detrusor contractility [237]. Third, ATP stimulation led to increased MMP-9 release from monocytes within 30 minutes and this increase was blocked by $P2X_7$ inhibition [237]. Lastly, in aortic smooth muscle cells, ATP stimulated MMP-2 release leading to collagen remodeling implying that purinergic signaling may provide a mechanistic link between biomechanical stress and inflammation [76].

Based on all my findings and previous literature, I propose the following pathway should be explored. First, compound 48/80 activates Mrgprb2 receptors expressed on the serosal membrane of umbrella cells. This assumption is made due to persistent effects of compound 48/80 irrespective of its administration in the bath or intravesically. Then, ATP (among other mediators) is released via pannexin and/or connexin hemichannels to act directly on P2X receptors expressed on detrusor smooth muscle cells. Alternatively, it is also possible that exogenous prostaglandins are synthesized and released from detrusor muscle upon ATP stimulation to increase detrusor contractility. Urothelial-derived ATP can also act on the

interstitial cells and/or detrusor smooth muscle cells to activate MMP-2 or release more active MMP-2 that would drive remodeling of collagen fibers in the ECM.

2. NOVEL FINDINGS

This dissertation outlines the nature and mechanism of the paradoxical effects of compound 48/80 on bladder function, and many findings have both significance and novelty. First, quantification of biomechanical properties in a whole bladder can be achieved accurately and precisely using our custom designed Pentaplanar reflected image macroscopy (PRIM) system and a custom developed mathematical model that accurately predicts the shape of the bladder as it fills *ex vivo*. Chapter 2 outlines the mathematical derivation used to create the formulae that we used to calculate wall stress, spherical stretch, and the wall thickness of empty bladder. While we know that changes in compliance accompany LUTS [238], studies that correlate altered compliance to OAB do not provide conclusions that are in consensus. Hence, my methods attempt to develop a model to specifically calculate alterations in mechanical compliance with simultaneous alterations in detrusor excitability.

Methods to measure clinical "compliance" exist; however, they are often inaccurately defined. As such, traditional clinical measures of compliance gives incomplete information since they don't account for changes in wall geometry influencing compliance. My experiments employed mathematical models that were designed to accurately calculate mechanical compliance, wall stress, and linearized stiffness of whole bladders. We measured bladder wall thickness and area to calculate wall stress and stretch as a measure of compliance [239]. The slope of the elastic (linear) region of a stress-stretch curve is equal to the linearized stiffness [158] indicating that we can derive information about the of the material properties of the bladder wall such as stiffness and elasticity along with compliance. Figure 18 shows that in the case of our experiments, conclusions deduced from comparing clinical compliance are similar to those deduced from analyzing mechanical compliance. However, the ability to determine continuous changes in

stretch and stiffness as the bladder pressurizes brings information about the material properties of bladder wall that was impossible to glean from clinical measurements of bladder pressure and volume alone. Additionally, it may be that the conclusions derived from both measures of compliance are similar in this isolated incident and this is not the case always. Hence, the stress-stretch curve is a better representation of the stiffness that the bladder wall inherently possess. My method uses the imaging data that we obtain from *ex vivo* experiments on the PRIM system to assess the geometrical parameters of bladder filling that are used to then calculate wall stress and stretch. My techniques show that more accurate measurements of the biomechanical properties of the bladder can be made when we consider changes in geometry of the bladder wall.

Second, data collected in chapter 2 also shows that profound changes in mechanical compliance can occur upon compound 48/80 exposure for 10-20 minutes. Surprisingly, increase in compliance was accompanied by a paradoxical increase in the amplitude and leading slope of transient pressure events suggesting that, while bladder wall can stretch more, the afferent outflow is likely increased [35]. These results were counterintuitive because, generally, bladder overactivity is associated with a decreased wall compliance [169]. Much like bladder wall alterations during spinal cord injury in rat bladder overactivity models where distensibility is increased [153], my results could mean that bladder wall remodeling begins with an initial loss of fibrillar collagens (increased compliance and overactivity) followed by deposition of improperly arranged collagen (decreased compliance and overactivity).

Third, my study shows that *Mrgprb2* receptors are expressed outside of mast cells and can be activated by the prototypical mast cell activator compound 48/80 suggesting that thee receptors are not only expressed outside of mast cells but they are functional. Effects of compound 48/80

on both compliance and contractility combined with the results obtained in chapter 3 imply that inflammatory mediators may be released downstream of Mrgprb2 activation. Traditionally, Mrgprb2 activation on mast cells release mediators such as histamine that could directly alter contractility [116]. Hence, it is likely that the cell type that expresses Mrgprb2 receptors in the urothelium acts like quasi-immune cells to drive ECM remodeling and overactivity. The significance of these findings are two-fold, in that I determined Mrgprb2 receptors are expressed in bladder umbrella cells, and I identified a quasi-immune role of umbrella cells that was not explored before.

Fourth, chapter 3 outlines the role of MMP mediated bladder ECM remodeling after Mrgprb2 agonism. To my knowledge, this is one of the first studies to determine changes in MMP activity in the absence of translational modifications upon activation of an inflammatory pathway in the bladder. Most studies that show MMP mediated alterations in bladder function talk about it only with respect to bladder cancer. My results indicate that the MMP and TIMP activities can be altered due to rapid inflammation and lead to ECM remodeling.

Lastly, it is likely from my findings that Mrgprb2 receptor activation increases urothelial signaling that leads to bladder wall remodeling and these effects occur without permeabilizing the urothelial barrier. This is one of the most interesting findings of my studies since it suggests that intravesical infusion of compound 48/80 may be a viable model for interstitial cystitis. Current models of IC/BPS have many shortcomings that make studies to understand pathophysiology of IC/BPS difficult. Bladder-centric models of interstitial cystitis use chemical irritants to mimic the pathological conditions of the bladder wall during cystitis. However, these studies are not entirely translational since even low doses of some of these irritants cause severe inflammation in the wall and denude the umbrella cell layer [240]. Hence, these models are more

aligned to acute hemorrhage which is not typical for either IC or BPS [241]. With compound 48/80 incubation, we observe bladder overactivity and increased compliance without any cell lysis or urothelial damage. Additionally, using compound 48/80, one may be able to analyze the changes in ECM structure and arrangement that occurs during IC/BPS giving us more information than just modulations in the neuronal pathway. An IC/BPS model that uses compound 48/80 is extremely significant to explore to uncover the pathological changes associated with inflammation.

3. LIMITATIONS AND ALTERNATIVES

My studies are not without shortcomings. There are many limitations in my experimental design, most of which are described in this section. Broadly, we assessed the effects of compound 48/80 on Mrgprb2 but these findings were not translated to the human ortholog, MRGPRX2. Moreover, the results were only obtained using 9–12-week-old male mice thereby limiting my conclusions with respect to sex and age differences.

3.1 Experimental Design

My experimental design does not account for sex or age differences that affect bladder function. Most inflammatory LUTS (IC/BPS) affect women more than men. There is also an increase in prevalence of LUTS with age [242]; however, studies presented in this dissertation were done on non-diseased bladders collected from male mice aged 9-12 weeks (mature adults). This was only done due to the simplicity of my research design. Additionally, my aims attempt to form a preliminary understanding about how labile the biomechanical characteristics of the bladder wall are in the presence of an inflammatory event and future studies will look at sex differences as well as disease models such as diabetes and aging.

In chapter 2, gelatin and collagen zymography was done to evaluate MMP and TIMP activity in the bladder after exposure to compound 48/80. However, zymography assays only provide a representation of total "potential activity" in the tissue. The spatial characteristics of MMP activation and TIMP inhibition of MMPs are lost during electrophoresis and the in-gel activity is always a more pronounced than in tissue [243]. This is because of the MMP2-TIMP2 interaction during their activation and inhibition. During electrophoresis, TIMP-2 dissociates from MMP-2, releasing the active MMP-2 and making activity seem more pronounced than it is *in vivo*. While it still acts as a great preliminary tool to measure MMP activity since any overestimation of

activity is consistent in all samples, more accurate measures of activity in real space and time can be made using *in situ* or *in vivo* zymography in the future. *In situ* zymography uses histological sections coated with fluorescent labelled matrix proteins where MMP activity can be observed as black holes on a fluorescent background. Even in the absence of in situ zymography results, my findings from in vitro zymography when combined with ex vivo biomechanical measurements provide a solid basis for my proposed pathway. The increase in compliance due to Mrgprb2 activation is prevented by MMP inhibition suggesting that MMPs are most likely a part of this pathway.

3.2 Measuring compliance as a mechanical measurement

Chapter 2 discusses the detailed method that was developed to measure compliance of murine bladders as they fill *ex vivo*. My methods use mechanical measurements of stress and stretch to calculate wall compliance however this was only possible during *ex vivo* filling. This method does not account for the abdominal pressure and its effects on the mechanical stress of the bladder wall. This is an important factor to account for since inside the body, the bladder pressure rises despite the forces on the bladder by virtue of neighboring organs. Abdominal pressure is not accounted for in our *ex vivo* setup due to two reasons. First, the Laplace law of stress that we apply to measure mechanical stress assumes that force on the outside of the wall is zero hence, this law cannot be applied if we account for abdominal pressure. Second, there is no way of measuring a consistent and accurate value of abdominal pressure inside the mouse since it varies due to several factors including breathing, digestion, body movement etc. Despite this limitation, the overall essence of our methods remains true; geometrical parameters influence wall compliance and should be accounted for. Similar measurements of bladder geometry can be taken in human bladders using ultrasound techniques [139] along with intravesical pressure

recordings. This would not only account for real time increases in intravesical pressure as an opposite entity to abdominal pressures but also account for the influence bladder wall geometry has on compliance.

3.3 Specificity of compound 48/80 on Mrgprb2

Basic secretagogues, such as substance P, compound 48/80, cortistatin-14, and PAMP 9-20, bind to Mrgprb2 and MRGPRX2, but also to their canonical targets NK-1 receptors and somatostatin receptors, respectively [139]. Similar to the agonists, antagonists that bind to Mrgprb2 and MRGPRX2 receptors (e.g., QWF) also block NK-1 [193]. The pharmacology of these agonists differs greatly between MRGPRX2, Mrgprb2 and their canonical receptors. For example, the affinity of substance P for NK-1 receptors is ~0.5 nM, for MRGPRX2 is ~150 nM and for Mrgprb2 is ~50 μM [176]. Due to a lack of specific compounds that only bind to Mrgprb2/X2, my studies are limited to using NK-1R agonists and antagonists. Even though NK-1R receptors are explored more in depth with respect to neuroinflammatory pathways that lead to bladder dysfunction, it is very difficult to compare the effects of NK-1R activation and Mrgprb2/X2 activation because of large discrepancies in their pharmacology. In the bladder, substance P and neurokinin A released from afferent nerve fibers can increase smooth muscle contractility mediated via NK-1 and NK-2 receptors [244]. Hence, it is possible that the effects due to compound 48/80 are mediated via NK-1R instead of Mrgprb2. Using specific NK-1R and NK-2R antagonists that have no affinity to Mrgprb2/X2 with compound 48/80 is necessary to confirm the Mrgprb2 mediated effects of compound 48/80. NK-1R KO mice can also be developed and used for the same purpose but neither of these approaches were used in my study. These approaches weren't used because my study acted as a preliminary measure to characterize

the effects of compound 48/80 on healthy mouse bladders. Even if the receptor mediating these effects is not Mrgprb2, the mechanism of these effects remain relevant and worth exploring.

Mrgprb2 is the mouse ortholog of orphan human GPCR MRGPRX2 [139]. Mouse models have been a great contribution to study MRGPRX2 receptor pharmacology since Mrgprb2 recognizes and binds to the same agonists as its human ortholog but, the huge difference in the affinities makes it difficult to translate the effects of Mrgprb2 to human MRGPRX2. My study does not show if the effects we see on Mrgprb2 using compound 48/80 would persist in humans. Humanized MRGPRX2 mice can be used in the future as a more translational approach to study the receptor.

4. FUTURE DIRECTIONS

4.1 Specificity, role, and location of Mrgprb2/X2

My studies use mouse models to study the effects of basic secretagogue compound 48/80 on bladder wall biomechanics but the specificity, exact location, and the translated effects of Mrgprb2/X2 were not revealed. First, to assess if the actions of compound 48/80 on compliance and contractility are Mrgprb2 mediated, the NK-1R antagonist aprepitant can be used with compound 48/80. This would shut off the effects of NK-1R; if the alteration in compliance and contractility persists, we would conclude that the effects of compound 48/80 on compliance and contractility are mediated via Mrgprb2. *Mrgprb2* KO and *NK-1R* KO mice could also be developed to confirm the specificity of effects that we study.

Second, more experiments need to be performed to determine if the effects of activating MRGPRX2 are the same as activating Mrgprb2. The experiments outlined in Chapter 2 hinged on the fact that Mrgprb2 and its human analogue MRGPRX2 share similar agonists and antagonists. Even though that is true, they differ greatly in their pharmacology [176]. My experiments need to be expanded further to determine if the effects of compound 48/80 persist on MRGPRX2. This is even more significant since there are no studies to my knowledge that explore the role of MRGPRX2 in driving inflammatory LUTS independent of mast cells. One of the most important findings of Chapter 2 is the effects of Mrgprb2 activation independent of mast cells and the mRNA expression of *Mrgprb2* in mast cell deficient mouse bladders. If this is true for human bladders as well, MRGPRX2 may represent a great target for LUTS outside of traditional inflammatory cells and molecules. Recently, humanized mouse models were developed by engraftment of human hematopoietic stem cells into an immune compromised mouse [245]. These mice express human mast cells and thus, MRGPRX2 is expressed on their

MCs instead of Mrgprb2. Similarly, mast cells transfected with MRGPRX2 can be used to aid in drug screening [120]. To accurately expand my studies, a humanized mouse model is needed that expresses MRGPRX2 everywhere Mrgprb2 is traditionally expressed. This would include all cell types even outside of mast cells and can be done using the CRISPR/Cas 9 system that can generate effective gene replacements. *Ex vivo* studies could be repeated using this mouse model to confirm the effects of compound 48/80 on compliance and detrusor excitability. While compound 48/80 is the canonical drug used to activate Mrgprb2/MRGPRX2, my experiments use no endogenous ligands to confirm the physiological relevance of these effects. This was only because the potency of substance P on Mrgprb2 is extremely low. Using humanized mouse models, the effects of compound 48/80 can be compared to those of substance P.

Third, we found that Mrgprb2 mRNA is expressed in mast cell-deficient mice as well, but no further data was shown regarding the expression of Mrgprb2 receptor protein. Figure 22 shows expression of Mrgprb2 receptors in the whole body of the mouse. Receptor expression throughout the skin aligns with previous findings [120]. Expression is also observed in the lower urinary tract, including in urethra, bladder, ureters, and the renal medulla. To explore specific bladder cell types that expresses Mrgprb2 receptor, bladders were pinned flat and visualized under a fluorescent microscope (Figure 23). Umbrella cells that can be morphologically identified by their shape express Mrgprb2 receptors. In the future, the Mrgprb2-ATG-Salsa6f mice can be used to study if Mrgprb2 receptors are expressed in cells other than umbrella cells. Cells can be separated using flow cytometry to then study the pathway downstream of Mrgprb2 using assays such as ELISA or more advanced Luminex assays. This is necessary to identify what G-protein Mrgprb2 is coupled with and if other intracellular pathways are activated upon its activation. Recently, umbrella cells have been studied for their intracellular calcium signaling

that promotes downstream pathways such as ATP signaling. Computational models also show the development of Piezo1 mediated calcium profiles on the apical surface [246]. I presume that my Mrgprb2-ATG-Salsa6f mouse model can be used to confirm these studies and provide a deeper analysis on calcium events within the umbrella cells. Additionally, this would further redefine the functions of umbrella cells that were previously assumed to be a barrier between urine and underlying bladder layers.

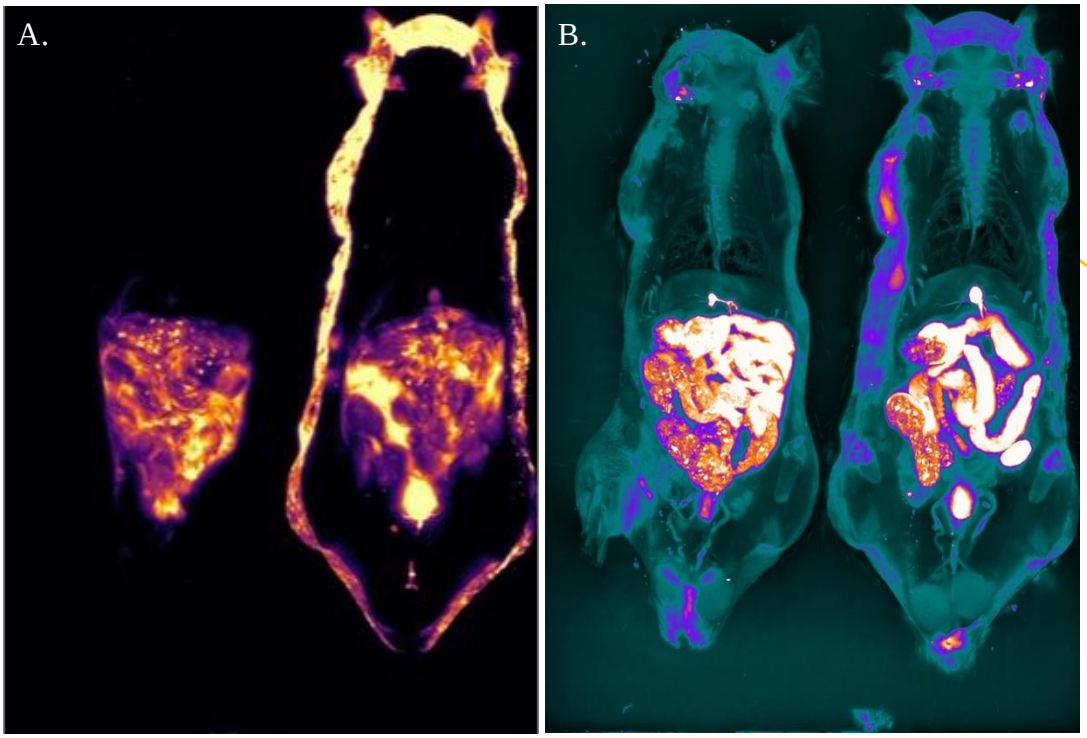

Figure 32 Mrgprb2 receptor expression in the whole mouse body. Mrgprb2-ATG-Salsa6f mice were embedded in OCT and imaged under XERRA imaging platform. Fluorescent images were taken for every 50 µm z-slice in the 555 nm (**A)** and 470 nm **(B)** channels. Wild-type C57Bl/6 mice were used as negative controls. **A,** Image shows a cross sectional view of WT-mice (left) and Mrgprb2-Salsa6f mouse (right). Mrgprb2 receptor expression (orange) can be seen in the skin and the urinary bladder (yellow arrows). Alfalfa (chlorophyll) rich diet fed to mice leads to autofluoresence in the abdominal region. B, Images obtained using the 470 nm channel showing the outline of both WT and Mrgprb2-Salsa6f mice. Receptor expression (white) can be seen in the bladder ad the skin (yellow arrows). (N=1)

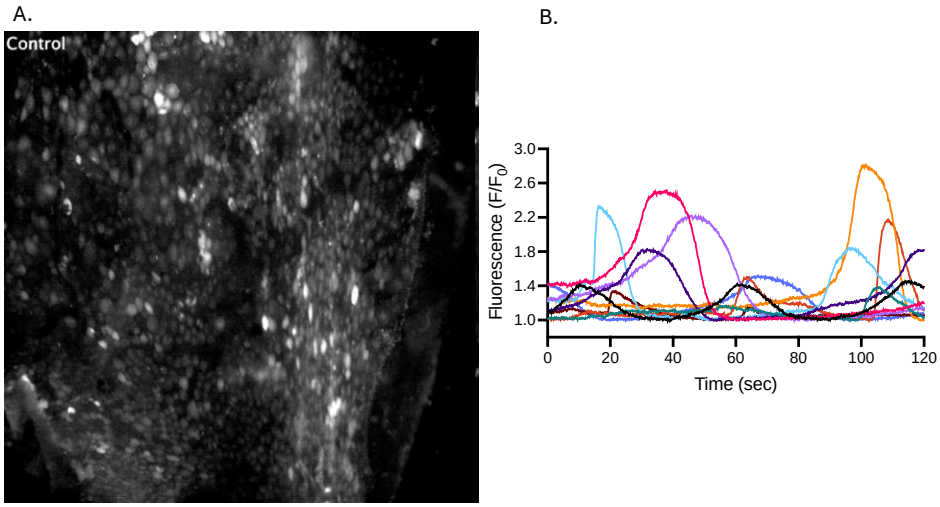

Figure 33 Mrgprb2 receptor expression in the urinary bladder. Bladder was dissected from Mrgprb2-Salsa6f transgenic mouse, pinned flat in a dish filled with Ca^{2+} containing PSS. Fluorescence intensity was measured for Mrgprb2 receptor expression. **A**, Urothelium side up bladder showing fluorescence in umbrella cells. **B**, Plot of fluorescence intensity ratio vs. time suggesting changes in fluorescence during video recording of the sample. Different colors represent different cells that were quantified. (n=10 cells from N=1 mouse)

4.2 Collagen arrangement in the bladder wall

My aims focus on visualizing collagen in living whole bladders. This becomes difficult as most microscopic techniques require the stability and resolution of fixed and sectioned tissue. Even though fixing tissues preserve the "life-like state" of cells and tissues, it also changes the inherent arrangement of ECM proteins [223]. In my experiments outlined in chapter 3, we used SHG signal generated by collagen fibers in whole bladders to assess the presence of collagen within the wall. However, due to the curvature of a full bladder, z-stacks were viewed perpendicularly to only study wall thickness. The complex arrangement of collagen fibers that could be obtained by viewing en face images were not observed hence, *en face* images were not studied. I also used a novel collagen hybridizing peptide (CHP) dye that specifically binds to degraded collagen [247] (Figure 24). These images show a stark difference between collagen fiber shape and tortuosity, but its specificity to degraded collagen is not observed. These experiments could either suggest that cutting the bladder tissue into strips imparts enough injury to the ECM and leads to remodeling of collagen fibers or that the CHP dye is not as specific as it promises to be. The former is unlikely because degradation was seen throughout the strip and not only on the edges. It could also mean that the constant stretch imparted on the bladder wall as it fills leads to the dynamic remodeling of collagen fibers. In the future, more data will be gathered using the same dye and *en face* images of collagen fibers visualized through SHG will be studied. Now that custom-designed imaging chambers exist, the CHP dye could also be instilled within the bladder to study collagen fiber arrangement in a full bladder. CHP dye can also be used in conjunction with Mrgprb2/X2 antagonists and MMP inhibitors to confirm if the collagen degradation we observe is mediated via Mrgprb2 and MMPs.

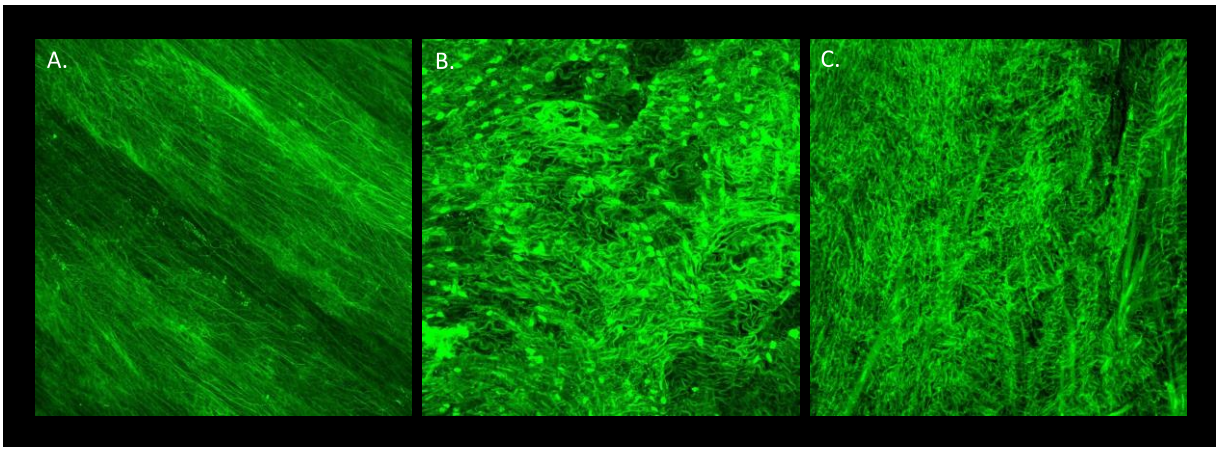

Figure 34 Compound 48/80 rapidly degrades collagen fibers. Bladder strips were pinned flat urothelium side up and exposed to either vehicle, compound 48/80 or 80° C heat for 30 minutes. Specific collagen hybridizing peptide was then put in the dish for 15 minutes and the dish was covered. **A,** Straight and stretched collagen fibers are visible in the unexposed strip **(B)** 10 µg/mL compound 48/80 degrades collagen fibers and breaks them into smaller fragments **(C)** Heat exposure also degrades collagen but the fibers appear more coiled than broken.

4.3 Effects of compound 48/80 on muscle contractility

Chapter 3 shows the dual effects of compound 48/80 on mechanical compliance and transient pressure events. Chapter 4 follows up with studies done to explore the mechanisms that drives increases in compliance; however, the increases in amplitude and leading slope of transient pressure events is not explored further. Non-voiding contractions that take place as the bladder fills plays a role in driving sensations of fullness to the brain [35]. Surprisingly, it was not the amplitude of each contraction but the rate of rise that is directly correlated to the magnitude of afferent outflow from the bladder to the central nervous system. Mrgprb2 activation increases compliance but paradoxically increases afferent outflow as measured via the leading slope of TPEs. Hence, properties of the transient pressure events are interesting to explore upon compound 48/80 incubation. Figure 2 shows that the effects of compound 48/80 on compliance and contractility are indeed both mediated by ATP. It is possible that activation of Mrgprb2 expressed on umbrella cells leads to release of ATP that increases detrusor contractility while also increasing MMP activity. Similar to the future experiments explained in section 4.1, separated cells or tissue extracts could be used to measure ATP release using colorimetric assays. Other than ATP, prostaglandins were also explored as a cause for increased contractility. The COX inhibitor indomethacin was also able to inhibit the dual effects of compound 48/80 (Figure 3). The proposed pathway for dual effects of compound 48/80 explains the possibility of ATP and prostaglandin release when mechanical stretch is induced hence, both modulators were explored.

4.4 Matrix metalloproteases and their role in driving LUTS

Chapter 4 of this dissertation outlines the mechanism by which compound 48/80 increases mechanical compliance. The most interesting finding from my experiments was the cumulative effects of MMP-2 activity and TIMP-2 inhibition on bladder ECM. We studied MMP-2 because: (1) it is the common MMP that degrades both non-fibrillar and fibrillar collagen types and (2) activated MMP-2 can further activate other MMPs to degrade their specific substrate [218]. My findings suggest that the balance of MMP and TIMP activity is extremely labile and influences the bladder biomechanics. While I lay a strong foundation for my hypothesis that MMPs drive alteration in mechanical compliance, more detailed studies are needed. MMPs have only been studied in bladder dysfunction in relation to bladder cancer. Hence, the role that MMP-TIMP imbalance plays in driving LUTS is not fully understood. Also, the techniques available to study this role are also not very well outlined. *In situ* proximity ligation assays could be performed to study MMP-TIMP interaction in the absence or presence of compound 48/80. This can also be done prior to taking mechanical measurements or collagen imaging to confirm if it is in fact MMP activity that leads to alteration in bladder biomechanics.

Another interesting finding that we bring to light is the effect of compound 48/80 on TIMP-2 activity. We show that inhibition of MMP-2 activity via TIMP-2 can be relieved by compound 48/80 and additively impact compliance. My conclusions need more evidence to confirm if the actions of compound 48/80 are due to proteolytic inactivation or just rapid degradation of TIMPs i.e., less activity was seen because less protein was present. The best approach to analyze MMP-TIMP interaction would be to perform *in situ* MMP-TIMP proximity ligation assays. This would not only give us information about their activity state but also help measure MMP-TIMP ratios.

5. PERSPECTIVES

Lower urinary tract symptoms significantly impact the quality of life of approximately 60% of the combined population with a slightly higher rate of incidence in men than women [83]. Pharmacological interventions including antimuscarinics and ß-3 agonists only seem to alleviate the symptoms of bladder dysfunction and are temporarily effective. Therefore, we studied the pseudo-inflammatory receptor Mrgprb2 [135] for its role in driving alterations in the bladder wall ECM and detrusor excitability to reveal new druggable targets for bladder dysfunction.

Overall, Mrgprb2/MRGPRX2 may seem like a very minor part of a bigger and more complex pathway. But, my studies show that activation of these receptors expressed on umbrella cells can rapidly alter wall compliance and increase excitability. Hallmark findings in this dissertation are indicative of the labile nature of bladder ECM. Even in the absence of any disease, an inflammatory pathway can trigger changes in stretch and stiffness, implying that inflammation may be an underlying cause for many bladder diseases that have not previously been explored as inflammatory in nature. Hence, it is worth exploring the effects of known inflammatory modulators on bladder wall biomechanics. The continuous remodeling of bladder ECM also implies that some level of remodeling may be reversible. If there are physiological processes by which collagen fibers rearrange themselves constantly, they can also be explored as a target for long term treatments for fibrosis in other organs as well. Even though our results imply that Mrgprb2 activation elicits a dual effect on bladder function (compliance and detrusor contractility) mediated via MMPs, ATP, and prostaglandins, it is likely that more mediators are involved that will be assessed in future studies.

BIBLIOGRAPHY

1. Hennig, G., et al., *Quantifying whole bladder biomechanics using the novel pentaplanar reflected image macroscopy system*. Biomechanics and Modeling in Mechanobiology, 2023.

2. Tykocki, N.R. and F.C. Monson, *Chapter Ten - Excitability and contractility in arterioles and venules from the urinary bladder*, in *Current Topics in Membranes*, W.F. Jackson, Editor. 2020, Academic Press. p. 301-326.

3. Cauwe, B. and G. Opdenakker, *Intracellular substrate cleavage: a novel dimension in the biochemistry, biology and pathology of matrix metalloproteinases.* Crit Rev Biochem Mol Biol, 2010. **45**(5): p. 351-423.

4. Jetti., S.R.B.N.O.R., *Histology, Bladder.* StatPearls, 2021.

5. Aitken, K.J. and D.J. Bagli, *The bladder extracellular matrix. Part I: architecture, development and disease.* Nat Rev Urol, 2009. **6**(11): p. 596-611.

6. Engel, P., L. Anagnostaki, and O. Brændstrup, *The Muscularis Mucosae of the Human Urinary Bladder.* Scandinavian Journal of Urology and Nephrology, 1992. **26**(3): p. 249-252.

7. Gentile, R., et al., *[Comparative microscopic anatomy of the urinary bladder of various domestic and wild ruminants].* Boll Soc Ital Biol Sper, 1984. **60**(8): p. 1473-9.

8. Apodaca, G., E. Balestreire, and L.A. Birder, *The uroepithelial-associated sensory web.* Kidney Int, 2007. **72**(9): p. 1057-64.

9. Bolla SR, O.N., Amraei R, et al. , *Histology, Bladder*. 2024, StatPearls.

10. Jafari, N.V. and J.L. Rohn, *The urothelium: a multi-faceted barrier against a harsh environment.* Mucosal Immunology, 2022. **15**(6): p. 1127-1142.

11. Khandelwal, P., S.N. Abraham, and G. Apodaca, *Cell biology and physiology of the uroepithelium*. American Journal of Physiology-Renal Physiology, 2009. **297**(6): p. F1477-F1501.

12. Hicks, R.M., *The mammalian urinary bladderan accommodating organ.* Biological Reviews, 1975. **50**(2): p. 215-246.

13. Carattino, M.D., et al., *Bladder filling and voiding affect umbrella cell tight junction organization and function.* American Journal of Physiology-Renal Physiology, 2013. **305**(8): p. F1158-F1168.

14. Yu, W., P. Khandelwal, and G. Apodaca, *Distinct apical and basolateral membrane requirements for stretch-induced membrane traffic at the apical surface of bladder umbrella cells.* Mol Biol Cell, 2009. **20**(1): p. 282-95.

15. Truschel, S.T., et al., *Stretch-regulated exocytosis/endocytosis in bladder umbrella cells.* Molecular biology of the cell, 2002. **13**(3): p. 830-846.

16. Birder, L.A. and W.C. de Groat, *Mechanisms of Disease: involvement of the urothelium in bladder dysfunction.* Nature Clinical Practice Urology, 2007. **4**(1): p. 46-54.

17. Birder, L. and K.-E. Andersson, *Urothelial Signaling.* Physiological Reviews, 2013. **93**(2): p. 653-680.

18. Birder, L.A., et al., *Adrenergic-and capsaicin-evoked nitric oxide release from urothelium and afferent nerves in urinary bladder.* American Journal of Physiology-Renal Physiology, 1998. **275**(2): p. F226-F229.

19. Chess-Williams, R., *Muscarinic receptors of the urinary bladder: detrusor, urothelial and prejunctional.* Autonomic & autacoid pharmacology, 2002. **22**(3): p. 133-145.

20. Vial, C. and R. Evans, *P2X receptor expression in mouse urinary bladder and the requirement of P2X1 receptors for functional P2X receptor responses in the mouse urinary bladder smooth muscle.* British journal of pharmacology, 2000. **131**(7): p. 1489-1495.

21. Wang, E.C., et al., *ATP and purinergic receptor–dependent membrane traffic in bladder umbrella cells.* The Journal of clinical investigation, 2005. **115**(9): p. 2412-2422.

22. Kanai, A., et al., *Origin of spontaneous activity in neonatal and adult rat bladders and its enhancement by stretch and muscarinic agonists.* American Journal of Physiology-Renal Physiology, 2007. **292**(3): p. F1065-F1072.

23. Chaiyaprasithi, B., et al., *Inhibition of human detrusor contraction by a urothelium derived factor.* The Journal of urology, 2003. **170**(5): p. 1897-1900.

24. Ferguson, D., I. Kennedy, and T. Burton, *ATP is released from rabbit urinary bladder epithelial cells by hydrostatic pressure changes--a possible sensory mechanism?* The Journal of physiology, 1997. **505**(Pt 2): p. 503.

25. Lewis, S.A. and J.R. Lewis, *Kinetics of urothelial ATP release.* American Journal of Physiology-Renal Physiology, 2006. **291**(2): p. F332-F340.

26. Jones, B.M., G.C. Mingin, and N.R. Tykocki, *The mast cell stimulator compound 48/80 causes urothelium-dependent increases in murine urinary bladder contractility.* Am J Physiol Renal Physiol, 2023. **325**(1): p. F50-f60.

27. Wang, X., et al., *Evidence for the Role of Mast Cells in Cystitis-Associated Lower Urinary Tract Dysfunction: A Multidisciplinary Approach to the Study of Chronic Pelvic Pain Research Network Animal Model Study.* PLoS One, 2016. **11**(12): p. e0168772.

28. Motta, P., *Ultrastructure of smooth muscle*. Vol. 8. 2012: Springer Science & Business Media.

29. Karl-Erik Andersson, a.A.A., *Urinary Bladder Contraction and Relaxation: Physiology and Pathophysiology.* Physiological Reviews, 2004. **84**(3): p. 935-986.

30. Andersson, K.-E., *Detrusor contraction.* Scandinavian Journal of Urology and Nephrology, 2004. **38**(215): p. 54-57.

31. Fetscher, C., et al., *M(3) muscarinic receptors mediate contraction of human urinary bladder.* Br J Pharmacol, 2002. **136**(5): p. 641-3.

32. Matsui, M., et al., *Increased relaxant action of forskolin and isoproterenol against muscarinic agonist-induced contractions in smooth muscle from M2 receptor knockout mice.* J Pharmacol Exp Ther, 2003. **305**(1): p. 106-13.

33. Bonev, A.D. and M.T. Nelson, *ATP-sensitive potassium channels in smooth muscle cells from guinea pig urinary bladder.* Am J Physiol, 1993. **264**(5 Pt 1): p. C1190-200.

34. Herrera, G.M., et al., *Urinary bladder instability induced by selective suppression of the murine small conductance calcium-activated potassium (SK3) channel.* J Physiol, 2003. **551**(Pt 3): p. 893-903.

35. Heppner, T.J., et al., *Transient contractions of urinary bladder smooth muscle are drivers of afferent nerve activity during filling.* Journal of General Physiology, 2016. **147**(4): p. 323-335.

36. Petkov, G.V., *Role of potassium ion channels in detrusor smooth muscle function and dysfunction.* Nat Rev Urol, 2011. **9**(1): p. 30-40.

37. Parekh, A., A. Brading, and T. Tomita, *Studies of longitudinal tissue impedance in various smooth muscles.* Progress in Clinical and Biological Research, 1990. **327**: p. 375-378.

38. Sperelakis, N. and J.D. Wood, *Frontiers in smooth muscle research: proceedings of the Emil Bozler International Symposium, held in Columbus, Ohio, May 19-20, 1989.* (No Title), 1990.

39. Brading, A.F., *Spontaneous activity of lower urinary tract smooth muscles: correlation between ion channels and tissue function.* The Journal of Physiology, 2006. **570**(1): p. 13-22.

40. Andersson, K.-E. and K.D. McCloskey, *Lamina propria: The functional center of the bladder?* Neurourology and Urodynamics, 2014. **33**(1): p. 9-16.

41. Paner, G.P., et al., *Further characterization of the muscle layers and lamina propria of the urinary bladder by systematic histologic mapping: implications for pathologic staging of invasive urothelial carcinoma.* The American journal of surgical pathology, 2007. **31**(9): p. 1420-1429.

42. Wu, C., G. Sui, and C. Fry, *Purinergic regulation of guinea pig suburothelial myofibroblasts.* The Journal of physiology, 2004. **559**(1): p. 231-243.

43. Wiseman, O., C. Fowler, and D. Landon, *The role of the human bladder lamina propria myofibroblast.* BJU international, 2003. **91**(1): p. 89-93.

44. Mukerji, G., et al., *Localization of M2 and M3 muscarinic receptors in human bladder disorders and their clinical correlations.* The Journal of urology, 2006. **176**(1): p. 367-373.

45. Nile, C.J., J. De Vente, and J.I. Gillespie, *Stretch independent regulation of prostaglandin E2 production within the isolated guinea-pig lamina propria.* BJU international, 2010. **105**(4): p. 540-548.

46. Rahnama'i, M.S., et al., *Prostaglandin receptor EP1 and EP2 site in guinea pig bladder urothelium and lamina propria.* The Journal of urology, 2010. **183**(3): p. 1241-1247.

47. De Jongh, R., et al., *Alterations to network of NO/cGMP-responsive interstitial cells induced by outlet obstruction in guinea-pig bladder.* Cell and Tissue Research, 2007. **330**: p. 147-160.

48. Smet, P., K. Moore, and J. Jonavicius, *Distribution and colocalization of calcitonin gene-related peptide, tachykinins, and vasoactive intestinal peptide in normal and idiopathic unstable human urinary bladder.* Laboratory investigation; a journal of technical methods and pathology, 1997. **77**(1): p. 37-49.

49. Miodoński, A.J. and J.A. Litwin, *Microvascular architecture of the human urinary bladder wall: a corrosion casting study.* The Anatomical Record: An Official Publication of the American Association of Anatomists, 1999. **254**(3): p. 375-381.

50. Piez, K.A., *History of extracellular matrix: a personal view*. Matrix Biol, 1997. **16**(3): p. 85-92.

51. Pompili, S., et al., *The Charming World of the Extracellular Matrix: A Dynamic and Protective Network of the Intestinal Wall.* Front Med (Lausanne), 2021. **8**: p. 610189.

52. Hynes, R.O., *The extracellular matrix: not just pretty fibrils.* Science, 2009. **326**(5957): p. 1216-9.

53. Lu, P., et al., *Extracellular matrix degradation and remodeling in development and disease.* Cold Spring Harb Perspect Biol, 2011. **3**(12).

54. Kristensen, J.H. and M.A. Karsdal, *Chapter 30 - Elastin*, in *Biochemistry of Collagens, Laminins and Elastin*, M.A. Karsdal, Editor. 2016, Academic Press. p. 197-201.

55. Mithieux, S.M. and A.S. Weiss, *Elastin.* Adv Protein Chem, 2005. **70**: p. 437-61.

56. Spofford, C.M. and W.M. Chilian, *The elastin-laminin receptor functions as a mechanotransducer in vascular smooth muscle.* American Journal of Physiology-Heart and Circulatory Physiology, 2001. **280**(3): p. H1354-H1360.

57. Saban, R., et al., *Bladder inflammatory transcriptome in response to tachykinins: Neurokinin 1 receptor-dependent genes and transcription regulatory elements.* BMC Urology, 2007. **7**(1): p. 7.

58. Hubschmid, U., et al., *In Vitro Growth of Human Urinary Tract Smooth Muscle Cells on Laminin and Collagen Type I-Coated Membranes under Static and Dynamic Conditions.* Tissue engineering, 2005. **11**: p. 161-71.

59. Kadler, K.E., A. Hill, and E.G. Canty-Laird, *Collagen fibrillogenesis: fibronectin, integrins, and minor collagens as organizers and nucleators.* Curr Opin Cell Biol, 2008. **20**(5): p. 495-501.

60. UPADHYAY, J., et al., *Integrins Expressed With Bladder Extracellular Matrix After Stretch Injury In Vivo Mediate Bladder Smooth Muscle Cell Growth In Vitro.* Journal of Urology, 2003. **169**(2): p. 750-755.

61. Singh, V.P., et al., *Advanced glycation end products and diabetic complications.* Korean J Physiol Pharmacol, 2014. **18**(1): p. 1-14.

62. Cheng, F., et al., *Layer-dependent role of collagen recruitment during loading of the rat bladder wall.* Biomechanics and Modeling in Mechanobiology, 2018. **17**(2): p. 403-417.

63. Gathercole, L.J. and A. Keller, *Crimp morphology in the fibre-forming collagens.* Matrix, 1991. **11**(3): p. 214-34.

64. Strauss, K. and J. Chmielewski, *Advances in the design and higher-order assembly of collagen mimetic peptides for regenerative medicine.* Current Opinion in Biotechnology, 2017. **46**: p. 34-41.

65. Exposito, J.-Y., et al., *Evolution of collagens.* The Anatomical Record, 2002. **268**(3): p. 302-316.

66. Fleischmajer, R., et al., *Type I and type III collagen interactions during fibrillogenesis.* Ann N Y Acad Sci, 1990. **580**: p. 161-75.

67. Stevenson, K., et al., *Functional changes in bladder tissue from type III collagen-deficient mice.* Molecular and Cellular Biochemistry, 2006. **283**(1): p. 107-114.

68. Chang, S.L., et al., *Role of type III collagen in bladder filling.* Neurourol Urodyn, 1998. **17**(2): p. 135-45.

69. Ewalt, D.H., et al., *Is lamina propria matrix responsible for normal bladder compliance?* J Urol, 1992. **148**(2 Pt 2): p. 544-9.

70. Bosman, F.T. and I. Stamenkovic, *Functional structure and composition of the extracellular matrix.* The Journal of Pathology: A Journal of the Pathological Society of Great Britain and Ireland, 2003. **200**(4): p. 423-428.

71. Brunner, A. and A. Tzankov, *The Role of Structural Extracellular Matrix Proteins in Urothelial Bladder Cancer (Review).* Biomarker Insights, 2007. **2**: p. BMI.S294.

72. Longhurst, P.A., et al., *Urinary bladder function in the tight-skin mouse.* The Journal of urology, 1992. **148**(5): p. 1611-1614.

73. Liapis, A., et al., *Changes in the quantity of collagen type I in women with genuine stress incontinence.* Urological research, 2000. **28**: p. 323-326.

74. McCawley, L.J. and L.M. Matrisian, *Matrix metalloproteinases: they're not just for matrix anymore!* Current Opinion in Cell Biology, 2001. **13**(5): p. 534-540.

75. Johnson, J.L., et al., *Activation of Matrix-Degrading Metalloproteinases by Mast Cell Proteases in Atherosclerotic Plaques.* Arteriosclerosis, Thrombosis, and Vascular Biology, 1998. **18**(11): p. 1707-1715.

76. Robinson, W.P., 3rd, et al., *ATP stimulates MMP-2 release from human aortic smooth muscle cells via JNK signaling pathway.* Am J Physiol Heart Circ Physiol, 2006. **290**(5): p. H1988-96.

77. Nagase, H., R. Visse, and G. Murphy, *Structure and function of matrix metalloproteinases and TIMPs.* Cardiovascular Research, 2006. **69**(3): p. 562-573.

78. Ra, H.-J. and W.C. Parks, *Control of matrix metalloproteinase catalytic activity.* Matrix biology, 2007. **26**(8): p. 587-596.

79. Mott, J.D. and Z. Werb, *Regulation of matrix biology by matrix metalloproteinases.* Current opinion in cell biology, 2004. **16**(5): p. 558-564.

80. Van Wart, H.E. and H. Birkedal-Hansen, *The cysteine switch: a principle of regulation of metalloproteinase activity with potential applicability to the entire matrix metalloproteinase gene family.* Proceedings of the National Academy of Sciences, 1990. **87**(14): p. 5578-5582.

81. Hamze, A.B., et al., *Constraining specificity in the N-domain of tissue inhibitor of metalloproteinases-1; gelatinase-selective inhibitors.* Protein Science, 2007. **16**(9): p. 1905-1913.

82. Yang, L., et al., *Imbalance between matrix metalloproteinase-1 (MMP-1) and tissue inhibitor of metalloproteinase-1 (TIMP-1) contributes to bladder compliance changes in rabbits with partial bladder outlet obstruction (PBOO).* BJU Int, 2013. **112**(4): p. E391-7.

83. Coyne, K.S., et al., *The prevalence of lower urinary tract symptoms (LUTS) and overactive bladder (OAB) by racial/ethnic group and age: Results from OAB-POLL.* Neurourology and Urodynamics, 2013. **32**(3): p. 230-237.

84. Siddiqui, N.Y., et al., *Biomarkers Implicated in Lower Urinary Tract Symptoms: Systematic Review and Pathway Analyses.* J Urol, 2019. **202**(5): p. 880-889.

85. Sibley, G., *The response of the bladder to lower urinary tract obstruction.* DM Theses, Oxford, 1984.

86. Stewart, W.F., et al., *Prevalence and burden of overactive bladder in the United States.* World J Urol, 2003. **20**(6): p. 327-36.

87. Steers, W.D., *Pathophysiology of overactive bladder and urge urinary incontinence.* Rev Urol, 2002. **4 Suppl 4**(Suppl 4): p. S7-s18.

88. Brading, A.F., *A myogenic basis for the overactive bladder.* Urology, 1997. **50**(6A Suppl): p. 57-67; discussion 68-73.

89. Brading, A. and W. Turner, *The unstable bladder: towards a common mechanism*. British journal of urology, 1994. **73**(1): p. 3-8.

90. de Groat, W.C., *A neurologic basis for the overactive bladder.* Urology, 1997. **50**(6A Suppl): p. 36-52; discussion 53-6.

91. Coolsaet, B.L., et al., *New concepts in relation to urge and detrusor activity.* Neurourol Urodyn, 1993. **12**(5): p. 463-71.

92. Drake, M.J., et al., *The potential role of unregulated autonomous bladder micromotions in urinary storage and voiding dysfunction; overactive bladder and detrusor underactivity.* BJU International, 2017. **119**(1): p. 22-29.

93. Kim, J.C., et al., *Nerve growth factor and prostaglandins in the urine of female patients with overactive bladder.* The Journal of urology, 2006. **175**(5): p. 1773-1776.

94. Suh, Y.S., et al., *Potential biomarkers for diagnosis of overactive bladder patients: urinary nerve growth factor, prostaglandin E2, and adenosine triphosphate.* International Neurourology Journal, 2017. **21**(3): p. 171.

95. Sun, Y. and T.C. Chai, *Augmented extracellular ATP signaling in bladder urothelial cells from patients with interstitial cystitis.* American Journal of Physiology-Cell Physiology, 2006. **290**(1): p. C27-C34.

96. Smith, C.P., et al., *Enhanced ATP release from rat bladder urothelium during chronic bladder inflammation: effect of botulinum toxin A.* Neurochemistry international, 2005. **47**(4): p. 291-297.

97. Jhang, J.-F., et al., *Clinical relevance of bladder histopathological findings and their impact on treatment outcomes among patients with interstitial cystitis/bladder pain syndrome: An investigation of the European Society for the study of interstitial cystitis histopathological classification.* The Journal of Urology, 2021. **205**(1): p. 226-235.

98. Grundy, L., A. Caldwell, and S.M. Brierley, *Mechanisms Underlying Overactive Bladder and Interstitial Cystitis/Painful Bladder Syndrome.* Front Neurosci, 2018. **12**: p. 931.

99. Malek, N., et al., *The importance of TRPV1-sensitisation factors for the development of neuropathic pain.* Mol Cell Neurosci, 2015. **65**: p. 1-10.

100. Jhang, J.-F., Y.-H. Jiang, and H.-C. Kuo, *Current Understanding of the Pathophysiology and Novel Treatments of Interstitial Cystitis/Bladder Pain Syndrome.* Biomedicines, 2022. **10**(10): p. 2380.

101. Brierley, S.M. and D.R. Linden, *Neuroplasticity and dysfunction after gastrointestinal inflammation.* Nature reviews Gastroenterology & hepatology, 2014. **11**(10): p. 611-627.

102. Abraham, S.N. and Y. Miao, *The nature of immune responses to urinary tract infections.* Nature Reviews Immunology, 2015. **15**(10): p. 655-663.

103. Yu, Z., et al., *Single-cell transcriptomic map of the human and mouse bladders.* Journal of the American Society of Nephrology, 2019. **30**(11): p. 2159-2176.

104. Mora-Bau, G., et al., *Macrophages subvert adaptive immunity to urinary tract infection.* PLoS pathogens, 2015. **11**(7): p. e1005044.

105. van Furth, R., et al., *The mononuclear phagocyte system: a new classification of macrophages, monocytes, and their precursor cells.* Bull World Health Organ, 1972. **46**(6): p. 845-52.

106. Sant, G.R. and T.C. Theoharides, *The role of the mast cell in interstitial cystitis.* Urol Clin North Am, 1994. **21**(1): p. 41-53.

107. Bowyer, G.S., et al., *Tissue Immunity in the Bladder.* Annual Review of Immunology, 2022. **40**(Volume 40, 2022): p. 499-523.

108. Li, Z., et al., *Adult connective tissue-resident mast cells originate from late erythro-myeloid progenitors.* Immunity, 2018. **49**(4): p. 640-653. e5.

109. Abraham, S.N. and A.L. St John, *Mast cell-orchestrated immunity to pathogens.* Nat Rev Immunol, 2010. **10**(6): p. 440-52.

110. Bauer, O. and E. Razin, *Mast cell-nerve interactions.* Physiology, 2000. **15**(5): p. 213-218.

111. Malik, S.T., et al., *Distribution of mast cell subtypes in interstitial cystitis: implications for novel diagnostic and therapeutic strategies?* J Clin Pathol, 2018. **71**(9): p. 840-844.

112. Tyagi, P., et al., *Urine cytokines suggest an inflammatory response in the overactive bladder: a pilot study.* International urology and nephrology, 2010. **42**: p. 629-635.

113. Smith, J., J.K.H. Tan, and C. Moro, *Mast cell distribution and prevalence in the murine urinary bladder.* BMC Urology, 2024. **24**(1): p. 51.

114. Fuentes-Corona, C.G., et al., *Second harmonic generation signal from type I collagen fibers grown in vitro.* Biomed Opt Express, 2019. **10**(12): p. 6449-6461.

115. Done, J.D., et al., *Role of mast cells in male chronic pelvic pain.* J Urol, 2012. **187**(4): p. 1473-82.

116. Stromberga, Z., R. Chess-Williams, and C. Moro, *Histamine modulation of urinary bladder urothelium, lamina propria and detrusor contractile activity via H1 and H2 receptors.* Scientific Reports, 2019. **9**(1): p. 3899.

117. Jones, B.M., G.C. Mingin, and N.R. Tykocki, *Histamine receptors rapidly desensitize without altering nerve-evoked contractions in murine urinary bladder smooth muscle.* Am J Physiol Renal Physiol, 2022. **322**(3): p. F268-F279.

118. Brothely Jones, G.M., Nathan Tykocki, *The mast cell activator Compound 48/80 causes phasic urinary bladder smooth muscle contractions independent of histamine release.* The FASEB Journal, 2021. **35**(S1).

119. Decuyper, I., et al., *In vitro diagnosis of immediate drug hypersensitivity anno 2017: potentials and limitations.* Drugs in R&D, 2017. **17**: p. 265-278.

120. McNeil, B.D., et al., *Identification of a mast-cell-specific receptor crucial for pseudo-allergic drug reactions.* Nature, 2015. **519**(7542): p. 237-241.

121. Marshall, J.S., *Mast-cell responses to pathogens.* Nature Reviews Immunology, 2004. **4**(10): p. 787-799.

122. Lieberman, P. and L.H. Garvey, *Mast cells and anaphylaxis.* Current allergy and asthma reports, 2016. **16**: p. 1-7.

123. Subramanian, H., K. Gupta, and H. Ali, *Roles of Mas-related G protein–coupled receptor X2 on mast cell–mediated host defense, pseudoallergic drug reactions, and chronic inflammatory diseases.* Journal of Allergy and Clinical Immunology, 2016. **138**(3): p. 700-710.

124. Herrera, J., C.A. Henke, and P.B. Bitterman, *Extracellular matrix as a driver of progressive fibrosis.* The Journal of clinical investigation, 2018. **128**(1): p. 45-53.

125. Xia, H., et al., *Low α2β1 integrin function enhances the proliferation of fibroblasts from patients with idiopathic pulmonary fibrosis by activation of the β-catenin pathway.* The American journal of pathology, 2012. **181**(1): p. 222-233.

126. Huang, S. and D.E. Ingber, *The structural and mechanical complexity of cell-growth control.* Nature cell biology, 1999. **1**(5): p. E131-E138.

127. Putnam, A.J., et al., *Microtubule assembly is regulated by externally applied strain in cultured smooth muscle cells.* Journal of cell science, 1998. **111**(22): p. 3379-3387.

128. Wyndaele, J.J., et al., *Bladder compliance what does it represent: can we measure it, and is it clinically relevant?* Neurourol Urodyn, 2011. **30**(5): p. 714-22.

129. Dörr, W., *Cystometry in mice—influence of bladder filling rate and circadian variations in bladder compliance.* The Journal of urology, 1992. **148**(1): p. 183-187.

130. Nagle, A.S., et al., *Quantification of bladder wall biomechanics during urodynamics: A methodologic investigation using ultrasound.* Journal of biomechanics, 2017. **61**: p. 232-241.

131. Treuting, P.M., S.M. Dintzis, and K.S. Montine, *Comparative anatomy and histology: a mouse, rat, and human atlas*. 2017: Academic Press.

132. Yamada, H., *Stress and Strain Analyses of Blood Vessels in Physiological and Pathological Conditions*, in *Clinical Application of Computational Mechanics to the Cardiovascular System*, T. Yamaguchi, Editor. 2000, Springer Japan: Tokyo. p. 29-38.

133. Damaser, M.S. and S.L. Lehman, *The effect of urinary bladder shape on its mechanics during filling.* J Biomech, 1995. **28**(6): p. 725-32.

134. Roccabianca, S. and T.R. Bush, *Understanding the mechanics of the bladder through experiments and theoretical models: Where we started and where we are heading.* Technology, 2016. **4**(1): p. 30-41.

135. Porebski, G., et al., *Mas-Related G Protein-Coupled Receptor-X2 (MRGPRX2) in Drug Hypersensitivity Reactions.* Frontiers in Immunology, 2018. **9**.

136. Al Hamwi, G., et al., *MAS-related G protein-coupled receptors X (MRGPRX): Orphan GPCRs with potential as targets for future drugs.* Pharmacology & Therapeutics, 2022. **238**: p. 108259.

137. Lembo, P.M., et al., *Proenkephalin A gene products activate a new family of sensory neuron--specific GPCRs.* Nat Neurosci, 2002. **5**(3): p. 201-9.

138. Subramanian, H., et al., *β-Defensins activate human mast cells via Mas-related gene X2.* The Journal of Immunology, 2013. **191**(1): p. 345-352.

139. Cao, C., et al., *Structure, function and pharmacology of human itch GPCRs.* Nature, 2021. **600**(7887): p. 170-175.

140. Dondalska, A., et al., *Amelioration of Compound 48/80-Mediated Itch and LL-37-Induced Inflammation by a Single-Stranded Oligonucleotide.* Front Immunol, 2020. **11**: p. 559589.

141. NIH, *MAS-related GPR, Member, B2*, in *National Center for Biotechnology Information*. 2018, Provided by MGI: National Center for Biotechnology Information.

142. Abdelwahab, O., et al., *27 MAST CELLS IN THE URINARY BLADDERS OF INTERSTITIAL CYSTITIS/BLADDER PAIN SYNDROME PATIENTS EXPRESS THE MAST CELL RELATED G-PROTEIN COUPLED RECEPTOR X2 (MRGPRX2): POTENTIAL ROLE IN THE PATHOGENESIS OF NEUROGENIC INFLAMMATION*. Continence, 2022. **2**: p. 100217.

143. Dorr, W., *Cystometry in mice--influence of bladder filling rate and circadian variations in bladder compliance.* J Urol, 1992. **148**(1): p. 183-7.

144. Nagle, A.S., et al., *Quantification of bladder wall biomechanics during urodynamics: A methodologic investigation using ultrasound.* J Biomech, 2017. **61**: p. 232-241.

145. Parekh, A., et al., *Ex vivo deformations of the urinary bladder wall during whole bladder filling: contributions of extracellular matrix and smooth muscle.* J Biomech, 2010. **43**(9): p. 1708-16.

146. Bouchard, M.B., et al., *Swept confocally-aligned planar excitation (SCAPE) microscopy for high speed volumetric imaging of behaving organisms.* Nat Photonics, 2015. **9**(2): p. 113-119.

147. Keller, P.J. and M.B. Ahrens, *Visualizing whole-brain activity and development at the single-cell level using light-sheet microscopy.* Neuron, 2015. **85**(3): p. 462-83.

148. Ren, Y.X., et al., *Parallelized volumetric fluorescence microscopy with a reconfigurable coded incoherent light-sheet array.* Light Sci Appl, 2020. **9**: p. 8.

149. Nagatomi, J., et al., *Changes in the biaxial viscoelastic response of the urinary bladder following spinal cord injury.* Ann Biomed Eng, 2004. **32**(10): p. 1409-19.

150. Gloeckner, D.C., et al., *Passive biaxial mechanical properties of the rat bladder wall after spinal cord injury.* J Urol, 2002. **167**(5): p. 2247-52.

151. Heppner, T.J., et al., *Transient contractions of urinary bladder smooth muscle are drivers of afferent nerve activity during filling.* J Gen Physiol, 2016. **147**(4): p. 323-35.

152. Ajalloueian, F., et al., *Bladder biomechanics and the use of scaffolds for regenerative medicine in the urinary bladder.* Nat Rev Urol, 2018. **15**(3): p. 155-174.

153. Tuttle, T.G., et al., *Remodeling of extracellular matrix in the urinary bladder of paraplegic rats results in increased compliance and delayed fiber recruitment 16 weeks after spinal cord injury.* Acta Biomater, 2022. **141**: p. 280-289.

154. Zwaans, B.M.M., et al., *Increased extracellular matrix stiffness accompanies compromised bladder function in a murine model of radiation cystitis.* Acta Biomater, 2022. **144**: p. 221-229.

155. Tykocki, N.R., et al., *The KV 7 channel activator retigabine suppresses mouse urinary bladder afferent nerve activity without affecting detrusor smooth muscle K(+) channel currents.* J Physiol, 2019. **597**(3): p. 935-950.

156. Chancellor, M.B., *Urodynamics Evaluation of Underactive Bladder*, in *The Underactive Bladder*, M.B. Chancellor and A.C. Diokno, Editors. 2016, Springer International Publishing: Cham. p. 25-50.

157. Maddra, K.M., et al., *Repeatability of Ultrasound-Defined Bladder Shape Metrics in Healthy Volunteers.* Res Rep Urol, 2022. **14**: p. 185-192.

158. Tuttle, T.G., et al., *Investigation of Fiber-Driven Mechanical Behavior of Human and Porcine Bladder Tissue Tested Under Identical Conditions.* J Biomech Eng, 2021. **143**(11).

159. Watanabe, H., et al., *A finite deformation theory of intravesical pressure and mural stress of the urinary bladder.* Tohoku J Exp Med, 1981. **135**(3): p. 301-7.

160. Neuhaus, J. and T. Schwalenberg, *Intravesical treatments of bladder pain syndrome/interstitial cystitis.* Nat Rev Urol, 2012. **9**(12): p. 707-20.

161. Regnier, C.H., et al., *The elastic behavior of the urinary bladder for large deformations.* J Biomech, 1983. **16**(11): p. 915-22.

162. van Mastrigt, R. and D.J. Griffiths, *An evaluation of contractility parameters determined from isometric contractions and micturition studies.* Urol Res, 1986. **14**(1): p. 45-52.

163. Schott, H.C. and J.B. Woodie, *Chapter 65 - Bladder*, in *Equine Surgery (Fourth Edition)*, J.A. Auer and J.A. Stick, Editors. 2012, W.B. Saunders: Saint Louis. p. 927-939.

164. Chaudhry, S.R., M.N.P. Liman, and D.C. Peterson, *Anatomy, Abdomen and Pelvis, Stomach*. 2021: StatPearls Publishing, Treasure Island (FL).

165. Parsons, B., et al., *The validation of a functional, isolated bladder model from a large animal.* Frontiers in Pharmacology, 2012. **3**(52).

166. Zhang, W., G. Huang, and F. Xu, *Engineering Biomaterials and Approaches for Mechanical Stretching of Cells in Three Dimensions.* Frontiers in bioengineering and biotechnology, 2020. **8**: p. 589590-589590.

167. Habteyes, F.G., et al., *Modeling the influence of acute changes in bladder elasticity on pressure and wall tension during filling.* J Mech Behav Biomed Mater, 2017. **71**: p. 192-200.

168. Murakumo, M., et al., *Three-Dimensional Arrangement of Collagen and Elastin Fibers in the Human Urinary Bladder: A Scanning Electron Microscopic Study.* The Journal of Urology, 1995. **154**(1): p. 251-256.

169. Parekh, A., et al., *Ex vivo deformations of the urinary bladder wall during whole bladder filling: Contributions of extracellular matrix and smooth muscle.* Journal of Biomechanics, 2010. **43**(9): p. 1708-1716.

170. Hinek, A. and M. Rabinovitch, *67-kD elastin-binding protein is a protective "companion" of extracellular insoluble elastin and intracellular tropoelastin.* Journal of Cell Biology, 1994. **126**(2): p. 563-574.

171. Koo, H.P., et al., *Temporal expression of elastic fiber components in bladder development.* Connect Tissue Res, 1998. **37**(1-2): p. 1-11.

172. Gacci, M., A. Sebastianelli, and M. Salvi, *Chapter 5 - Metabolic Syndrome and LUTS/BPH*, in *Lower Urinary Tract Symptoms and Benign Prostatic Hyperplasia*, G. Morgia and G.I. Russo, Editors. 2018, Academic Press. p. 89-111.

173. Grover, S., et al., *Role of inflammation in bladder function and interstitial cystitis.* Ther Adv Urol, 2011. **3**(1): p. 19-33.

174. Rudick, C.N., et al., *Mast Cell-Derived Histamine Mediates Cystitis Pain.* PLoS ONE, 2008. **3**(5): p. e2096.

175. Azimi, E., et al., *Substance P activates Mas-related G protein–coupled receptors to induce itch.* Journal of Allergy and Clinical Immunology, 2017. **140**(2): p. 447-453.e3.

176. Azimi, E., et al., *Dual action of neurokinin-1 antagonists on Mas-related GPCRs.* JCI Insight, 2016. **1**(16).

177. Hamamura-Yasuno, E., et al., *Identification of the dog orthologue of human MAS-related G protein coupled receptor X2 (MRGPRX2) essential for drug-induced pseudo-allergic reactions.* Sci Rep, 2020. **10**(1): p. 16146.

178. Ibrahim, A., Y. Ryu, and M. Saidpour, *Stress Analysis of Thin-Walled Pressure Vessels.* Modern Mechanical Engineering, 2015. **Vol.05No.01**: p. 9.

179. Jay D. Humphrey, S.L.D., *An Introduction to Biomechanics*. 1 ed. 2004: Springer New York, Ny.

180. Saban, R., et al., *Mast cells mediate substance P-induced bladder inflammation through an NK(1) receptor-independent mechanism.* Am J Physiol Renal Physiol, 2002. **283**(4): p. F616-29.

181. Ali, H., *Mas-related G protein coupled receptor-X2: A potential new target for modulating mast cell-mediated allergic and inflammatory diseases.* J Immunobiol., 2016. **1**.

182. Berrozpe, G., et al., *The W(sh), W(57), and Ph Kit expression mutations define tissue-specific control elements located between -23 and -154 kb upstream of Kit.* Blood, 1999. **94**(8): p. 2658-66.

183. Watanabe, T., et al., *Comparative analysis of bladder wall compliance based on cystometry and biosensor measurements during the micturition cycle of the rat.* Neurourol Urodyn, 1997. **16**(6): p. 567-81.

184. Li, C., et al., *Quantitative elasticity measurement of urinary bladder wall using laser-induced surface acoustic waves.* Biomed Opt Express, 2014. **5**(12): p. 4313-28.

185. Minevich, E. and C.A. Sheldon, *Chapter 117 - Reconstruction of the Bladder and Bladder Outlet,* in *Pediatric Surgery (Seventh Edition)*, A.G. Coran, Editor. 2012, Mosby: Philadelphia. p. 1467-1485.

186. Schemann, M., et al., *The mast cell degranulator compound 48/80 directly activates neurons.* PLoS One, 2012. **7**(12): p. e52104.

187. Fitzgerald, J.J., et al., *Evidence for the role of mast cells in colon–bladder cross organ sensitization.* Autonomic Neuroscience, 2013. **173**(1-2): p. 6-13.

188. Frenz, A.M., T.J. Christmas, and F.L. Pearce, *Does the mast cell have an intrinsic role in the pathogenesis of interstitial cystitis?* Agents Actions, 1994. **41 Spec No**: p. C14-5.

189. Eglezos, A., et al., *Activation of capsaicin-sensitive primary afferents in the rat urinary bladder by compound 48/80: a direct action on sensory nerves?* Arch Int Pharmacodyn Ther, 1992. **315**: p. 96-109.

190. Sam P, N.A., LaGrange CA, *Anatomy, Abdomen and Pelvis, Bladder Detrusor Muscle.* . 2022, StatPearls treasure island (FL).

191. Macarak, E.J., et al., *The collagens and their urologic significance.* Scand J Urol Nephrol Suppl, 1997. **184**: p. 173-178.

192. Stromberga, Z., R. Chess-Williams, and C. Moro, *Alterations in histamine responses between juvenile and adult urinary bladder urothelium, lamina propria and detrusor tissues.* Scientific reports, 2020. **10**(1): p. 4116-4116.

193. Ogasawara, H., et al., *Novel MRGPRX2 antagonists inhibit IgE-independent activation of human umbilical cord blood-derived mast cells.* Journal of Leukocyte Biology, 2019. **106**(5): p. 1069-1077.

194. Wang, C., et al., *Synthetic imperatorin derivatives alleviate allergic reactions via mast cells.* Biomedicine & Pharmacotherapy, 2022. **150**: p. 112982.

195. Fujisawa, D., et al., *Expression of Mas-related gene X2 on mast cells is upregulated in the skin of patients with severe chronic urticaria.* J Allergy Clin Immunol, 2014. **134**(3): p. 622-633.e9.

196. Liu, Q. and X. Dong, *The role of the Mrgpr receptor family in itch.* Handb Exp Pharmacol, 2015. **226**: p. 71-88.

197. Dong, X., et al., *A diverse family of GPCRs expressed in specific subsets of nociceptive sensory neurons.* Cell, 2001. **106**(5): p. 619-32.

198. Piipponen, M., D. Li, and N.X. Landén, *The Immune Functions of Keratinocytes in Skin Wound Healing.* Int J Mol Sci, 2020. **21**(22).

199. Yoshida, M., et al., *The forefront for novel therapeutic agents based on the pathophysiology of lower urinary tract dysfunction: pathophysiology and pharmacotherapy of overactive bladder.* J Pharmacol Sci, 2010. **112**(2): p. 128-34.

200. Lu, P., et al., *Extracellular Matrix Degradation and Remodeling in Development and Disease.* Cold Spring Harbor Perspectives in Biology, 2011. **3**(12): p. a005058-a005058.

201. Wilson, C.B., et al., *Extracellular matrix and integrin composition of the normal bladder wall.* World Journal of Urology, 1996. **14**(1).

202. Deen, S. and R.Y. Ball, *Basement membrane and extracellular interstitial matrix components in bladder neoplasia--evidence of angiogenesis.* Histopathology, 1994. **25**(5): p. 475-81.

203. Rodriguez Faba, O., et al., *Matrix Metalloproteinases and Bladder Cancer: What is New?* ISRN Urol, 2012. **2012**: p. 581539.

204. Hastings, G.W., *Cardiovascular biomaterials*. 2012: Springer Science & Business Media.

205. Wagenseil, J.E. and R.P. Mecham, *Vascular extracellular matrix and arterial mechanics.* Physiological reviews, 2009. **89**(3): p. 957-989.

206. Saxena, P., et al., *Compound 48/80 increases murine bladder wall compliance independent of mast cells.* Scientific Reports, 2023. **13**(1): p. 625.

207. Margot S Damaser, S.L.L., *THE EFFECT OF URINARY BLADDER SHAPE ON ITS MECHANICS DURING FILLING*. J. Biomechanics, 1995. **28**: p. 725-732.

208. Sounni, N.E., et al., *MT-MMPS as Regulators of Vessel Stability Associated with Angiogenesis.* Frontiers in Pharmacology, 2011. **1**.

209. Soccal, P.M., et al., *Matrix metalloproteinases correlate with alveolar-capillary permeability alteration in lung ischemia-reperfusion injury.* Transplantation, 2000. **70**(7): p. 998-1005.

210. Bernardo, M.M. and R. Fridman, *TIMP-2 (tissue inhibitor of metalloproteinase-2) regulates MMP-2 (matrix metalloproteinase-2) activity in the extracellular environment after pro-MMP-2 activation by MT1 (membrane type 1)-MMP*. Biochem J, 2003. **374**(Pt 3): p. 739-45.

211. Iskratsch, T., H. Wolfenson, and M.P. Sheetz, *Appreciating force and shape—the rise of mechanotransduction in cell biology.* Nature reviews Molecular cell biology, 2014. **15**(12): p. 825-833.

212. Humphrey, J.D., E.R. Dufresne, and M.A. Schwartz, *Mechanotransduction and extracellular matrix homeostasis.* Nature reviews Molecular cell biology, 2014. **15**(12): p. 802-812.

213. Bellucci, C.H.S., et al., *Increased detrusor collagen is associated with detrusor overactivity and decreased bladder compliance in men with benign prostatic obstruction.* Prostate Int, 2017. **5**(2): p. 70-74.

214. Gelman, R.A., D.C. Poppke, and K.A. Piez, *Collagen fibril formation in vitro. The role of the nonhelical terminal regions.* Journal of Biological Chemistry, 1979. **254**(22): p. 11741-11745.

215. Chase, A.J. and A.C. Newby, *Regulation of matrix metalloproteinase (matrixin) genes in blood vessels: a multi-step recruitment model for pathological remodelling.* Journal of vascular research, 2003. **40**(4): p. 329-343.

216. GINEYTS, E., et al., *Racemization and isomerization of type I collagen C-telopeptides in human bone and soft tissues: assessment of tissue turnover.* Biochemical Journal, 2000. **345**(3): p. 481-485.

217. Cabral-Pacheco, G.A., et al., *The Roles of Matrix Metalloproteinases and Their Inhibitors in Human Diseases.* Int J Mol Sci, 2020. **21**(24).

218. Kapoor, C., et al., *Seesaw of matrix metalloproteinases (MMPs).* Journal of Cancer Research and Therapeutics, 2016. **12**(1): p. 28-35.

219. Cui, N., M. Hu, and R.A. Khalil, *Biochemical and Biological Attributes of Matrix Metalloproteinases.* Prog Mol Biol Transl Sci, 2017. **147**: p. 1-73.

220. Jackson, H.W., et al., *TIMPs: versatile extracellular regulators in cancer.* Nature Reviews Cancer, 2017. **17**(1): p. 38-53.

221. Grundy, L., et al., *Experimentally Induced Bladder Permeability Evokes Bladder Afferent Hypersensitivity in the Absence of Inflammation.* Frontiers in Neuroscience, 2020. **14**.

222. GuhaSarkar, S. and R. Banerjee, *Intravesical drug delivery: Challenges, current status, opportunities and novel strategies.* J Control Release, 2010. **148**(2): p. 147-59.

223. Turunen, M.J., et al., *Effects of tissue fixation and dehydration on tendon collagen nanostructure.* Journal of Structural Biology, 2017. **199**(3): p. 209-215.

224. Roccabianca, S. and T. Bush, *Understanding the mechanics of the bladder through experiments and theoretical models: Where we started and where we are heading.* TECHNOLOGY, 2016. **04**: p. 1-12.

225. Yang, T.H., F.C. Chuang, and H.C. Kuo, *Urodynamic characteristics of detrusor underactivity in women with voiding dysfunction.* PLoS One, 2018. **13**(6): p. e0198764.

226. Jaskowak, D., et al., *Mathematical modeling of the lower urinary tract: A review*. Neurourol Urodyn, 2022. **41**(6): p. 1305-1315.

227. Alkanfari, I.S., *The Role of MRGPRX2/Mrgprb2 in Regulating Mast Cell Function.* Dential Theses 2019. **41**.

228. Porebski, G., et al., *Mas-Related G Protein-Coupled Receptor-X2 (MRGPRX2) in Drug Hypersensitivity Reactions.* Front Immunol, 2018. **9**: p. 3027.

229. Tomoe, S., et al., *Comparison of substance P-induced and compound 48/80-induced neutrophil infiltrations in mouse skin.* Int Arch Allergy Immunol, 1992. **97**(3): p. 237-42.

230. Liu, J., et al., *Assay considerations for fluorescein isothiocyanate-dextran (FITC-d): an indicator of intestinal permeability in broiler chickens.* Poult Sci, 2021. **100**(7): p. 101202.

231. Amidzadeh, Z., et al., *Assessment of different permeabilization methods of minimizing damage to the adherent cells for detection of intracellular RNA by flow cytometry.* Avicenna J Med Biotechnol, 2014. **6**(1): p. 38-46.

232. Stromberga, Z., R. Chess-Williams, and C. Moro, *The five primary prostaglandins stimulate contractions and phasic activity of the urinary bladder urothelium, lamina propria and detrusor.* BMC Urology, 2020. **20**(1): p. 48.

233. Nishiguchi, J., et al., *Detrusor overactivity induced by intravesical application of adenosine 5'-triphosphate under different delivery conditions in rats.* Urology, 2005. **66**(6): p. 1332-7.

234. Chuang, Y.C., et al., *Intravesical protamine sulfate and potassium chloride as a model for bladder hyperactivity.* Urology, 2003. **61**(3): p. 664-70.

235. Shabir, S., et al., *Functional expression of purinergic P2 receptors and transient receptor potential channels by the human urothelium*. American Journal of Physiology-Renal Physiology, 2013. **305**(3): p. F396-F406.

236. O'REILLY, B.A., et al., *A quantitative analysis of purinoceptor expression in human fetal and adult bladders.* The Journal of urology, 2001. **165**(5): p. 1730-1734.

237. Drumm, B.T., et al., *Calcium signalling in Cajal-like interstitial cells of the lower urinary tract.* Nature reviews Urology, 2014. **11**(10): p. 555-564.

238. Liao, J.Y., et al., *Monitoring bladder compliance using end filling detrusor pressure: Clinical results and related factors.* Taiwan J Obstet Gynecol, 2015. **54**(6): p. 709-15.

239. Roccabianca, S. and T.R. Bush, *Understanding the mechanics of the bladder through experiments and theoretical models: where we started and where we are heading.* Technology, 2016. **4**(01): p. 30-41.

240. Malley, S.E. and M.A. Vizzard, *Changes in urinary bladder cytokine mRNA and protein after cyclophosphamide-induced cystitis.* Physiological genomics, 2002. **9**(1): p. 5-13.

241. Birder, L. and K.E. Andersson, *Animal Modelling of Interstitial Cystitis/Bladder Pain Syndrome.* Int Neurourol J, 2018. **22**(Suppl 1): p. S3-9.

242. Coyne, K.S., et al., *The impact of overactive bladder, incontinence and other lower urinary tract symptoms on quality of life, work productivity, sexuality and emotional well-being in men and women: results from the EPIC study.* BJU Int, 2008. **101**(11): p. 1388-95.

243. Ren, Z., J. Chen, and R.A. Khalil, *Zymography as a Research Tool in the Study of Matrix Metalloproteinase Inhibitors*. 2017, Springer New York. p. 79-102.

244. Chien, C.-T., et al., *Substance P via NK1 receptor facilitates hyperactive bladder afferent signaling via action of ROS.* American Journal of Physiology-Renal Physiology, 2003. **284**(4): p. F840-F851.

245. Tanaka, S., et al., *Development of mature and functional human myeloid subsets in hematopoietic stem cell-engrafted NOD/SCID/IL2rγKO mice.* The Journal of Immunology, 2012. **188**(12): p. 6145-6155.

246. Gupta, A. and R. Manchanda, *Computational modeling of stretch induced calcium signaling at the apical membrane domain in umbrella cells.* Computer Methods in Biomechanics and Biomedical Engineering, 2022. **26**: p. 1-10.

247. Marino, M., et al., *Molecular-level collagen damage explains softening and failure of arterial tissues: A quantitative interpretation of CHP data with a novel elasto-damage model.* Journal of the Mechanical Behavior of Biomedical Materials, 2019. **97**: p. 254-271.

APPENDIX

CONFERENCE ABSTRACTS

1. Experimental Biology, 2020

Title: Smooth Muscle Tone Contributes to Bladder Wall Stiffness during Filling

Authors: Pragya Saxena, Sara Roccabianca, and Nathan R. Tykocki

Sensations of bladder fullness are conveyed to the central nervous system by sensory nerves as a response to distention of the urinary bladder. This distention is accompanied by non-voiding transient pressure events and contractions called "micromotions" that are responsible for the majority of sensory outflow during bladder filling. Changes in smooth muscle contractility along with alterations in wall stiffness and sensory feedback are observed in most UB pathologies. Thus, the mechanical properties of bladder wall may play a crucial role in communicating a sense of bladder fullness. We hypothesize that the contractile apparatus of the urinary bladder is actively involved in maintaining bladder wall stiffness during filling.

Whole mouse bladders were dissected and mounted in a custom designed pentaplanar reflected image macroscopy (PRIM) system, for simultaneous measurement of bladder wall micromotions, bladder volume, intravesical pressure, bladder wall stress, and bladder wall strain during ex vivo bladder filling. Bladders were filled at a constant rate (30 µl/min) until intravesical pressure reached 25 mmHg. During filling, bladder wall micromotions led to transient pressure events (0–2 mmHg in amplitude). These micromotions began on the lateral sides of the bladder wall near the trigone and expanded upwards as the bladder filled. Baseline bladder pressure, however, remained relatively low over a large infused volume (~350 µL). Next, we derived the stress versus strain relationship of the bladder wall from the pressure-volume recordings during filling. At baseline pressures >15 mmHg, intravesical pressure

rapidly increased and transient pressure events could no longer be distinguished implying that wall compliance is maintained until larger infused volumes, after which bladder wall stress with respect to strain increases rapidly. To determine if smooth muscle tone altered bladder wall stress during filling, bladder was exposed to myosin inhibitor blebbistatin (10 μM) or PI3 kinase inhibitor wortmannin (10 μM). Both blebbistatin and wortmannin effectively diminished the micromotions and shifted the stress vs strain curve to the right, indicating that the smooth muscle contractile apparatus and smooth muscle tone contribute to bladder wall stiffness, but predominantly only at higher filling volumes. These findings suggest that smooth muscle tone directly increases bladder wall stiffness and that changes in this tone could alter sensory feedback during bladder filling.

2. Experimental Biology, 2021

Title: The mast cell activator Compound 48/80 increases bladder compliance through matrix metalloprotease release

Authors: Pragya Saxena, Sara Roccabianca, and Nathan R. Tykocki

Bladder wall stiffness and elasticity is essential to its storage and voiding functions. In addition to smooth muscle contractility, the integrity of the extracellular matrix plays a crucial role in maintaining the optimal balance between wall stiffness and compliance as the bladder distends. Lower urinary tract symptoms (e.g., bladder overactivity and fibrosis) can be caused by mast cell activation and inflammation, which increases wall stiffness and matrix remodeling. Thus, we hypothesize that mast cell activation increases muscle contractility and decreases compliance. Whole mouse bladders were dissected and mounted in a custom-designed pentaplanar reflected image macroscopy (PRIM) system for simultaneous measurement of the following parameters during ex vivo bladder filling: intravesical pressure, bladder volume, wall deformation, mechanical stress, and mechanical stretch. Bladders were filled at a constant rate (30 µl/min) until intravesical pressure reached 25 mmHg, at which point bladders were emptied and allowed to recover for approximately 10 minutes prior to the next fill cycle. During filling, baseline bladder pressure remained relatively low over a large infused volume (~350 µL), after which pressure increased rapidly. Transient contractions began on the lateral sides of the bladder wall near the trigone, expanded upwards as the bladder filled, and corresponded to transient increases in intravesical pressure (0-2 mmHg). Using the pressure-volume curves and associated image data, we next calculated the bladder wall compliance (defined as the stress vs stretch relationship of the bladder wall). As with pressure, wall stress was relatively low over a large change in stretch, implying that bladder wall was highly

compliant until larger infused volumes. Subsequent exposure to the mast cell activator Compound 48/80 (10 µg/ml) significantly increased the amplitude of transient pressure events but decreased wall stress per change in stretch, indicating a paradoxical increase in compliance. Incubation with the matrix metalloprotease inhibitor doxycycline (10 µM) prior to addition of compound 48/80 prevented this increase in compliance without preventing the increased amplitude of transient pressure events. These findings suggest that Compound 48/80 activates bladder mast cells to release at least two things: (1) matrix metalloproteases that rapidly degrade the extracellular matrix and increase bladder wall compliance; and (2) compounds that increase smooth muscle excitability. Thus, both decreases in stiffness and increases in smooth muscle excitability may accompany inflammatory bladder pathologies such as diabetes and interstitial cystitis.

3. Society for Basic Urological Research, 2021

Title: Calculation and Analysis of Bladder Wall Biomechanics During Ex Vivo Filling

Authors: Pragya Saxena, Sara Roccabianca, and Nathan R. Tykocki

Background: Optimal wall compliance is essential to urinary bladder storage and voiding functions. Changes in compliance occur in many lower urinary tract symptoms (LUTS), however compliance is poorly defined. Clinically, bladder compliance is the change in bladder volume per change in intravesical pressure, but without regard to wall structure or wall volume. Thus, it is unknown if the true mechanical properties of the bladder wall affect bladder function during filling. Thus, we developed a novel method to accurately calculate bladder wall compliance as a measure of the mechanical stress vs stretch instead of pressure vs volume.

Methods: Whole mouse bladders were mounted in our novel Pentaplanar Reflected Image Macroscopy (PRIM) System for simultaneous measurement of intravesical pressure (Pves), infused volume and video during ex vivo filling. The PRIM allows simultaneous visualization of the bladder in 5 planes. Mechanical forces acting on the bladder wall were calculated by assuming the bladder to be an ellipsoid formed with planar areas equal to those measured from the PRIM recordings. Values of wall thickness and wall volume were calculated and used to measure wall stress as $[(Pves)(radius)(stretch^2)]/Thickness$. Stretch was calculated from the infused volume as a function of the relative change in diameter from the start of filling. Volume measurements were validated by comparing the calculated volume in full bladder to the sum of infused and residual volumes.

Results: The calculated volume measurements were comparable to the measured infused volumes. Wall stress only increased rapidly when intravesical pressure exceeded 15 mmHg,

implying that wall compliance is maintained until larger infused volumes. At large volumes, bladder wall stress with respect to strain increases rapidly.

Conclusions: Accurate analysis of bladder compliance is an essential step towards understanding the underlying changes in wall tension and geometry during distention. This study demonstrates how wall tension, stress and stretch can be quantified and used to accurately define wall compliance. This method can be used to explore underlying changes in biomechanics of the bladder wall that accompany LUTS.

4. Experimental Biology, 2022

Title: Compound 48/80 increases bladder wall compliance independent of mast cells

Authors: Pragya Saxena, Sara Roccabianca, and Nathan R. Tykocki

Changes in wall compliance are seen in many bladder pathologies, such as fibrosis and diabetes. Some of these pathologies can be caused by basic secretagogues like Compound 48/80 and its endogenous analogue, Substance P. Traditionally it is believed that basic secretagogues rapidly degranulate mast cells and release inflammatory mediators by acting on an orphan receptor, Mas-related G protein-coupled receptor B2 (Mrgprb2). While Compound 48/80 does increase wall compliance, the exact location and function of Mrgprb2 in the urinary bladder are still unknown. We hypothesize that changes in bladder wall compliance caused by Compound 48/80 are mediated through Mrgprb2 receptors but independent of mast cell degranulation.

Whole mouse bladders from C57Bl/6 (wild-type) and C-kit$^{W\text{-}sh}$ (mast cell-deficient) mice were dissected and mounted in a custom designed pentaplanar reflected image macroscopy (PRIM) system for simultaneous measurement of transient pressure events, intravesical pressure, bladder volume, wall stress, and wall stretch during ex vivo bladder filling. Wall compliance was derived as a measure of the stress versus stretch relationship using the pressure-volume curves and associated imaging data. To test our hypothesis, bladders were exposed to either vehicle or Compound 48/80 (10 µg/ml) during ex vivo filling. Compound 48/80 significantly increased the leading slope of transient pressure events in both wild-type and mast cell-deficient mice. Compliance was also increased, as shown by decreased stress per change in stretch. We also collected urothelium and detrusor layers from C57Bl/6 and C-kit$^{W\text{-}sh}$ mouse bladders. Layers were separated using blunt dissection, and RNA was isolated for

measurement of Mrgprb2 expression using qRT-PCR. No significant difference in the expression of Mrgprb2 mRNA was observed between the two mouse models in either the urothelium or detrusor layers. These findings suggest that Mrgprb2 receptors are also expressed outside of mast cells in the urinary bladder wall and, when activated by Compound 48/80, increase wall compliance and the leading slope of transient pressure events.

5. Society for Basic Urological Research, 2022

Title: Bladder Wall Biomechanics Differ between Male and Female Mice

Authors: Pragya Saxena, Sara Roccabianca, Bernadette Zwaans, Michael Chancellor, Sarah Bartalone, Elijah P. Ward and Nathan R. Tykocki

Background: The high compliance of the bladder wall allows for the storage of relatively large volumes of urine, while simultaneously providing enough structure so that the detrusor muscle can generate forceful voiding contractions. Changes in the structure of the urinary bladder wall and alterations in bladder compliance are present in numerous urinary bladder pathologies. Yet, we know very little about how mechanical properties of the bladder wall differ between sexes even though bladder dysfunction is more prevalent in females than males. Thus, we measured and compared the mechanical properties of normal bladders from male and female mice.

Methods: Voiding behavior was measured from age-matched male and female mice using the void spot assay. Whole mouse bladders were then dissected and mounted in our novel Pentaplanar Reflected Image Macroscopy (PRIM) System for simultaneous measurement of intravesical pressure, infused volume, and bladder shape. These measurements were used to calculate bladder wall stress and stretch during *ex vivo* bladder filling as intravesical pressure increased from 0 to 25 mmHg.

Results: No significant differences in quantity of void spots, void spot volume, or primary void volume were noted between sexes. However, bladder wall compliance was significantly increased in male mice *versus* female mice.

Conclusions: This study uncovered that the mechanical properties of the bladder wall differ between sexes, even in the absence of bladder dysfunction. These data suggest that the relationship between the mechanical properties, structure, and function of the bladder wall are key in

understanding how bladder dysfunction can develop in both sexes. These data also suggest that "normal" clinical bladder compliance may differ between sexes. Future studies will investigate how the arrangement and expression of extracellular matrix proteins differ between male and female mice.

6. International Continence Society, 2022

Title: Mechanism of Increased Detrusor Contractility Induced by Mast Cell Activator Compound 48/80 in Murine Urinary Bladder

Authors: Pragya Saxena, Sara Roccabianca, and Nathan R. Tykocki

HYPOTHESIS/AIMS OF STUDY: A balance between stiffness and compliance is essential to normal bladder function. Inflammatory processes, such as mast cell activation, can affect the integrity of the bladder wall and lead to increased stiffness. The resultant bladder wall remodeling ultimately leads to many lower urinary tract symptoms. Compound 48/80 is a basic secretagogue that rapidly degranulates mast cells and brings about release of multiple inflammatory mediators including prostaglandins, and matrix metalloproteases (MMPs). These mediators alter urinary bladder smooth muscle contractility as well as wall compliance. In this study, we explored if and how compound 48/80 alters urinary bladder smooth muscle contractility and wall compliance.

STUDY DESIGN: Whole mouse bladders were dissected and mounted in the custom designed Pentaplanar Reflected Image Macroscopy (PRIM) System for simultaneous measurement of transient pressure events, bladder volume, intravesical pressure, wall stress and wall stretch during *ex vivo* bladder filling. Using the recorded intravesical pressures, infusion volumes, image data, we next calculated the bladder wall compliance (defined as the stress versus stretch relationship of the bladder wall). To test our hypothesis, bladders were exposed to either broad spectrum MMP inhibitor Doxycycline (20 μM) or Cyclooxygenase inhibitor Indomethacin (10 μM) prior to the addition of vehicle or the mast cell activator compound 48/80 (10 μg/ml).

RESULTS: Compound 48/80 alone significantly increased the amplitude and leading slope of transient contractions while increasing bladder wall compliance. The broad spectrum MMP inhibitor doxycycline prevented the increase in compliance caused by compound 48/80; however,

the amplitude and leading slope of transient contractions was unaffected. Interestingly, the non-selective cyclooxygenase inhibitor indomethacin prevented all effects of compound 48/80 implying that the mechanism through which compound 48/80 acts is two-fold and parallel.

CONCLUSIONS: Our study discovered that the effects of Compound 48/80 on the urinary bladder are multi-faceted, in that it rapidly activates mast cells to release of prostaglandins, which then increase bladder smooth muscle contractility and activate MMP-mediated increases in bladder wall compliance. Thus, bladders can show signs of overactivity while actually increasing in compliance. Furthermore, changes in compliance and urinary bladder contractility can occur simultaneously and independently. This pathway paves the way for reframing our knowledge on treatments offered for bladder dysfunction that is accompanied by inflammation.

7. American Society for Pharmacology and Experimental Therapeutics, 2023

Title: Compound 48/80 increases bladder wall mechanical compliance via activation of MMP-2

Authors: Pragya Saxena, Sara Roccabianca, and Nathan R. Tykocki

Background: Alteration in wall stiffness and bladder compliance can disrupt normal bladder function and lead to lower urinary tract symptoms (LUTS). Urinary bladder fibrosis due to inflammation is implicated in many clinical cases of LUTS. Mast cell activation represents a key target to understand the fibrotic inflammatory pathways within the bladder wall. Our lab has previously shown that mast cell activation using Compound 48/80 increases mechanical compliance and detrusor contractility, and prostaglandins and matrix metalloproteases (MMPs) released from mast cells can directly alter the mechanical properties of the bladder wall. Blocking the release of prostaglandins blocks the increase in both mechanical compliance and detrusor contractility; however, the specific MMPs responsible for driving changes in compliance are unknown. Thus, in this study we pharmacologically investigated the role of specific MMPs in driving the increase in compliance upon mast cell activation. We hypothesized that MMP-2 is present in the urinary bladder wall and is responsible for the increase in mechanical compliance caused by mast cell degranulation.

Methods: Whole mouse bladders from C57Bl/6 (wild-type) mice were dissected and mounted in the custom-designed pentaplanar reflected image macroscopy (PRIM) system for simultaneous measurement of transient pressure events, intravesical pressure, bladder volume, wall stress, and wall stretch during *ex vivo* bladder filling. Wall compliance was derived as a measure of the stress *versus* stretch relationship using the pressure-volume curves and associated wall geometry gathered from imaging data. Bladders were exposed to Compound 48/80 (10 μg/ml) in the presence of vehicle, the broad-spectrum MMP inhibitor marimastat (10 μM), or the MMP2

inhibitor ARP-100 (10μM) during *ex vivo* filling. MMP-2 protein expression in whole urinary bladder protein isolates was also determined using western blot analysis.

Results: Western blot analysis showed that MMP-2 is present in the bladder wall in both detrusor and urothelium layers. Both marimastat and ARP-100 completely abolished the increase in compliance caused by Compound 48/80. However, neither altered the increase in amplitude of transient pressure events.

Conclusions: These findings suggest that the effects of mast cell activation are dual in nature: mast cell activation causes a release of prostaglandins that directly alter detrusor contractility and also increase wall compliance by activating MMP-2. Increases in excitability and profound bladder wall remodeling also occur in minutes after degranulation, suggesting these mechanisms are initiated rapidly after inflammatory insult.

8. American Physiological Society, 2023

Title: Alteration in Mechanical Compliance via Mast Cell Activation in Juvenile and Adult Urinary Bladder

Authors: Pragya Saxena, Sara Roccabianca, and Nathan R. Tykocki

Biomechanical properties such as mechanical compliance and stiffness are directly influenced by the integrity of the extracellular matrix (ECM) and its interaction with urinary bladder smooth muscle (UBSM). While normal bladder function differs between juveniles and adults, it is unclear if these differences are due solely to increases in bladder size. Differences in the mechanical properties of the wall may also exist and are unexplored. Changes in mechanical compliance are implicated in the pathophysiology of many lower urinary tract symptoms (LUTS) such as overactivity and fibrosis due to inflammation. Interestingly, juvenile bladders are particularly susceptible to inflammatory LUTS by various factors (e.g., early life stress) compared to their adult counterparts. We were interested in how bladders from juvenile and adult mice respond to inflammation, specifically driven by mast cell degranulation. We hypothesized that: (1) juvenile bladders are inherently more compliant than adult bladders and (2) mast cell degranulation increases mechanical compliance in both juvenile and adult mouse bladders.

Whole mouse bladders from juvenile (4–5 weeks old) and adult (12–14 weeks old) C57Bl/6 male mice were dissected and mounted in a custom designed pentaplanar reflected image macroscopy (PRIM) system for simultaneous measurement of transient pressure events, intravesical pressure, bladder volume, wall stress, and wall stretch during *ex vivo* bladder filling. Mechanical properties of the bladder wall were measured as the relationship between mechanical stress *versus* stretch. Properties of the transient contractions were calculated using acquired pressure-volume curves.

Measurements were performed in the absence or presence of the mast cell activator Compound 48/80 (10 µg/mL).

Mechanical stress in adult mouse bladders was higher compared to juvenile bladders, implying that adult bladders were stiffer. In presence of Compound 48/80, both age groups show similar effects. Mechanical compliance increased with a paradoxical increase in amplitude of transient contractions. Together, these data suggest that while juvenile mouse bladders are less stiff, they respond to mast cell activation in a similar manner as adult bladders. Consequently, rapid degranulation of mast cells in juvenile bladders leads to increased mechanical compliance and contractility. Thus, preventing mast cell degranulation could represent a viable target for treating LUTS in children as well as adults.

9. American Society for Pharmacology and Experimental Therapeutics, 2024

Title: Compound 48/80 alters mechanical compliance via activation of Gelatinases (MMP-2 and -9) in an ATP-dependent manner

Authors: Pragya Saxena, Sara Roccabianca, and Nathan R. Tykocki

Many lower urinary tract symptoms (LUTS) that arise due to alteration in mechanical compliance of the bladder are also accompanied by increased urothelial signaling which leads to release of transmitters such as ATP. While traditionally assumed to be a high-resistance barrier, urothelial cells can respond to inflammatory insult, signal to cells in the bladder wall, and potentiate the downstream release and activation of matrix metalloproteases (MMPs). MMPs are responsible for degrading components of the extracellular matrix (ECM) and causing bladder wall remodeling. Previously, we discovered that the Mas-related G protein-coupled receptor B2 (Mrgprb2) agonist Compound 48/80, increased bladder wall compliance in an MMP dependent manner. However, the mechanism underlying MMP activation downstream of Mrgprb2 is not understood. We hypothesized that Mrgprb2 activation causes breakdown of collagen in the bladder ECM *via* the ATP-dependent activation of MMP-2 and MMP-9.

Whole mouse bladders from C57Bl/6 mice were dissected and mounted in a custom designed pentaplanar reflected image macroscopy (PRIM) system for simultaneous measurement of transient pressure events, wall stress, and wall stretch during *ex vivo* bladder filling. Bladders were exposed to Compound 48/80 (10 µg/mL) in absence or presence of the MMP-9 inhibitor JNJ-0966 (500 nM) or MMP-2 inhibitor ARP-100 (200 nM). MMP-2 and MMP-9 content and activity in the bladders exposed to either vehicle or Compound 48/80 was also determined using Western blot analysis and Gelatin zymography respectively.

ARP-100 and JNJ-0966 completely abolished the increase in compliance caused by Compound 48/80. However, they had no effect on the increases in transient pressure events caused by Compound 48/80. Western blot analysis showed no difference in the expression of pro-MMP-2/MMP-2 and pro-MMP-9/MMP-9 between bladders that were exposed to vehicle or Compound 48/80 prior to protein isolation. The activity level of pro-MMP-2 and MMP-2 was increased in bladders that were exposed to Compound 48/80.

These findings suggest that Compound 48/80 brings about MMP activation which drives collagen degradation in the bladder wall. Future experiments will study the mechanistic pathway that leads to MMP activation after exposure to Compound 48/80.